Hochschule für Angewandte Wissenschaften Hamburg
Hamburg University of Applied Sciences

Master Thesis

Malte Hinsch

Two-bladed floating offshore wind turbines - Comparison of existing floating support structure concepts and aero-hydro-servo-elastic simulation

Fakultät Technik und Informatik
Department Maschinenbau und Produktion

Faculty of Engineering and Computer Science
Department of Mechanical Engineering and Production Management

Malte Hinsch

Two-bladed floating offshore wind turbines - Comparison of existing floating support structure concepts and aero-hydro-servo-elastic simulation

Masterarbeit eingereicht im Rahmen der Masterprüfung

im Studiengang Produktionstechnik und -management
am Department Maschinenbau und Produktion
der Fakultät Technik und Informatik
der Hochschule für Angewandte Wissenschaften Hamburg

Erstprüferin: Prof. Dr. Vera Schorbach
Zweitprüfer: Prof. Peter Dalhoff

Abgabedatum: 01.09.2022

Summary

Name of Student

Malte Hinsch

Title of the Master Thesis

Two-bladed floating offshore wind turbines - Comparison of existing floating support structure concepts and aero-hydro-servo-elastic simulation

Keywords

FOWT, floating offshore wind turbine, assessment of FOWT, numerical simulation, VolturnUS

Abstract

The application area of the bottom fixed wind turbines is limited to shallow waters up to 60m water depth. To use offshore wind turbines economically also in deeper waters, new foundation technologies must be applied. With the help of a floating offshore wind turbine (FOWT), areas of application with water depths up to 1000m can be opened up. The potential of the young expanding floating wind market has already been recognized by many companies, leading to a high variety of support structure concepts. For this reason, the first objective of this paper is to get an overview of commercial concepts and to assess those based on economic and environmental flexibility criteria. With the help of individual concept scores, suitable criteria and an appropriate weighting of those, the designs with the greatest potential for offshore wind farm deployment are to be identified.

The second part of this work consists of a numerical simulation that investigates the IEA 15 MW wind turbine that is mounted on the semi-submersible VolturnUS from UMaine. The focus is on the investigation of nacelle accelerations and substructure displacements resulting from an extreme design load case. Three different models are investigated which differ regarding their applied calculation methods. The hydrodynamic loads acting on the substructure are modeled with a boundary element method (BEM), the Morison’s equation, and a combination of both. The simulation tool Bladed by DNV calculates the diffraction, radiation, and hydrostatic loading for the BEM models with coefficients from response amplitude operators.

Zusammenfassung

Name des Studierenden

Malte Hinsch

Thema der Masterthesis

Schwimmende Zweiblatt-Windenergieanlagen - Vergleich kommerzieller schwimmender Tragwerkskonzepte und aero-hydro-servo-elastische Simulation

Stichworte

FOWT, schwimmende Windkraftanlage, Vergleich von Tragwerkstrukturen für schwimmende Windkraftanlagen, numerische Simulation, VolturnUS

Kurzzusammenfassung

Der Einsatzbereich von bodenfesten Offshore-Windkraftanlagen ist beschränkt auf flache Gewässer von bis zu 60 m Wassertiefe. Um Offshore-Windenergieanlagen auch in tieferen Gewässern wirtschaftlich nutzen zu können, müssen neue Gründungstechnologien eingesetzt werden. Mit Hilfe einer schwimmenden Windenergieanlage können Einsatzgebiete mit Wassertiefen bis zu 1000 m erschlossen werden. Das Potenzial dieses jungen Marktes wurde bereits von vielen Unternehmen erkannt, was zu einer großen Vielfalt an Tragwerkskonzepten geführt hat.

Aus diesem Grund fokussiert sich der erste Teil dieser Arbeit darauf, einen Überblick über die kommerziellen Konzepte zu geben und diese anhand von wirtschaftlichen und ökologischen Flexibilitätskriterien zu bewerten. Mit Hilfe individueller Konzeptbewertungen, geeigneter Kriterien und einer angemessenen Gewichtung dieser Kriterien sollen jene Tragwerkskonzepte identifiziert werden, welche das größte Potenzial für den Einsatz in Offshore-Windparks aufweisen.

Der zweite Teil dieser Arbeit besteht aus einer numerischen Simulation, welche die IEA 15-MW-Windenergieanlage in Verbindung mit dem Halbtaucherkonzept VolturnUS von UMaine untersucht. Der Schwerpunkt liegt dabei auf der Untersuchung von Beschleunigungen der Gondel sowie Auslenkungen der Tragstruktur, die aufgrund eines Extremlastfalls resultieren. Es werden drei verschiedene Modelle untersucht, die sich hinsichtlich der verwendeten Berechnungsmethoden unterscheiden. Die auf die Tragstruktur wirkenden hydrodynamischen Lasten werden mit einer Randelementmethode (BEM), der Morison-Gleichung und einer Kombination aus beiden modelliert. Das Simulationsprogramm Bladed vom DNV berechnet die hydrodynamischen und -statischen Lasten für die BEM-Modelle mit Hilfe von Koeffizienten aus einer Übertragungsfunktionen (RAOs).

Task description - Master Thesis

Name of Student

Malte Hinsch

Matriculation number

[redacted]

Title of the Master Thesis

Two-bladed floating offshore wind turbines - Comparison of existing floating support structure concepts and aero-hydro-servo-elastic simulation

Task description

State of the Art and Research for floating support structure concepts for floating offshore wind turbines (FOWT):

- Floating offshore wind market overview.
- Identification of existing support structure concepts.
- Elaboration of requirements for FOWT.

Comparison of the support structure concepts:

- Selection of an appropriate method for comparing the different structures.
- Definition of suitable criteria for the comparison.
- Identifying the structure with the most potential for offshore wind farm deployment.

Aero-hydro-servo-elastic simulation of the floating offshore wind turbine:

- Creating a numerical model of a floating support structure (inclusive a mooring system)
- Performing an aero-hydro-servo-elastic simulation of the floating wind structure based on one extreme load case.
- Investigation of the nacelle accelerations and support structure displacements.

Summary of results and findings

Aufgabenstellung – Masterthesis

Name des Studierenden

Malte Hinsch

Matrikelnummer

[redacted]

Thema der Masterthesis

Two-bladed floating offshore wind turbines - Comparison of existing floating support structure concepts and aero-hydro-servo-elastic simulation

Aufgabenstellung

Stand der Technik und Forschung für schwimmende Tragwerkskonzepte für schwimmende Offshore-Windkraftanlagen (FOWT):

- Überblick über den schwimmenden Offshore-Windmarkt.
- Erfassung von existierenden schwimmenden Tragstrukturkonzepten.
- Erarbeitung von Anforderungen für FOWT.

Vergleich der Tragstrukturkonzepte:

- Auswahl einer geeigneten Methodik zum Vergleich der verschiedenen Strukturen.
- Definition von geeigneten Kriterien für den Vergleich.
- Identifizierung der Struktur mit dem größten Potenzial für den Einsatz in Offshore-Windparks.

Aero-hydro-servo-elastische Simulation der schwimmenden Offshore-Windkraftanlage:

- Erstellung eines numerischen Modells von einer schwimmenden Tragstruktur (einschließlich eines Verankerungssystems).
- Durchführung einer aero-hydro-servo-elastischen Simulation der schwimmenden Windkraftanlage auf der Grundlage eines Extremlastfalls.
- Untersuchung der auftretenden Gondel-Beschleunigungen und Tragstruktur-Auslenkungen.

Zusammenfassung der Ergebnisse und Erkenntnisse

Contents

I Symbol directory

A	Wave amplitude	[m]
A_{jk}	Added mass matrix for kth element	[-]
B_{jk}	Damping matrix for kth element	[-]
cos	Cosine	[-]
C_D	Drag coefficient	[-]
$C_{D,C}$	Drag coefficient for columns	[-]
$C_{D,P}$	The drag coefficient for pontoons	[-]
C_{jk}	Stiffness matrix for kth element	[-]
C_M	Inertia (added mass) coefficient	[-]
$C_{M,IC}$	Inertia coefficient for inner columns	[-]
$C_{M,OC}$	Inertia coefficient for outer columns	[-]
$C_{M,P}$	Inertia coefficient for pontoons	[-]
$cs_{floater}$	Cost share of floater	[-]
$cs_{floater\&foundation,total}$	Cost share of floater and foundation in total costs	[-]
$cs_{installation,total}$	Cost share of installation in total costs	[-]
$cs_{mooring}$	Cost share mooring system	[-]
$cs_{O\&M,total}$	Cost share of O&M in total costs	[-]
$cs_{RNA\ \&\ tower,total}$	Cost share of RNA and tower in total costs	[-]
cs_{tower}	Cost share tower	[-]
cs_{total}	Cost share of selected criteria in total costs	[-]
D	Diameter of cylinder	[m]
dF	Horizontal force	[N]
d_p	Diameter of equivalent pontoon	[m]
dz	Strip length	[m]
e	Euler's number	[-]
F	External excitation force vector	[N]
$f_{F,manufacturing}$	Factor manufacturing in category floater	[-]
$f_{F,material,i}$	Material factor for ith element in category floater	[-]
$f_{O\&M,accessibility}$	Factor accessibility in category maintenance	[-]
$f_{M,anchor}$	Factor anchor type in category mooring system	[-]
$f_{M,line}$	Factor mooring line in category mooring system	[-]
$f_{T,design}$	Factor tower design in category tower	[-]
g	Acceleration of gravity	[m/s^2]
H	Wave height	[m]
h	Water depth	[m]
h_p	Height of pontoon	[m]
k	Wave number	[1/m]
KC	Keulegan-Carpenter number	[-]
KC_{IC}	KC number for inner columns	[-]
KC_{OC}	KC number for outer columns	[-]
$m_{F,i}$	Material mass for ith element	[ton]
M_{jk}	Mass matrix for kth element	[-]
N	Number of wave components	[-]
n	Number of flexibility criteria	[-]
n_{lines}	Number of mooring lines	[-]
$n_{anchors}$	Number of anchors	[-]
n_p	Number of pairwise comparisons	[-]
$r_{inverse}$	Inverse ranking	[-]
S	Total weighted score of a concept	[-]

s	Unweighted score of a concept	[-]
sin	Sine	[-]
s_{anchor}	Score anchor	[-]
$s_{base\ case}$	Unweighted score base case	[-]
$s_{floater}$	Unweighted score floater	[-]
$s_{F,manufacturing}$	Score manufacturing in category floater	[-]
$s_{F,raw\ material}$	Score raw material in category floater	[-]
$s_{installation}$	Unweighted score installation	[-]
$s_{I,floater}$	Score installation floater in category installation	[-]
$s_{I,mooring}$	Score installation mooring system in category installation	[-]
$s_{I,turbine}$	Score installation turbine in category installation	[-]
$s_{O\&M}$	Unweighted score maintenance	[-]
$s_{O\&M,strategy}$	Score maintenance strategy in category maintenance	[-]
$s_{mooring}$	Unweighted score mooring system	[-]
$s_{M,line}$	Score mooring line in category mooring system	[-]
$s_{rankings}$	Sum of rankings	[-]
s_{tower}	Unweighted score tower	[-]
$s_{T,typology}$	Score tower by typology in category tower	[-]
S_u	Normalized and unweighted score of a concept	[-]
$S(\omega)$	Wave spectrum	[m²/s]
T	Wave period	[1/s]
t	Time	[s]
u	Flow velocity	[m/s]
$\dot{u}$	Flow acceleration	[m/s²]
u_h	Horizontal particle velocity	[m/s]
u_0	Water particle velocity amplitude	[m/s]
u_v	Vertical particle velocity	[m/s]
V	Fluid velocity vector	[-]
v_m	Maximum orbital particle velocity	[m/s]
w	Criterion weight	[-]
w_F	Weight of flexibility criterion	[-]
$w_{floater}$	Criterion weight floater	[-]
$w_{F,sum}$	Sum of flexibility criteria weights	[-]
$w_{installation}$	Criterion weight installation	[-]
$w_{O\&M}$	Criterion weight maintenance	[-]
$w_{mooring}$	Criterion weight mooring system	[-]
w_p	Width of pontoon	[m]
w_{tower}	Criterion weight tower	[-]
γ	Peak enhancement factor	[-]
∂	Functional derivative	[-]
ϵ	Random phase angle of a wave component	[rad]
ζ	Wave elevation	[m]
ζ_a	Wave amplitude	[m]
$\eta_k, \dot{\eta_k}, \ddot{\eta}_k$	Motion, velocity and acceleration for kth element	[m], [m/s], [m/s²]
λ	Wavelength	[m]
ρ	Density of water	[kg/m³]
ϕ	Velocity potential	[-]
ω	Circular wave frequency	[Hz]
$\Delta\omega$	Difference between succussive frequencies	[Hz]

II List of abbreviations

2B	Two-bladed
3B	Three-bladed
AEP	Annual energy production
CAPEX	Capital expenditure
CTV	Crew transfer vessel
COB	Center of buoyancy
COG	Center of gravity
DEA	Drag embedment anchor
DECEX	Decommissioning expenditure
DLC	Design load case
DOF	Degree of freedom
FOWT	Floating offshore wind turbine
kW	Kilowatt
LCOE	Levelized cost of energy
Metocean	Meteorology and oceanography
MW	Megawatt
O&M	Operations and maintenance
OPEX	Operational expenditure
RNA	Rotor nacelle assembly
Spar	Single Point Anchor Reservoir
Semi-sub	Semi-submersible
SKS	Station keeping system
SOV	Service operation vessel
TLP	Tension Leg platform
UK	United Kingdom
WTG	Wind turbine generator

III List of tables

IV List of figures

1 Introduction

1.1 Background

It is estimated that about 80% of the offshore wind potential is found at water depths greater than 60 meters. [1] The economic efficiency of the market-dominating bottom-fixed wind turbines is coupled with the water depth and there is evidence to suggest that for depths greater than 50 meters those foundation types become less profitable. [2] To maintain the economic viability of offshore wind in deeper waters, floating offshore wind turbines (FOWT) could provide relief. Moreover, sites in cost-effective, near-shore, shallow-water locations are limited, so sooner or later it will be necessary to switch to deeper waters. [3]

At this point in time, floating wind turbines cannot yet match the electricity generation costs of bottom-fixed foundations. [4] Reducing the diversity of concepts would allow the supply chain, infrastructure as well as manufacturing of the substructure to be more efficiently aligned with one technology and thereby reducing costs. [5]

Currently, the share of FOWT in the total offshore wind market is only 0,1 % but is expected to grow to 6,1 % by 2030. [6] The potential of this young expanding market has also been recognized by many companies, resulting in a wide variety of floating substructure concepts. Approximately 50 concepts can be identified in the market, varying in maturity from concept design to demonstration projects. The individual advantages and disadvantages of these concepts vary with respect to different technical and economic criteria, making it difficult to identify a clear trend towards a particular design.

1.2 Objective and methodology

Since the market offers a wide variety of commercial concepts, but a smaller number of designs could positively impact profitability, the first main objective of this work is to evaluate substructure concepts for floating single-rotor wind turbines. As a first step the identification of main support structure typologies including their respective response characteristics and mooring systems is presented (Section2.1). The subsequent market research is intended to give an overview of the development of floating wind projects. Furthermore, commercial floater designs are identified in the market and an overview of the share per typology is given. (Section 2.2)

Subsequently, the Levelized Cost of Energy (LCOE) of floating wind turbines including its influencing factors will be discussed in more detail. The main focus is on the life cycle costs that are influenced by the floater typology and its individual design. (Section 3)

In addition, a literature review is performed focusing on the results of concept assessment conducted in studies. In a first step, results of studies are presented that evaluate concepts based on weighted qualitative and quantitative criteria. The following section examines cost studies that have determined the LCOE for various floater typologies. Finally, the last section of the literature review elaborates perspectives from which the concepts can be compared. (Section 4)

In the following chapter, the identified commercial concepts are assessed with the help of a two-dimensional weighted point analysis. The first dimension evaluates those concepts based on life cycle costs, that are directly affected by the floater typology and its design. For this purpose, individual concept scores are determined in five different cost categories and multiplied by the respective criteria weighting that is dependent on their cost share in the total LCOE. (Section 5.2) The second dimension assesses concepts based on their respective limitations and restrictions for site conditions. Depending on the typology and design of the substructure, the requirements for water depth, waves, current, and soil conditions are considered. (Section 5.3)

The second main objective of this study is a numerical simulation of a generic semi-submersible concept. The substructure model is based on the concrete support structure VolturnUS developed collaboratively by the University of Maine (UMaine) and the U.S. Department of Energy. A generic steel version of the semi-submersible by UMaine is investigated by the National Renewable Energy Laboratory (NREL) in “IEA Wind TCP Task 37: Definition of the IEA Wind 15-Megawatt Offshore Reference Wind Turbine” [7] which supports the International Energy Agency (IEA) 15 MW reference wind turbine. In the first part of the numerical simulation the theory background for waves, loads on floating wind turbines as well as response amplitude operators (RAO) is presented. Afterwards, the numerical model is introduced, which is modelled on the basis of the platform and mooring system properties as well as RAOs conducted in [7] by NREL. Based on an extreme load case the numerical model is investigated in terms of nacelle accelerations and support structure displacements and compared with the results determined in the report by NREL.

2 Review of floating wind

This chapter is intended to provide basic insights into the technology of support structures for floating wind turbines as well as an overview of the floating wind market. Therefore, in Section 2.1 the general classification of support structure concepts is presented including its respective response characteristics and mooring systems. In Section 2.2 an overview of the floating wind market is provided which points out the development of FOWT projects and the distribution of commercial concepts according to floater typology.

2.1 Floating wind support structures

Although there are approximately 50 individual designs on the market, they can be classified in a few main floater typologies. The classification helps to handle the high number of concepts in the further course of this work. Therefore, in Section 2.1.1 the most common classification of support structures is presented. Afterwards the Section 2.1.2 is intended to provide an overview of the response characteristics by floater typology. Finally in Section 2.1.3 an overview of mooring systems including its line configurations as well as anchor typologies is presented.

2.1.1 Classification of support structures

The floating support structure provides the required stability for operating the offshore wind turbine under the influence of environmental loads. The way in which the support structure achieves its floating stability is used to classify substructure concepts. As a result, similar geometries of support structures could potentially be classified in different categories. [3] Basically, there are three main possibilities for a floating support structure to generate the necessary counteracting or restoring moment which can be seen in Figure 1. [3], [8] These stabilization principles and its variations or hybrids are presented in the following.

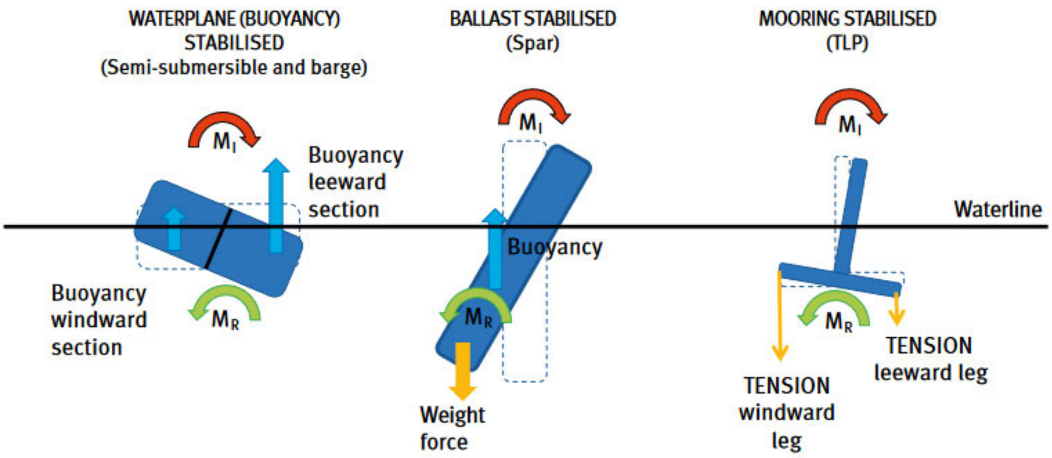

Figure 1: Primary principles of generating restoring forces of a FOWT [3]

Ballast stabilized platform

The vertically swimming Single Point Anchor Reservoir (Spar) buoy is stabilized by exploiting the buoyancy force in combination with the weight force of its ballast. The relatively long and slender structure is ballasted at the bottom end with either water, concrete, or sand to increase the vertical distance between the center of gravity (COG) and the above located center of buoyancy (COB). When the structure is forced to incline the center of the buoyancy force is not anymore vertically aligned with the center of gravity. This horizontal distance between the COG and the COB results in a restoring moment that prevents the structure from tipping over (see Figure 1). [3], [8]

Since a large distance between COB and COG is beneficial for the stability of the structure, spar buoys often have a relatively high draft which ranges typically from 70-100m. As a result, ballast stabilized platforms are most likely deployed in water depths of over 100 meters. Depending on the design and the turbine size the diameter of spar buoys is typically in the range of 10-20 m. [5]

Waterplane (buoyancy) stabilized platform

The large (continuous) waterplane area of a barge provides its static floating stability. By inclining the platform, the buoyancy leeward section has a larger submerged volume than the buoyancy windward section. This disequilibrium between the submerged volume of those two sections leads to a higher buoyancy force at the leeward site than at the windward site (see Figure 1). This results in a restoring moment (MR) counteracting the wind inclining moment (MI). [3] [8]

Due to its stabilization principle barges have typically the smallest draft among the other typologies with a draft smaller than 10 meters. The typical width and length ranges between 40 to 50 m. [5]

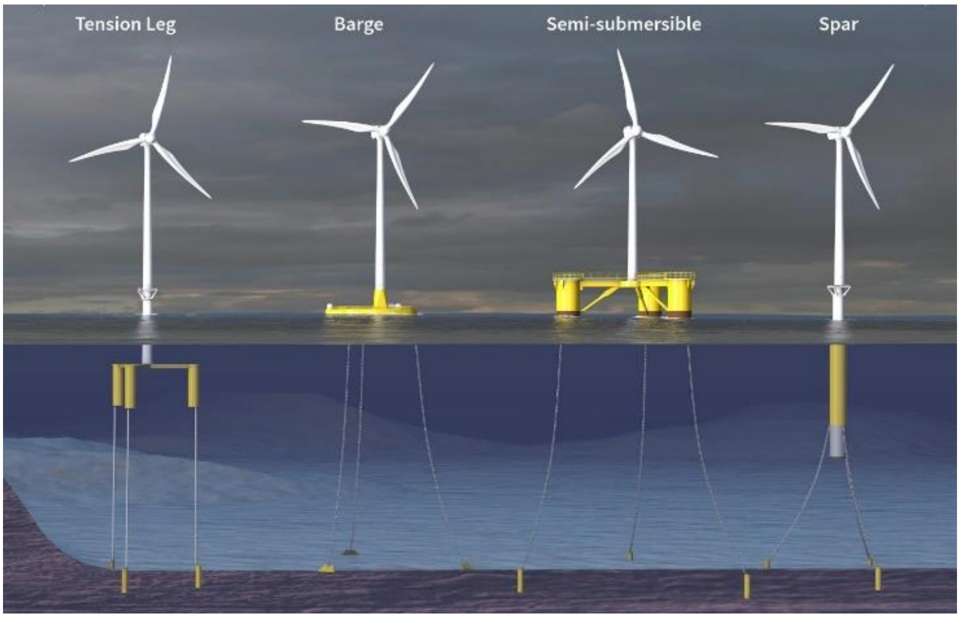

Figure 2: Examples for main floater typologies[9]

Mooring stabilized platform

The Tension Leg Platform (TLP) achieves its floating stability due to its tensioned mooring lines which connect the platform with the seabed. The buoyancy force of the platform is significantly greater than the weight force resulting in strongly and continuous tensioned lines. [5] An inclination of the structure results in higher tensioned tendons on the windward site compared to the ones connected to the leeward side. This difference causes a restoring moment (MR) counteracting the inclining moment (MI) (Figure 1). [3] The TLP is normally not stable without its tendons being attached. [8]

Usually, TLP's consists of a vertical center column with outward running submerged arms on which the tendons are attached. With 15-25 m the typical draft of a TLP is smaller than the draft of a spar buoy but slightly larger than the draft of a barge and semi-submersible. [3], [5] Their typical length and width is between 20-35 m but can vary significantly between different designs. [5]

Column stabilized platform

Since the semi-submersible achieves its static stability with their widely spaced columns it is named column stabilized platform. This typology combines the ballast stabilization principle with the waterplane stabilization principle. [10] If the structure is inclined, the outer columns provide a restring moment due to differences of the buoyancy forces. Next to that these columns are ballasted at their bottom end to lower the center of gravity of the substructure leading to the ability of exploiting the buoyancy stabilization principle. [8] [3] This combination of these two stabilization principles categorizes the semi-Submersible between the spar buoy and the barge (Figure 3). Although the semi-submersible achieves its stability with a combination of two main stabilization principles it is usually considered as a separate category in the literature and industry.

Due to the smaller columns connected far away from the inclination axis usually, the semi-submersible has greater outer dimensions than the barge foundation [11], [5] Typically the length and width of a column stabilized floater is ranging between 60-80m and the draft of this platform is 10-20 meters. [5] To decrease the dimensions of the structure some designs have heave plates attached to the bottom end of the columns and thus providing additional damping forces. [8]

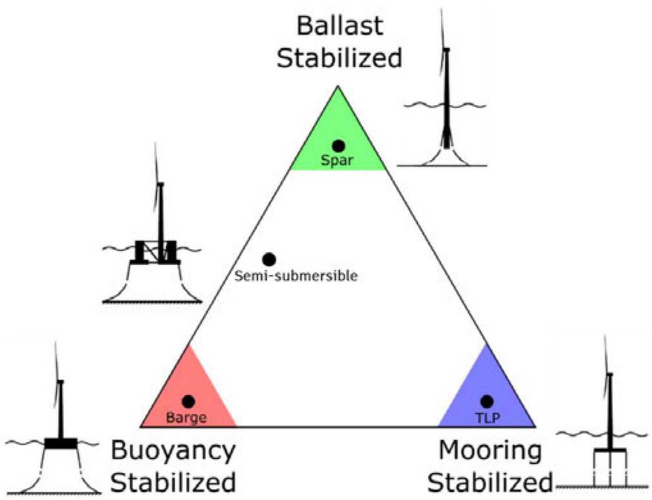

Figure 3: Stability triangle for main floater typologies [author's illustration adapted from [11]]

2.1.2 Response characteristics of support structures

In general, a floating support structure has six global modes of motions in a three-dimensional space, which often are called degrees of freedom (DOF). [10] Surge, sway and heave refer to the three translational directions of motions whereas roll, pitch and yaw describe the rotational degrees of freedom around the three axes (see Figure 4).

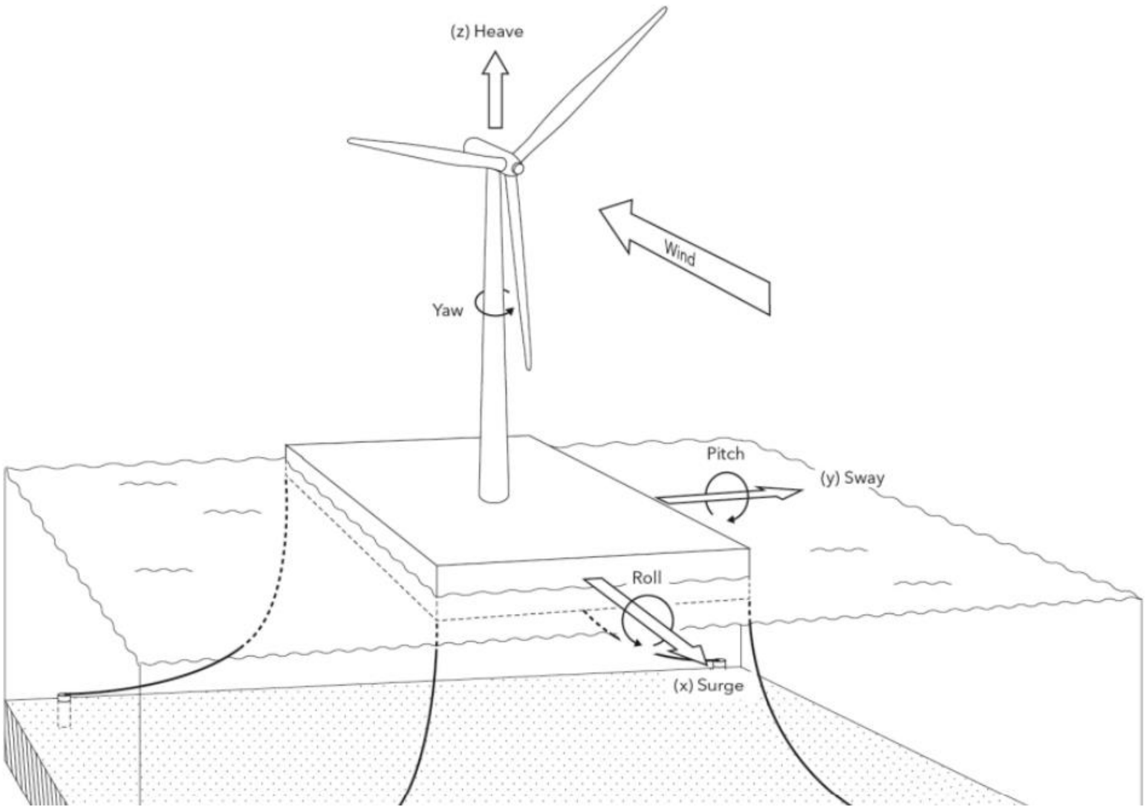

Figure 4: Degrees of freedom of a floating wind turbine [10]

The DNV [10] classifies the six degrees of freedom for each floater typology into restrained and compliant modes (see Table 1). Compliant indicates that motions and inclinations are possible, whereas restrained means that nearly no platform displacement can occur. Nearly no implies in this context that only small displacements in the order of centimeters are possible. [10]

According to [10] the spar buoy, the barge, and the semi-submersible have no restrained modes, so these platforms allow significant motions in all six degrees of freedom. The TLP allows displacements in surge, sway and yaw but is restrained regarding heave, roll and pitch motions. [8], [10]

Furthermore, Table 1 provides information about the natural frequencies of a floater typology. If a particular motion is compliant the natural period of the floater is above the typical wave frequency. Restrained implies that usually, the wave frequency is below the natural period of the substructure. [8], [12] Depending on the sea state and the location, the first-order wave frequencies are in the range of about 5-25 seconds. [10] The frequencies of the waves are a key criterion in the design process of the floating support structure. To avoid natural frequency excitations, it is important that the natural periods of the substructure are outside of the wave frequencies. [12]

Table 1: Motion characteristics by floater typology (C denotes compliant, R denotes restrained) [10]

Platform type	Surge	Sway	Heave	Roll	Pitch	Yaw
Barge	C	C	C	C	C	C
Semi-submersible	C	C	C	C	C	C
Spar buoy	C	C	C	C	C	C
TLP	C	C	R	R	R	C

Outside of the first-order frequencies, second-order wave loads can occur which may lead to additional loads on the platform. For TLP's this may result in ringing-springing type responses that occur within the range of 0-5 second wave periods. On the other side for compliant platforms in the horizontal axis (especially barges and semi-submersibles) second-order loads can lead to slow drift forces for periods above 25 seconds. [8]

In Figure 5 typical FOWT responses of a semi-submersible, spar buoy and TLP are illustrated.

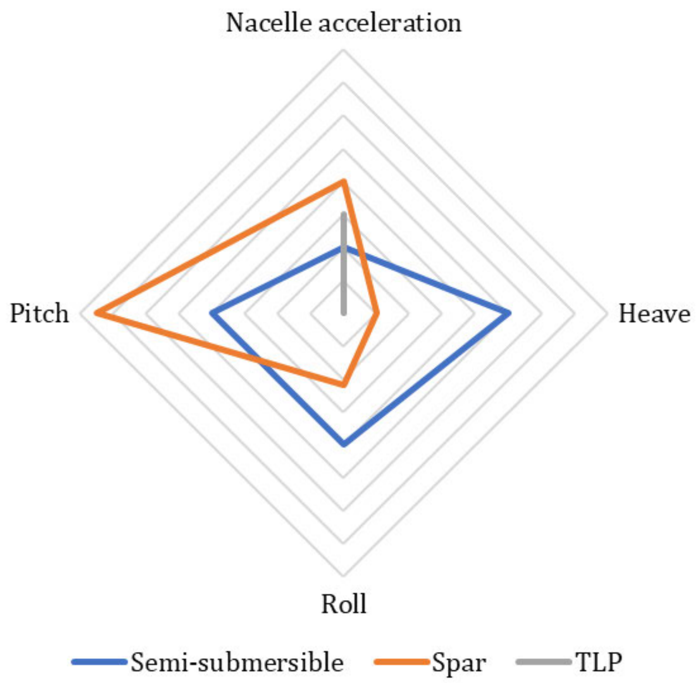

Figure 5: Motion permissible for floating wind foundation typologies [author's illustration adapted from [4]]

The **barge** substructure is not illustrated but due to its large waterplane area and relatively small draft, barges are susceptible to waves which can possibly result in larger nacelle accelerations and support structure displacements. [8], [10], [13] Especially the susceptibility of adverse pitch and roll motions can lead to higher turbine and tower loads. [14], [11]

Semi-submersibles have small distributed waterplane areas resulting in a natural period for the heave mode slightly above 20 seconds. As a result, the semi-submersible has smaller vertical motions when comparing it to a monohull floater (barge). [12] However, compared to the spar buoy and the TLP, semi-submersibles show the highest heave motions (see Figure 5).

Due to their large draft **spar buoy**s are usually characterized by small heave motions. On the other side the large, submerged area makes the platform more susceptible to surge motions caused by currents. In addition, the long slender design of the spar buoy increases its susceptibility to pitching and rolling motions which can lead to higher tower fatigue loads. [4], [14] Spar buoys also tend to low frequency vortex-induced motions which can increase the current forces. Strakes at the outside of the hull can reduce the vortex induced motions but would lead to a higher mass and increased drag forces. [12] Because of its small distance between the center of gravity in the horizontal plane and the mooring connection point the spar buoy shows a low resistance against yawing. This must be compensated by a specialized mooring system e.g., delta connection. [8]

The response characteristics of a **TLP** differ between the horizontal and vertical plane. In general, the motions of a TLP in the horizontal plane (surge, sway, yaw) are similar to those of a semi-submersible. [12] Due to the vertical tendons with a small anchor radius, it has a small yaw stiffness which may increase the rotational motion. The response characteristics in the vertical plane of a TLP behave more like a fixed structure with nearly no motions. [12]

2.1.3 Mooring system

The mooring system (also station keeping system (SKS)) of a floating wind turbine connects the floating substructure with the seabed. The main task of mooring systems is to provide station-keeping and prevent the floater from drifting away from of the wind farm. For TLPs, mooring lines also provide the necessary stability that keeps the FOWT in an upright position (see Section 2.1.1). [15]

Mooring lines

By deforming and activating reaction forces mooring lines provide resistance to environmental loading. A displacement of the substructure from its neutral equilibrium leads to a restoring force which counteracts the applied loading. The so called "tension spring effect" of the lines can result from a hanging catenary effect (gravity force acting vertically on line) or an elastic effect (elastic stretch over the length on line). [12] The mooring configuration describes which type of tension spring effect is applied for generating the restoring forces.

Usually, barges, semi-submersible and spar buoys apply a catenary or semi-taut mooring configuration (combination out of the catenary and tension effect). Due to their stabilization principle TLP's require a taut leg mooring system which relies on the tension spring effect. [4] In Table 2 the mooring configurations with their respective properties are presented.

Table 2: Characteristics of different mooring configurations [4], [16], [17]

Parameter	Catenary	Semi-taut	Taut leg
Functionality	Restoring force by the weight of the hanging chain	Elasticity of synthetic line section and restoring force by weight of ground chain	Tension of the lines
Line material	Steel chain, steel wire	Synthetic fiber, steel wire or steel chain	Synthetic fiber or steel wire
Footprint	Large	Medium	Small
Direction of anchor loading	Horizontal loading at anchoring point	Horizontal and vertical loading at anchoring point	Vertical loading at anchoring point
Loads on anchor	Long mooring lines, partly resting on the seabed, reduce loads on the anchors	Medium loads on the anchors	Large loads acting on the anchors - requires anchors which can withstand vertical forces
Impact on floater	Greater freedom of movement than taut leg	Greater freedom of movement than taut leg	High tension limits floater motion (pitch/roll/heave) to maintain excellent stability
Installation effort	Relatively simple Installation procedure	Relatively simple Installation procedure	Challenging installation procedure

Anchors

The choice of the anchor type is dependent on several factors such as the mooring configuration, the seabed conditions, and the required holding capacity. For greater distances between shore and site, higher water depths, and more challenging weather conditions the practicability of the anchor type becomes a more important selection criterion. [16]

The stabilization principle of the FOWT determines to a large extent the bandwidth of anchor choice selection. TLPs rely on anchor types that can withstand a high vertical loading e.g., driven piles, suction piles, and gravity anchors. Since drag-embedment anchors (DEA) are only able to withstand small uplift angles, this anchor type is well suited for catenary moorings with mainly horizontal anchor loading. Semi-taut moorings can lead to vertical anchor loads, which is why vertical load anchors are often used. Heavy bottom line sections in a semi-taut configuration can reduce the anchor uplift angle and make the system applicable for a drag embedment anchor. In Table 3 the most common anchor types with their respective properties are presented.

Table 3: Overview anchor types and characteristics [4], [16], [17]

Parameter	Drag-embedded	Driven pile	Suction pile	Gravity anchor
Functionality of holding capacity	Resistance of soil in front of anchor	Combination of friction and lateral soil resistance	Combination of friction and lateral soil resistance	Weight of material
Soil conditions	Cohesive soils	Wide range of soils	Not suitable for loose sandy or too stiff soils	Medium to hard soil conditions
Loading	Horizontal with only small uplift angles	Horizontal and vertical	Horizontal and vertical	Horizontal and vertical
Installation	Dragging by using tugboats	Requires a hammer for piling leading to high noise emissions	Relatively simple with suction pumps	High weight and large dimensions can increase costs
Decommissioning	Simple recoverable	Difficult to remove	Easily removable	Difficult to remove

2.2 Market overview

This section is intended to give an overview of the current floating wind market and its forecast for the next decades. Furthermore, the development of installed demonstrators and commercial projects is pointed out. Next to that the distribution of concepts and market shares, as well as a more detailed review of representative floater concepts, is conducted.

From 2012 to 2021, the installed offshore wind energy capacity increased by a factor of ten. [18] The growth forecast for offshore wind power predicts that offshore wind will increase its installed capacity by 2030 to over 240 GW. [19] Until today most of the capacity is installed in countries with coasts of shallow waters. [18] In deeper waters, such as the coast of the USA, no offshore wind farms have been installed so far. [1] To date, a total of nearly 124 MW of floating wind turbines have been deployed around the world. The largest share of this installed capacity have the Hywind Pilot Park in the UK (30 MW), the WindFLoat Atlantic 2 in Portugal (25 MW) and, the Kincardine – phase 2 park in the UK (48 MW). In the next years, many demonstrator projects as well as commercial wind farms will increase this capacity. According to [19] by 2030 the installed power of floating wind turbines will reach 11 GW. Projections from [20] and [6] show that by 2030 the biggest floating wind market will be in Europe. It is expected that the industry is currently shifting away from the demonstrator stage towards commercial scale floating wind farms. [20]

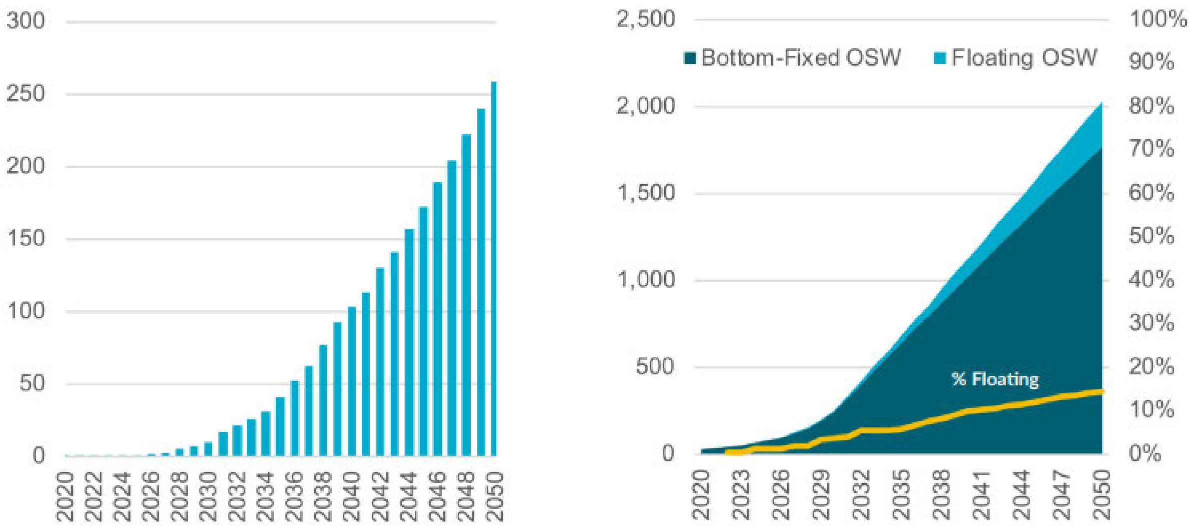

Figure 6: Left: FOWT global forecast, right: FOWT in a Net Zero Emissions by 2050 scenario [21]

2.2.1 Development of floating wind deployment

The first floating wind turbine was deployed by Blue H Engineering in December 2007. The small-scale Tension Leg Platform combined with an 80-kilowatt turbine was located in the Adriatic Sea, 22 km off the coast of Apulia in 113 meters deep water. [8], [22]

Two years later in September 2009 the oil and gas company Equinor installed the first multimegawatt floating wind turbine in the North Sea in Norway. The 2,3 MW turbine from supplier Siemens was mounted on the 100 m deep draft spar platform. [23], [24]

The world's first commercial floating wind farm named Hywind Scotland Pilot Park was commissioned by Equinor in 2017 and has an overall capacity of 30 MW. According to Equinor, the floating wind farm achieves a cost reduction up to 70% compared to the Hywind Demo project in Norway. Each of the five spar-type substructures features a 6 MW turbine which can supply combined nearly 20.000 UK homes with energy. [25]

Equinor plans to install the 95 MW floating wind farm Hywind Tampen which shall provide electricity for the Gullfaks and Snorre offshore field operations in the Norwegian North Sea in the third quarter of 2022. Each of the spar platforms is equipped with an 8,6 MW wind turbine from Siemens Gamesa. The water depth of the wind farm which is located 140 km off the coast is between 260-300 m. [26]

In 2011 the WindFloat, a semi-submersible concept of Principle Power, was deployed in the Atlantic Ocean, 5 km off the Portuguese coast. The turbine of the WindFloat 1 project which has since been decommissioned had a power of 2 MW and was delivered by Vestas. [27]

The first commercial wind farm of Principle Power, the WindFloat Atlantic, is operating 20 km offshore from Viana do Castelo in Portugal since 2019. In total, the three 8.4 MW turbines from Vestas have a combined capacity of 25 MW. [27]

2 years later in 2021 Principle Power delivered five of their semi-submersibles for the Kincardine Offshore Wind Farm. 15km off the coast of Aberdeen each of the WindFloat units hosts a 9,5 MW turbine from Vestas. [27]

The 1:6 model of the spar type foundation called SWAY were tested in real-life conditions off the coast of Bergen in June 2011. The innovative downwind configuration floater is moored with a single tendon which shall reduce the costs for the mooring system. Due to harsh wave conditions in November 2011 water could enter the platform through the j-tube for the cable connection and forced it to sink. [8], [28]

In June 2013, the University of Maine deployed the first grid-connected offshore wind turbine in the USA. The semi-submersible is a 20 kW 1:8 scale model of the VolturnUS and operated for 18 months off the coast of Castine.

New England Aqua Ventus I is an 11 MW floating offshore wind pilot project which will test the full-scale concrete foundation VolturnUS in the next years. [29], [30] The Fukushima floating offshore wind farm demonstration project (FORWARD), consisting of three floating wind turbines and a floating substation, were deployed between 2013 and 2016 approximately 23 km off the town of Naraha (coast of Fukushima).

In the fourth quarter of 2013, the 2 MW compact semi-submersible floating wind turbine Fukushima Mirai was the first platform that was installed.

The 7 MW v-shaped semi-submersible Fukushima Shinpuu arrived in July 2015 its testing area. One year later June 2016 the Fukushima Hamakze was deployed. The 5 MW advanced spar type floating wind turbine has a comparatively small draft of 33 m and is moored with six catenary steel chain mooring lines. [31], [32], [33]

In October 2013 Toda Corporation installed a 2 MW hybrid spar floating wind turbine Sakiyama 5 km off the coast of Kabashima Goto in Japan. The lower part of the foundation is made from concrete while the upper part consists of steel segments. [34], [35]

In 2018 BW Ideol deployed within the Floatgen project the first demonstrator barge foundation off the coast of Le Croisic. The concrete support structure called Damping Pool which is equipped with a 2 MW turbine is moored with six synthetic fiber (nylon) mooring lines in 33 meters of water depth. [36]

Within the Hibiki project a steel variant of Ideols Damping Pool was commissioned off the coast of Japan in the same year (2018). The Barge foundation floats in a 55 meters deep water and features a 3 MW turbine. [37]

In 2020 Saitec Offshore Technologies deployed the BlueSATH in Spain - their first 1:6 scale prototype of a 10 MW wind turbine. The hull of the self-aligning barge platform is made of steel and concrete and is located off the coast of Santander. 2022 the 2 MW first full-scale prototype of Saitec will be tested in BiMEP, an open-sea test site in the Basque Country. [38]

Stiesdals TetraSpar is a tetrahedral floating platform which is being tested since July 2021 at the Marine Energy Test Centre, 10 kilometers off Karmøy in Norway. A keel is attached to the 3,6 MW spar type foundation with leads to a more efficient installation process compared to a conventional spar (see Section 2.2.2 and 3.2.4) [39]

The energy provider China Three Gorges installed the semi-submersible by Wison Offshore & Marine at their 400 MW wind farm off the coast of Yangjiang City in Guangdong Province. The substructure supports a 5,5 MW MingYang wind turbine and the system was commissioned in December 2021. The steel floater is moored in a 30 m deep water and shall test the role of floating wind turbines in shallow waters. [40]

2.2.2 Review of floating wind concepts in the market

At the time of this work, 52 different support structure concepts for floating wind turbines can be identified in the market. However, it is assumed that more designs are under development that are not captured by the market here. As this thesis focuses only on single rotor FOWT floater concepts for multi-rotor turbines are not included in this market overview.

The concept breakdown in Figure 7 presents the commercial concept share by typology. Since it is not clearly identifiable, some of the concepts presented here may no longer be followed by some manufacturers. However, the concept breakdown shows that concepts for all four floater typologies are represented in the market, yet the semi-submersible makes up the largest share with about 58 %. According to [4] the main reason for the large share is its flexibility in terms of site selection combined with the lower infrastructural requirements for installation. With a share of 9%, the spar has the second highest number of concepts. Although no commercial wind farm uses a TLP to date, this platform typology has the third largest share when mixture concepts (TLP&semi-Sub and Spar&Semi-sub) are left aside. The barge concept is currently represented on the market with the fewest concepts among all other floater typologies.

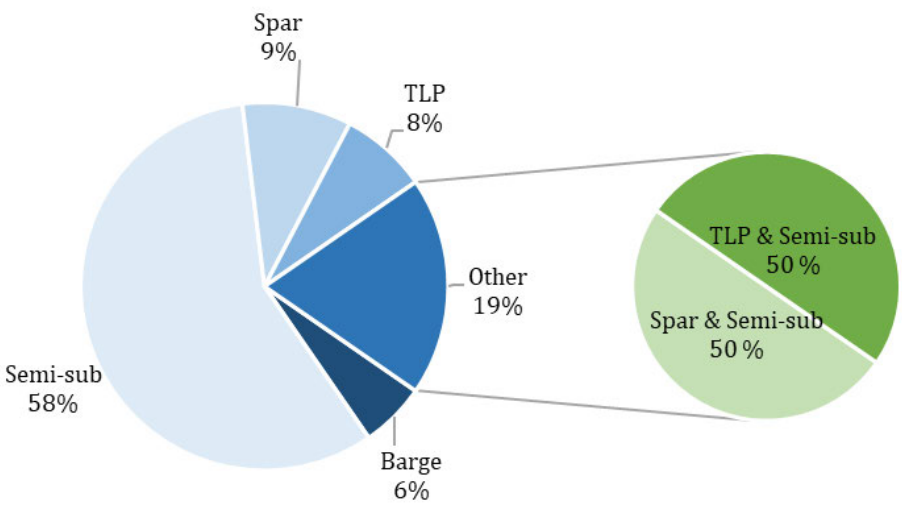

Figure 7: Concept share by floating foundation typology [author's illustration]

Mixture concepts combine characteristics of two floater typologies to exploit the advantages while eliminating the disadvantages of each concept. Those designs do not necessarily combine two different types of stabilization, but the combination rather refer to aspects related to the manufacturing, installation and maintenance methodologies. An example of a spar buoy-semi-submersible-mixture concept is the TetraSpar of the Danish company Stiesdal (see Figure 8) which is already mentioned in Section 2.2.1. Although this floater makes use of the ballast stabilizing principle the FOWT can be fully assembled in port. Due to the usually large draft of ballast stabilized floaters spar buoys require a sufficient water depth for mounting the turbine and tower onto the substructure. This in-port assembly of the TetraSpar is possible due to the flexible ballast keel, which is attached to the floater near the water surface in the harbor and can be lowered in deeper waters [41]. Some companies also combine the TLP structure with a semi-submersible foundation. An example is the Gazelle Windpower concept which combines a low weight platform (50 % weight reduction compared to a semi-submersible) with an 80% tension reduction in the tendons. [42], [43] About every fifth concept is a mixture of two or more concepts. The share of mix concepts is divided equally between the TLP & Semi-sub mixture and the Spar & Semi-sub mixture.

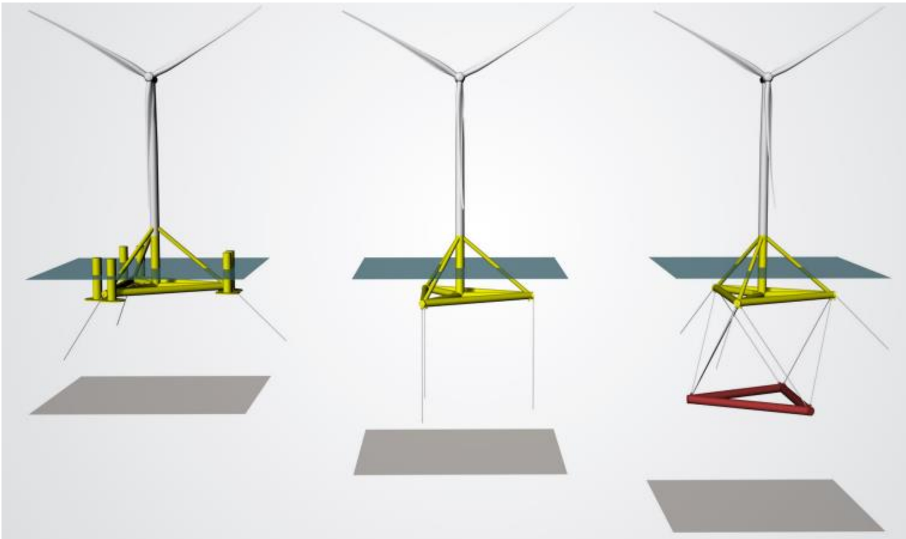

Figure 8: Floater concepts from Stiesdal – from left to right: TetraSub, TetraTLP and TetraSpar [41]

A self-aligning wind turbine can align itself with the wind direction. These concepts are based on a passive wind tracking and a turret anchoring system which allows the platform to rotate around the vertical axis of its mooring connection. Usually, the rotor provides the necessary forces to align the system with the wind. Some systems also have an aerodynamically shaped tower which generates a self-aligning yaw moment due to its horizontal lift forces. [44] Depending on the individual concept, self-aligning systems are based on one of the main floater typologies (refer to Section 2.1.1). The distribution of self-aligning concepts among the main typologies and their mixture is illustrated in Figure 9. Eight floaters or nearly 15 % of all concepts identified in the market are self-aligning floating platforms. More than the half of those concepts are semi-submersibles. The barge, spar buoy and mixture between TLP and semi-submersible have each one provider of a self-aligning floating design.

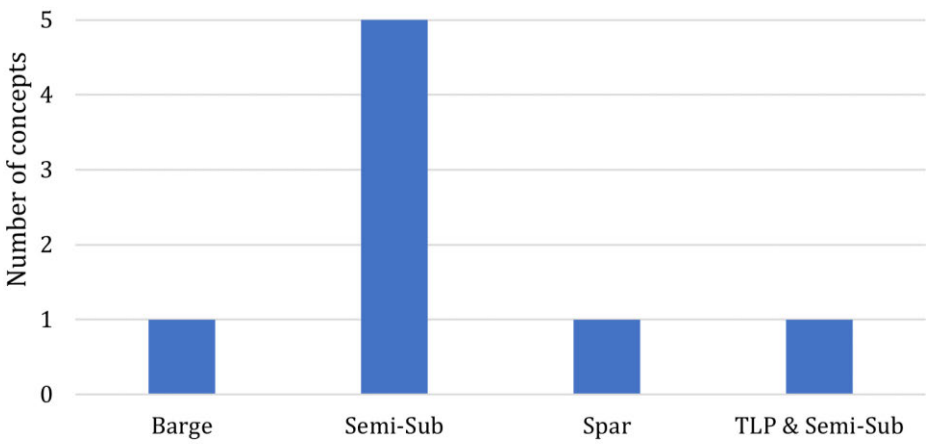

Figure 9: Number of mix concepts by floater typology [author's illustration]

In Figure 10 operating, under construction, upcoming and decommissioned FOWT capacity by typology is illustrated. All data are based on the market overview of [20]. Again, in this comparison only single turbine concepts are included. Next to that, the project Blyth - phase 2 is not included in the figure since it is not clear at the moment of this study which floater typology will be selected. [45] The biggest share of installed capacity among all other concepts has the semi-submersible with nearly 80 MW. This is mainly because of the floating wind projects from PrinciplePower which are mentioned in Section 2.2.1. The 88 MW wind farm Hywind Tampen is responsible for the fact that the spar buoy has the largest capacity which is currently under construction. Looking at the upcoming projects, the semi-submersible again has the highest capacity among the other floater typologies. The largest upcoming projects in terms of capacity are the Erebus wind farm with a planned installed power of about 96 MW (first power in 2028) and the floating wind farm Groix & Belle-Île in France which is going to have a capacity of 28,5 MW (first power in 2024). [20]

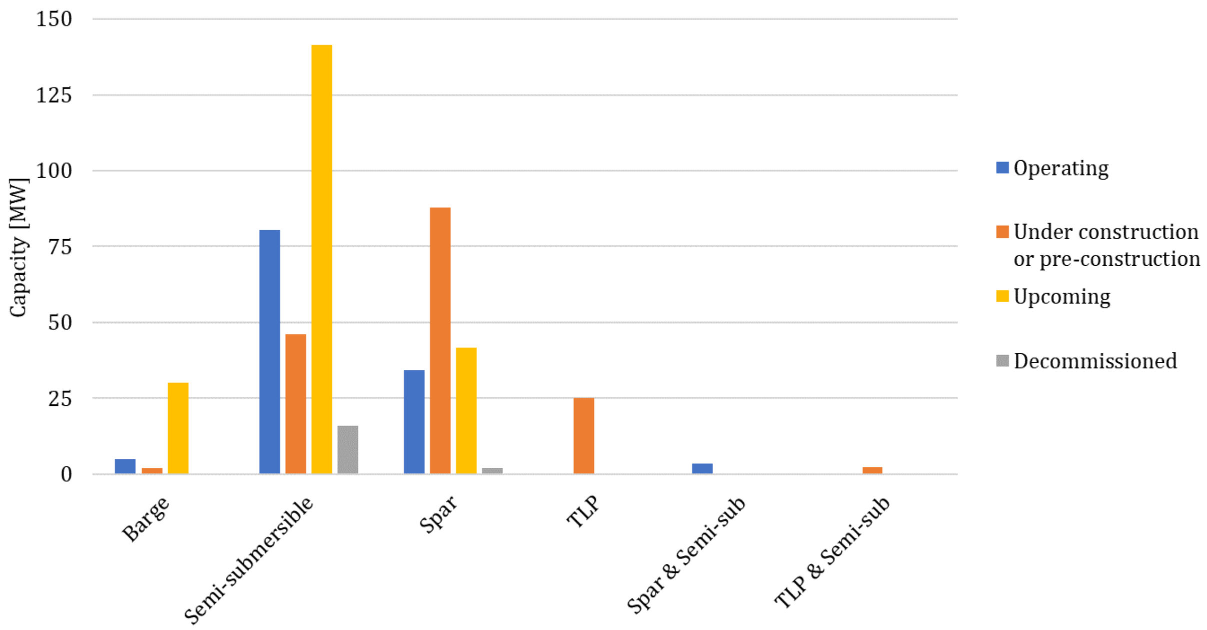

Figure 10: FOWT capacity by typology (values from [20], [author's illustration])

The following sections are intended to provide a more detailed overview of the designs of the various floaters. For this purpose, some concepts shall be described in more detail representative for each typology. All statements were taken from the respective manufacturer and could not be verified by an independent authority.

Barge

The single point mooring platform SATH by Saitec is built on two horizontal cylindric concrete elements which provide the necessary buoyancy. The frame structure which connects the cylinders has a large heave plate mounted on the bottom of the floater(see Figure 11). According to Saitec, their plug & play system leads to an easy installation enabling a quick connection and disconnection of the mooring lines and the power cable. [46]

Another barge concept is the Damping Pool developed by Ideol which uses entrapped water inside in its central opening to minimize floater motions. The tower is placed on an outer side of the substructure. The platform offers the possibility of using steel or concrete as primary hull material and thus increasing the material selection flexibility. Concrete as primary hull material reduces susceptibility to steel price fluctuations and also enables mass production with on-site construction and high local content. [4], [36], [37]

Figure 11: Barges (from left to right): Sath from Saitec, Damping Pool from Ideol [46], [4]

Semi-submersible

The OO-Star concept by Olav Olsen consists of a tri-star shaped pontoon which supporting three buoyancy cylinders as well as one central shaft which connects the substructure with the tower end. The substructure can be made of concrete, steel or a combination out of both materials allowing a material selection according to optimal design and cost fabrication facilities. According to Olav Olsen the fabrication of the floater can take place in a dock, on a barge or on a quay and is well suited for a modular fabrication. Heave plates are connected to the lower end of the pontoons which increase the damping. Next to that the low draft substructure is equipped with a passive ballast system. [47]

The columns of the updated three-legged substructure called VolturnUS are connected at the bottom by rectangular pontoons and at the top with cylindrical struts. The turbine is mounted on the center column of the semi-submersible. According to [29] a concrete version of the VolturnUS gives several benefits over one made out of steel. Industrialized pre-cast bridge construction techniques can be applied for its fabrication resulting in lower total costs per ton. Next to that the hull of this structure is heavier than an equivalent steel floater which leads to a greater distance between the center of gravity and center of buoyancy resulting in good wave motion resistance. To reduce the complexity, this system does not feature an active ballast system, heave plates or hanging masses. The rectangular shape of the bottom beams add more wave motion resistance than cylindrical Sections according to [29].


Figure 12: Concrete semi-submersibles (from left to right): OO-Star from Olav Olsen, VolturnUS from UMaine [48], [49]

The triangular steel structure WindFLoat designed by Principle Power consists of three outer columns whereby the wind turbine is placed off-centric on one of those. Heave plates fitted at the bottom of each column add hydrodynamic mass to the system enabling the platform to stay light while performing like a heavier structure. A “smart hull trim system” which moves water from column to column is able to compensate changes in wind conditions to keep the towers mean pitch at a constant angle. Since the structure is built from only three subcomponent modules (columns, truss elements, damping plates) the structure enables a separately performed manufacturing for the components by several companies. The off-centric tower placement leads to the fact that the structure can be positioned adjacent to the quay which minimizes the crane outreach requirements. [50]

One of Stiesdal’s three floater concepts is the TetraSub. The turbine is placed off centric on a central column of the platform. At each of the three corners two vertical columns are attached, which are equipped with heave plates at their lower end. According to Stiesdal their semi-submersible can be deployed in waters deeper than 60 meters. The unballasted draft of the structure is around 8 to 10 meters allowing a shallow water launch. Stiesdals three concepts combine advantages to accelerate the cost reduction of floating wind power: low cost production, fast assembly and easy installation of turbine on foundation using onshore cranes. [51]

Mitsui Engineering & Shipbuilding designed and installed the 2 MW downwind semi-submersible called Mirai (also compact semi-submersible) within the Fukushima FORWARD Project. The structure consists of four columns -one center column supporting the wind turbine and three outer columns providing stability. The structure is reinforced with diagonal struts that run between the inner and outer columns. [52]

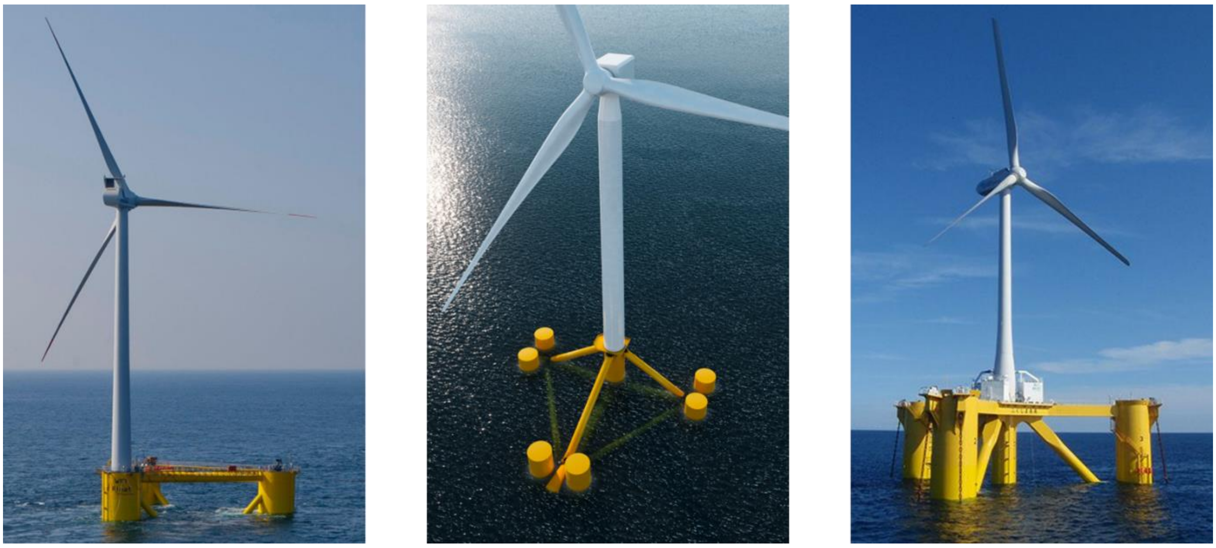

Figure 13: Triangular semi-submersibles (from left to right): WindFloat from Principle Power, TetraSub from Stiesdal, Mirai from Mitsui Engineering & Shipbuilding Co., Ltd. (MES) [53], [41], [54]

Two examples for lightweight steel semi-submersibles can be seen in Figure 14.

The wing modules of the tri-star shaped MOLO by Clovers AS are connected to the center column through upper and lower flanges providing a simple and lightweight connection. The stability is achieved by the total of seven columns, two of which are attached to each of the wings. The higher number of outer columns on each wing shall reduce their diameter which makes them suitable for automatic manufacturing. On the bottom of the structure flat regular stiffened panels are used to add hydrodynamic mass. In addition, the MOLO is using flat panels on the lower end of the substructure instead pontoons to reduce the manufacturing effort by enabling a fabrication with automated production facilities. [55]

The three outer columns of the steel semi-submersible OCG-Wind by Ocergy are connected to the central one at the lower and upper ends by horizontal cylindric elements. Each arm is reinforced with two diagonal struts which run between the two horizontal cylindrical beams. According to Ocergy their foundation weights under 200 ton per megawatt and thus minimizing CAPEX, CO2 footprint and its exposure to steel market variations. The low draft of under ten meters makes it compatible with most local port infrastructures. The four sub-assemblies of the modular substructure can be produced from most shipyards and wind tower manufacturers. [56]

Figure 14:Lightweight semi-submersibles (from left to right): Molo from Clovers, OCG-Wind from Ocergy [55], [56]

Two examples of square support structures can be seen in Figure 13.

Each of the four outer column of the XCF by Mareal is connected at the lower end with the central column as well as to their respective two neighbor columns. According to Mareal the regular grade concrete and the simple modular structure of the floater allows a universally available and manufacturable solution. The two axes symmetry of the four columns increasing its stability and making it suitable for cyclonic and multi-directional wind sites. Next to that a concrete platform minimizes the painting and corrosion protection of the hull. [57]

Nautlius is developed by Nautilus Floating Solutions, S.L. a technological and industrial consortium consisting of Subsea 7 and Vicinay Marine Innovación. The lower pontoons each connect the neighboring columns, while upper the struts converge in the center and thus providing a central deck for the wind turbine tower. According to Nautilus Floating Solutions a low-cost manufacturing is achieved through compact structure dimensions, modular steel construction without tubular joints and pontoon and deck enabling common shipbuilding structural solutions. [58]

Figure 15: Square semi-submersibles (from left to right): XCF from Mareal, Nautilus from Nautilus Floating Solutions [57], [58]

Spar buoy

The monolithic spar buoy Windcrete is built in a continuous piece, including both the tower and the substructure. The concrete foundation is manufactured horizontally using a slipform in a dry dock. A unique differentiator of this concept compared to other spar buoys is its installation process. The structure (substructure and tower) can be towed out horizontal by simple tug boats. After the erection of the platform 90% of the floater can be submerged, allowing a turbine installation in 20 meters height above mean sea level. This offers the possibility of using a smaller catamaran ship (or similar vessel) and thus reducing costs for cost intensive heavy lifting floating cranes. [59]

The Stinger Keel developed by Floating Energy systems (FES)is a hybrid platform using a truss spar to separate the ballast tanks from the upper buoyancy units. According to FES due to its tubular based components allowing for steel rolling mills the floater is suitably for a modular assembly which can maximize the production. The stinger (ballast arm) of the structure can be tilted to a horizontal position in port reducing the draught and thus allowing a shallow water assembly and transport. [60]

The already mentioned TetraSpar by Stiesdal is a tetrahedral structure which can be assembled from tubular steel components. As mentioned the foundation and keel can be assembled without the need of welding in port. The keel, which is attached to the foundation with ropes, allows a port side integration of the turbine and a simple transit to the wind farm. [39]

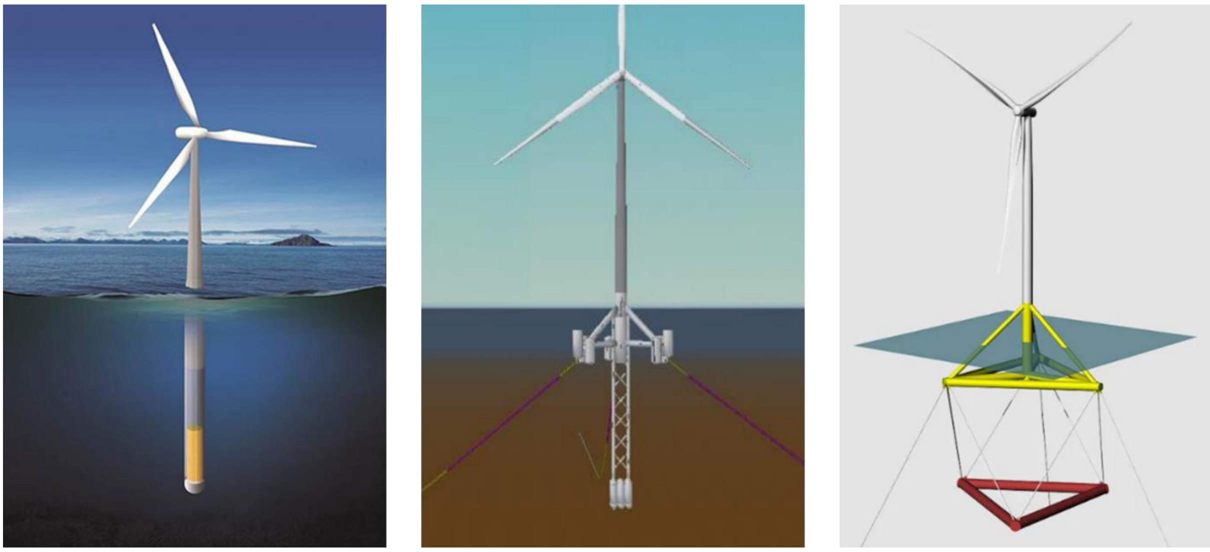

Figure 16: Spar buoys (from left to right): Windcrete from WindCrete, Stingerkeel from Floating Energy Systems, TetraSpar from Stiesdal [61], [60], [41]

TLP

The Float4Wind by SBM is their second generation of floater concept based on the TLP technology. The simple design with less components enables automated welding and a fast assembly time. In order to reduce the risk of losing a tendon, the floater is moored with redundant mooring lines. A special feature are the inclined tendon legs with reduce the nacelle motion. [62]

Marine Power Systems designed the PelaFlex, a tetrahedral substructure with only four distinct parts allowing a fast assembly at yard. According to Marine Power Systems its steel lightweight substructure achieves a weight of under 200 tons per megawatt. The response characteristics resulting in zero tilt maximizing the energy yield and reducing the wind turbine controller modifications Next to that the low accelerations can reduce the turbine wear and tear. The shallow draft and its towing stability lead to an easy assembly and installation of system. [63]

According to Glosten their design of the star-shaped structure Pelastar combines minimal motion with minimal steel weight and a complete quayside assembly. The concept enables a port side assembly of the turbine and can be towed out with a specialized support barge with makes heavy lift crane obsolete. [64], [65]

Figure 17: TLP concepts (from left to right): Float4Wind from SBM, PelaFlex from Marine Power Systems, PelaStar from Glosten [62], [63], [64]

The concept Gicon-SOF combines advantages of a TLP with those of a semi-submersible while eliminating the respective disadvantages of both designs. The lowerable gravity anchor acts as a barge during transit to provide stability whereby the structure can be towed out using simple tug boats. The tendons are pre attached on the bottom of the floater and the anchor. At site the gravity anchor is be lowered by ballasting which simplifies the mooring system installation at the wind farm. After installation, the response characteristics of the SOF are those of a conventional TLP. [66]

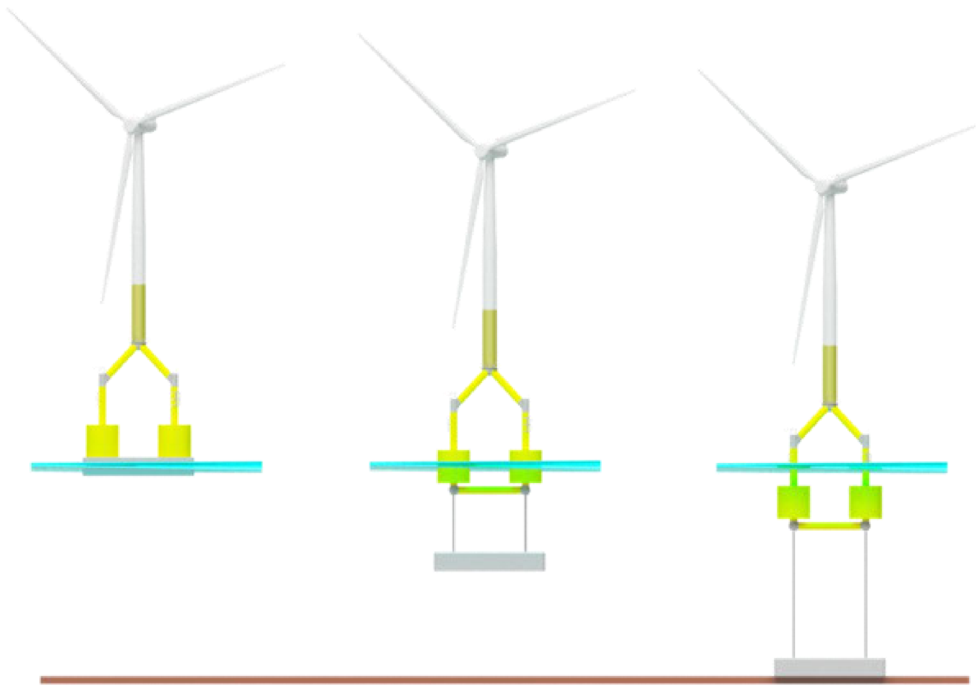

Figure 18: Transit and installation of TLP concept Gicon-SOF from Gicon [66]

Self-aligning platform

The platform X1 Wind is a combination of a semi-submersible and a TLP resulting in a lightweight structure which can be easily installed due to its free-floating stability. The turbine is supported by a pyramidal tower, allowing the platform to be as light as a TLP or a fixed foundation. Due to the fact that downwind-configurations do not need tilt angles, rotor coning or the use of pre-bent blades is not necessary so that manufacturing costs can be reduced. [67]

Each of the four corners of Eolink's semi-submersible supports a mast of the pyramidical tower. According to Eolink the weight of turbine is distributed evenly among those four tower masts. Next to that Eolink claims that their multi mast system is 40% lighter compared to a single mast solution which leads to a reduction of the LCOE of about 10%. The lightweight structure achieves a total mass of 200 tons per MW. Since the blades rotate around an axis between the front and rear tower elements the distance between the blades and tower is increased. This allows the blade to be more flexible without risking a collision with the tower. Next to that due to the tower mass savings the blades can be lengthened. [68]

The platform of Nezzy from Aerodyn engineering is based on pre-stressed concrete elements supporting a load optimized and profiled tower. The central tower element is stabilized by preloaded steel ropes which are attached at the three corners of the platform. For self-alignment the RNA is designed as a two-bladed downwind rotor configuration. [69]

Figure 19: Self-aligning concepts (from left to right): X1 Wind from X1 Wind, Eolink from Eolink, Nezzy from Aerodyn [70], [68], , [69]

2.3 Potential of two-bladed wind turbine for floating wind

In the last decades, three-bladed wind turbines dominated the offshore wind market. The expanding FOWT market can offer new possibilities for a comeback of two-bladed wind turbines. To date, there has been little research work on the potential of two-bladed systems in the area of floating wind. However, the market research has revealed that some companies are currently already using or planning to use two-blade systems for their substructure concept. An example is the company Aerodyn which is already mentioned in Section 2.2.2. Their self-aligning system can be equipped with either one or two downwind turbines. According to [69] two blades can reduce the top mass of the RNA since the rotor mass is 25 % lower compared to a three-bladed turbine and thus reducing the investment and energy production costs. [71] Another company which is focusing on two-bladed floating wind turbines is Seawind [72]. According to [72] their twin-bladed turbine technology that is mounted on a concrete semi-submersible can operate at higher wind speeds than conventional wind turbines.

Furthermore, 2B turbines can potentially expand the field of application and offer a deployment in regions with typhoons. This is possible due to their comparatively small wind attack surface when the rotor is parked in a vertical position. [69], [71]

As a result of the more complex dynamic-cyclic loads acting on a two-bladed wind turbine compared to a 3B turbine, such systems are often equipped with a teetering hinge. It allows the more heavily loaded rotor blade to swing backwards and thus decrease the resulting moment acting on the rotor that is passed to the wind turbine. [73] The combination of a light and flexible rotor translates into further material savings for the gearbox, tower, and foundation. [74] Next to that, the additional rotor flexibility around its horizontal axis can reduce the impact of the pitch movements of the substructure. [75]

In [76] a code-to-code comparison is carried out for a modified version of the VolturnUS floater with the IEA 15MW wind turbine. It is investigated that the first natural tower frequency is lower compared to the results in the NREL study [77]. As a result, the tower stiffness and thus its mass had to be increased around 20% to avoid resonance frequencies between the 3P rotor frequency and the first natural frequency of the tower. As two-bladed wind turbines offer greater rotor frequency flexibility [77], the tower stiffness could be reduced which can lead to a mass reduction of the tower.

Moreover, two-bladed wind turbines also open up cost-saving potentials in other life cycle phases. While three-bladed rotors must be assembled on site, two-bladed rotors can be transported pre-installed to the wind farm. [78] The assembled rotor package fits better on ships and its low mass can be lifted more easily onto the tower. Therefore, especially for floating wind structures that are installed with floating cane vessels at the wind farm, two bladed-wind turbines can help to reduce installation costs. The lower number of blades can also positively favor the maintenance effort which can lower the expenses for the O&M compared to 3B turbines. [71]

3 Costs of a floating wind turbine

In Section 3.1 the costs occurring during the different life cycle phases of a FOWT are presented. In a first step, the lifecycle phases are outlined and LCOE are introduced. Afterwards, the lifecycle costs of a floating wind turbine are presented and compared to those of a bottom-fixed wind turbine. In the Section 3.2, the most important life cycle costs that are affected by the floater typology and its individual design are conducted. Furthermore, parameters are examined that influence the expenditures in the different life cycle cost categories.

3.1 Life cycle costs

One possibility to summarize the life cycle phases of an offshore wind turbine can be seen in Figure 20.

Figure 20: Life cycle phases of an offshore wind turbine [author's illustration based on [79]]

An overview of the contents of the various life cycle phases is shown below:

1. Development	Planning of the wind farm.
2. Fabrication	Procurement and manufacturing of the materials, parts, components, e.g., nacelle, blades, tower, floater, mooring system.
3. Installation	Construction of the plant until its commissioning e.g., transport from port to wind farm, mounting of tower and RNA on foundation, erection of the foundation, power cable connection.
4. Operations and maintenance (O&M)	Ensures the operation of the wind turbine and wind farm e.g., inspection of parts and components, repairs.
5. Decommissioning	Removal of the wind farm and recycling of the components.

The LCOE is defined as the total costs invested for construction and operation per unit over an assumed lifetime and compares this with the amount of energy produced. [80]. This offers the possibility to compare costs of different methods of electricity generation (e.g., wind, solar, gas etc.). The first input parameter for the calculation of the LCOE are the capital expenditures which include all investment costs before the commercial operation of the power plant. The second input parameter are the operational expenditures (OPEX), and it includes all costs incurred during the operation of the plant. The costs associated with decommissioning and site area clearance are described with the decommissioning expenditures (DECEX). The total costs generated during the life cycle of a power plant are set in relation to the energy produced – the average annual energy production (AEP): [81], [82], [83]

$$LCOE = \frac{CAPEX + OPEX + DECEX}{AEP} \tag{1}$$

A reduction of LCOE can be achieved due to reduced costs (advanced technology for manufacturing, installation, or operations phase), an increased energy production (more effective technology or reducing energy loss) or an expansion of the lifetime of the project. In the recent decades, a sustained trend of cost reduction has been achieved for bottom-fixed wind turbines. The matured supply chain with larger volumes increased the investment in design, manufacturing, and installation tools suited for a volume production. Furthermore, the strengthened cross-disciplinary collaboration has contributed to an evolution of the supply chain. Another cost reduction potential offers an increasing turbine size. In the last 20 years, the turbine capacity has increased from 2MW to 10 MW. Although a lot of cost reductions could be achieved the LCOE can still vary for different projects. A key driver for this variation is the site conditions (waves and current, wind, water depth, soil condition) of a wind farm. Extreme environmental conditions can for example drive design changes that can add costs. Furthermore, extreme wind and wave conditions can increase challenges for installation and maintenance. [82] The water depth and the soils mainly influence the costs for the foundation of an offshore wind turbine. [84], [85] The distance to shore affects the costs for the export cable as the cable length increases. Next to that a longer distance to the port leads to higher installation times resulting in additional costs. Maintenance strategies for wind turbines can change due to longer times for access. Furthermore, installation vessel day rates can have a significant impact on the LCOE of an offshore wind turbine. [82]

Figure 21 shows the cost ratio between CAPEX, OPEX, and DECEX for a floating wind turbine. The costs are based on [83] in which the costs for the VolturnUS are investigated. With about two third of the total expenditures, the biggest cost share is associated with the CAPEX of the FOWT. The largest cost components are the expenditures for turbine, foundation, electrical infrastructure, and the wind farm installation. Approximately one third of the total costs arising from the OPEX, which includes the costs for the operations and the maintenance of the floating wind turbine. Usually, the DECEX have a relatively small influence on the LCOE and sums up to 1-3 % of the total costs.

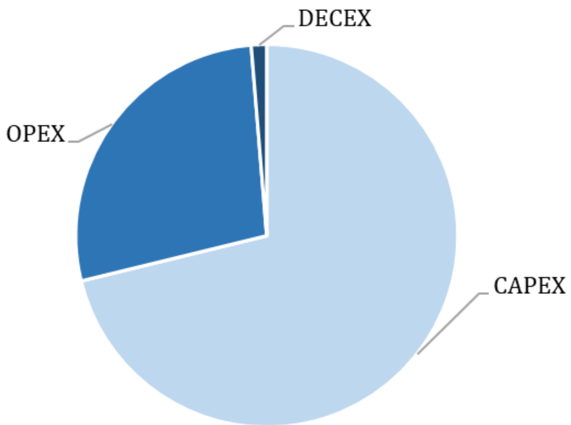

Figure 21: Cost ratio - CAPEX, OPEX and DECEX [author's illustration, data based on [83]]

Since very few floating wind farms are in operation, there is little collected data on the LCOE of floating wind farms to date. As a consequence, the cost estimations have a high uncertainty of what must be taken into account when interpreting results of cost studies for FOWTs. [11]

Currently, floating wind turbines tend to be more cost-intensive than bottom fixed wind turbines. The main reason for this is primarily the high cost of the foundation of the FOWT, which includes the floater and the mooring system. However, to reach achieve cost competitiveness against bottom-fixed offshore wind turbines, cost reduction must be achieved across the full project lifecycle. [4], [11] In terms of CAPEX reduction, the manufacturing of the structures must be automated using standard parts which can easily be assembled. Next to that dedicated vessels with high charter rates should be avoided. One possibility to lower the OPEX is to reduce the fatigue damage to the system to improve its reliability. Simplifying the maintenance operations is also an important aspect to lower the OPEX. The energy production can be increased with better control strategies for floating wind turbines and bigger turbine sizes. [11]

Besides cost reduction aspects in terms of the life cycle phases an important factor to enable further cost reductions offers the economies of scale. Higher and more consistent FOWT deployment rates as well as improving the capability and efficiency of the supply chain would lead to cost savings. [5]

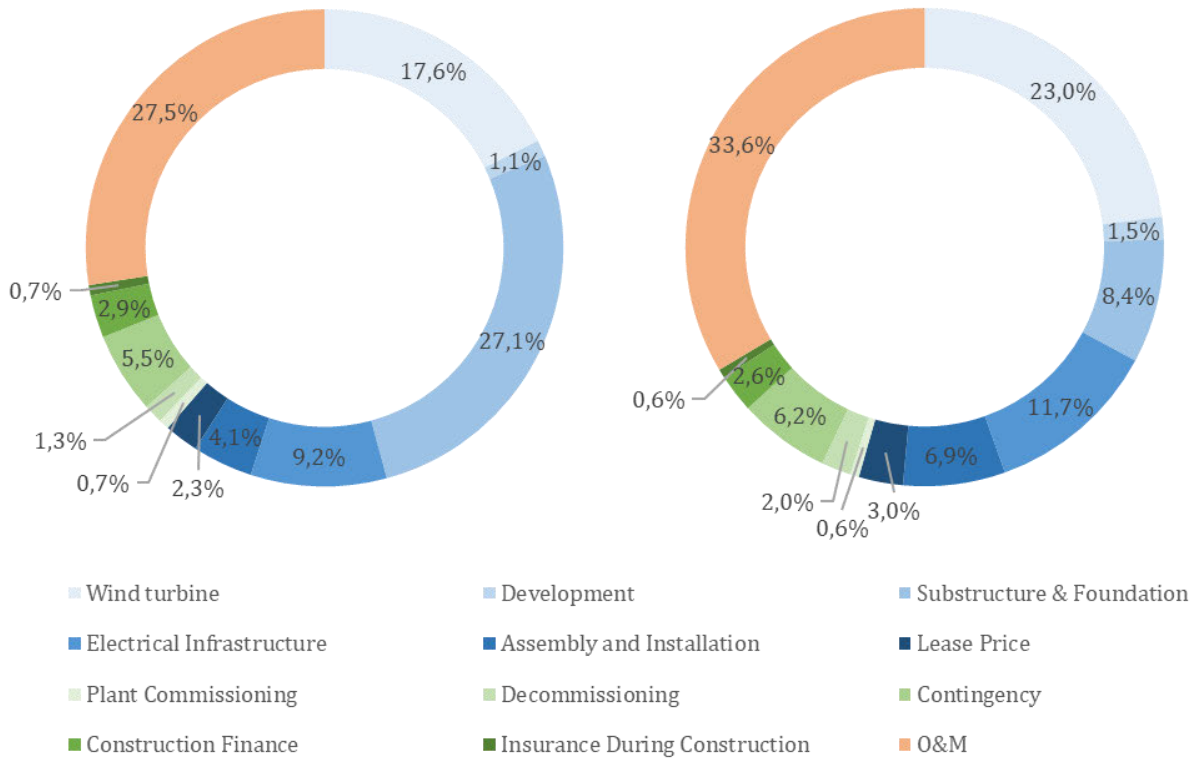

Figure 22: Cost comparison floating vs. bottom-fixed wind turbine [author's illustration, data based on [83]

3.2 Life cycle costs affected by the floater typology

In Figure 23 an overview of the most important cost categories of a floating wind farm are illustrated more in detail. The capital expenditures can be categorized into turbine, floater electrical infrastructure and installation expenses. The costs of the wind turbine can be divided further into the costs for the nacelle, the rotor and the tower. The expenses for the mooring system and the floater sum up to the total costs for the substructure and foundation. The electrical infrastructure includes the expenses for the cables (inner array cables and export cable) and for the substation (offshore and onshore). During installation there are costs for the turbine, floater, mooring system and substructure and electrical infrastructure. The operational expenditures sum up from the costs of operation and maintenance. Since the DECEX have a small influence on the overall lifetime costs (see Figure 21) they are not included in this figure.

The cost parameters highlighted in light blue (floater, tower, mooring system, installation of turbine, floater and mooring system and O&M) are presented in more detail in the following sections. Since this work is concerned with the comparison between concepts and the differences between those, only the costs that are influenced by the typology and design are described in the following. Furthermore, those parameters that are responsible for the cost differences between the floater typologies and designs are pointed out. These cost categories including its cost influencing parameters were selected based on studies that focuses on the calculation of life cycle costs for different floater typologies. Cost differences may also occur in other categories, but since their influence is estimated to be small and there is no study basis for this, they are not included in this thesis.

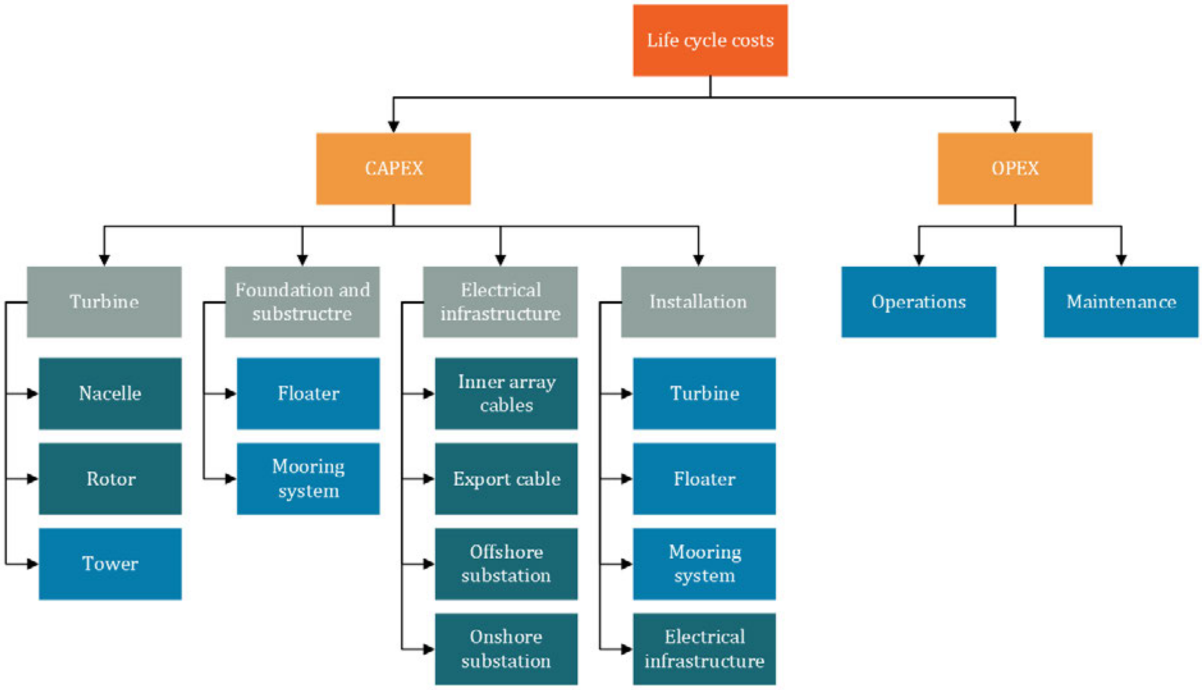

Figure 23: Overview life cycle costs [author's illustration, data based on [81] and [86]]

3.2.1 Floater

As mentioned in Figure 22 the costs of a floating support structure is a key driver for the LCOE of a FOWT. In Figure 24 the most important parameters which influence the expenses for procurement and manufacturing of a floater are summarized.

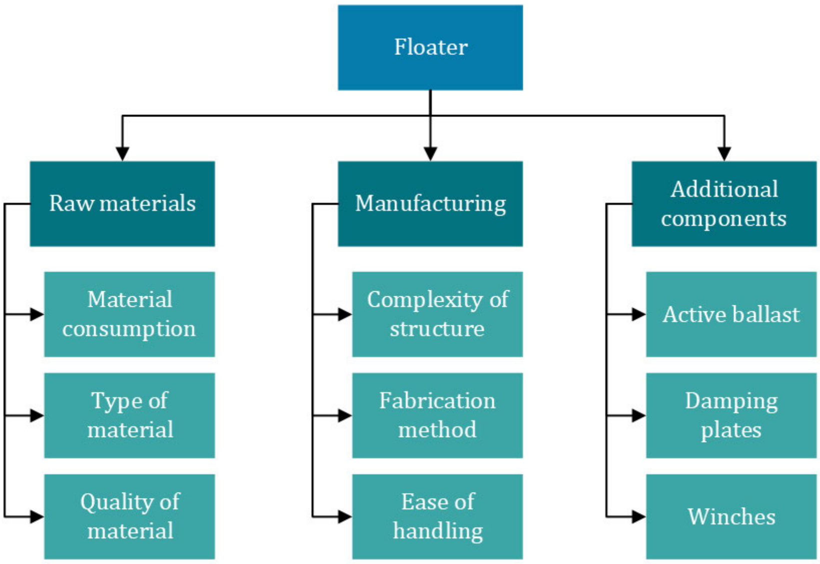

Figure 24: Parameters influencing the costs of the floater [author's illustration]

Raw materials

The overall costs for the floater materials rely to a high amount on its the required material consumption. [4] Therefore in Table 4 floater masses by typology are shown. Comparing the pre-ballasted weight of the spar buoy, the semi-submersible, and the TLP, it can be seen that the TLP is the lightest platform among all others. When comparing the more mature concepts the spar (~1750 tons) and the semi-submersible (~1900 tons) are nearly equal in weight and have about twice the mass of the TLP. [4] No data for the hull mass of the barge are given in [4]. However, since this platform realizes its stability by means of a continuous waterplane area, it can be assumed that the barge has the highest hull mass among all other concepts. [1] Looking at the structure weights after ballasting, these mass differences between the concepts change slightly. The weight of the TLP stays the same because of its stabilization principle which usually does not require a ballast. In contrast to this the weight of the semi-submersible triples after ballasting. As discussed in Section 2.1.1 the spar buoy remains its stability with the help of its heavy ballast at the lower platform. This is the reason why the weight of the structure is significantly increased after ballasting. [4]

Table 4: Ballasted and unballasted platform masses by floater typology for a 6 MW turbine (data based on [4])

Ballast status	Semi-submersible [ton]	Spar buoy [ton]	TLP [ton]
Unballasted	1918	1404	1039
Ballasted	6011	8311	1055

It should be noted, however, that the masses of the floater typologies are also influenced to a large extent by the respective design. Therefore, the values in Table 4 are only a mass indication and are not universallly valid. Further floater masses from other studies can be seen in Appendix B.

The unit price of material is dependent on the material quality. [4] In [4] unit prices for different steel grades of floaters are presented. It is mentioned that the TLP structure tends to require higher steel grades compared to the semi-submersible and the spar buoy. The increased grade of the steel is one reason why the unit price for the steel of the TLP is higher than that for the semi-sub and the spar buoy.

Furthermore, the type of material can impact the unit price of a material. In [87] a steel and a concrete variant of Ideol's Damping Pool are compared with each other. Depending on the current market situation it is assumed that the material unit prices of steel are nearly eight times higher than those for concrete. Although the concrete structure requires nearly four times as much hull material compared to the steel variant, the investigated concrete floater is half the cost of the steel floater. It should be mentioned that these results are highly dependent on the current material prices and can vary significantly within time or between manufacturing countries. [87], [4] In [88] the results for bottom-fixed foundations show that the changes of the LCOE are much higher for steel structures than for concrete platforms due to the higher fluctuance of the steel prices. [88]

Manufacturing

Support structures for floating wind turbines have the potential to be fabricated in a similar way to shipbuilding, allowing manufacturers to leverage existing shipbuilding facilities. However, some modifications of the shipbuilding facilities must be conducted to meet all the requirements for the fabrication of floating wind turbine platforms. Especially the draft as well as the large dimensions of the floaters lead to challenges for the port facilities. To achieve cost competitiveness against bottom-fixed wind turbines the port infrastructure should enable a serial fabrication and assembly of the platforms with a sufficient length of the quayside, suitable heavy lift cranes, and a wet storage area. [84], [89] The results of an analysis in which 96 European ports were examined regarding their suitability for the production of floaters showed that only five are up to these challenges. [84] Therefore, an important factor in the way of increasing the economic efficiency of FOWTs is to design the substructure for cost-effective manufacturing and assembly (DfMA). [89] Essential parameters which should be considered for DfMA are the supply chain capabilities, port, marshalling, and assembly infrastructure as well as the required heavy lift vessels and cranes [89] Examples of assembly-friendly substructures are the TetraSpar, TetraSub, and TetraTLP by Stiesdal (see Figure 25). The main components of their floaters are connected by pin joints, allowing a no on-site manufacturing and an assembly with no welding nor painting. [41]

The manufacturing of steel floaters includes plate cutting, bending, rolling, welding, and coating. [4] According to [89] the manufacturing process of components and the assembly of the substructure shall take place in two separate locations. Specialized facilities should produce components and parts in a serial manufacturing process. These components could then be transported e.g., by sea to the port, where they would be assembled. Next to that, the separation of manufacturing and assembly at two different locations can relieve the assembly port. Another aspect which is often mentioned by providers is to use simple standard parts which can be fabricated automatically in volume productions. [55], [68], [90]

Figure 25: Substructure assembly of TetraSpar from Stiesdal [41]

Concrete platforms for floating wind turbines are manufactured differently than steel floaters. The fabrication process can rather be compared to caisson or bridge production. [89] Usually, reinforced concrete is used for the floater hull and the platform will be constructed through a slipform process where it can be formed without joints. Due to the large dimensions and the heavy weight of the (unballasted) structure a large area with a quay which has a sufficient load bearing is required. [89] Concrete structures have the potential to enable local content and reduce the CO2 emissions which occur while production. [4] [87] According to [91] concrete constructions enable a greater independence in terms of production site selection. With the help of mobile construction sites, concrete support structures have the potential to offer cost and time savings. [91]

After the platform is manufactured, it must be launched into the water. This can be done with a heavy lift crane, with a slipway, or with the help of a dry dock. Due to the low availability of heavy lift cranes, which can lift weights up to 2.000 tons, the first variant poses great challenges for the port facility. [4] Assembly on a dry dock can also be cost an intensive solution due to its limited number. [84]

Figure 26 presents platform weights and costs by typology. The spar buoy tends to be the most cost-effective concept due to its low steel grade and its simple fabrication process with well-established steel rolling techniques. Although the TLP has the lowest material consumption among all other concepts its platform cost is about the same as that of a spar buoy. The main reasons for that are the high steel grade and the complexity of the structure. Semi-submersibles tend to be the least economic concept in terms of platform costs. In addition to its high material consumption, the structural complexity is decisive for the high platform costs. [4] There are hardly any sources in the literature that compare the costs of a barge with those of other floaters. However, in [14] it is mentioned that the barge floater is relatively expensive compared to other typologies.

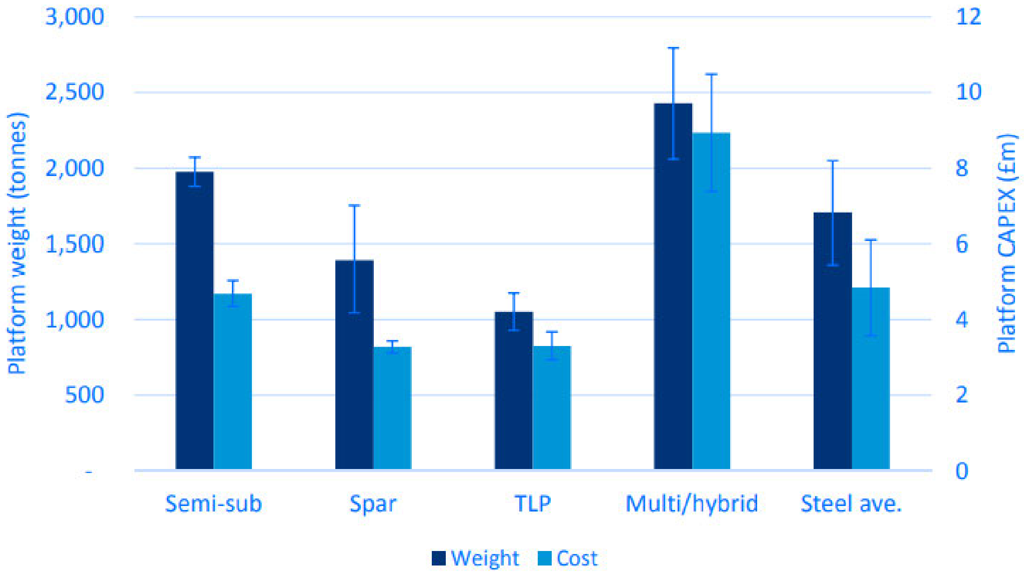

Figure 26: Platform costs by typology [4]

Additional components

Some floaters require additional components like active ballast systems, which shifts a fluid ballast between corners or columns. The main advantage of this system is to reduce the pitch angle of the turbine and thus increase the energy yield. [92] This benefit is countered by the fact that active ballast can generate additional costs. [4]

Heave Plates shall increase the hydrodynamic added mass of the floating structure and thus provide potential material savings. [8], [92] Due to its additional fabrication effort heave plates can result in a cost increase. [29] There are other systems like winches or hanging masses that can influence the costs of a support structure for floating wind turbine, but they are not discussed further here.

3.2.2 Tower

Studies that deal with the influence of the floater typology on tower costs could not be identified in the literature review. However, it is assumed that the motions (and thus loads on the tower) of the platform as well as the tower design influence its costs. This assumption is based on the comparison from [77, p. 547] which describes the cost of a wind turbine tower depending on its typology (tubular steel tower, hybrid tower, lattice tower) and its height. As the tower height increases, so does the required mass and thus the tower costs.

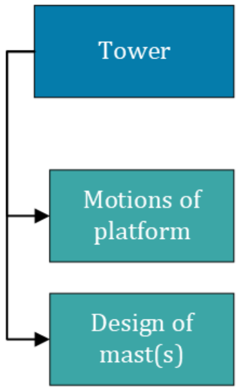

Figure 27: Parameters influencing the costs of the tower [author's illustration]

In [93] the model test campaign of the DeepCwind consortium where the motion characteristics of three floating wind systems (TLP, spar buoy, and semi-submersible) are compared is summarized. One part of the test campaign was the investigation of the tower bending moments for the investigated platform types.

Due to the large pitch angles, the spar buoy has the highest tower bending moments among all other systems. Similar to [13] the TLP has the lowest loads on the tower. The semi-submersible has slightly lower bending moments than the spar buoy. It is mentioned that the pitch motion of the systems could be reduced with some control methodologies which were not applied for this test campaign. [93]

In [13] the dynamic responses of three floating wind turbine concepts (ITI Energy barge, OC3-Hywinds Spar buoy, and MIT/NREL TLP) are investigated and compared to those of a land-based wind turbine. In Figure 28 the results of the ratios of different bending moments between sea and land wind turbines are presented. As a result, all investigated floating foundations show increased loads on the tower base compared to land-based wind turbine towers. The barge achieves by far the highest motion-induced ultimate and fatigue loads compared to the other two investigated platforms. The tower base bending moments of the OC3-Hywind spar buoy are nearly 50% higher compared to the bending moments of the TLP. However, it should be noted that the weight of the investigated barge is the lowest, whereas the TLP has the highest structural weight. According to [4] usually, the TLP is the lightest concept of the compared platform types. The reduced overall mass of the barge may have an impact on the tower loads.

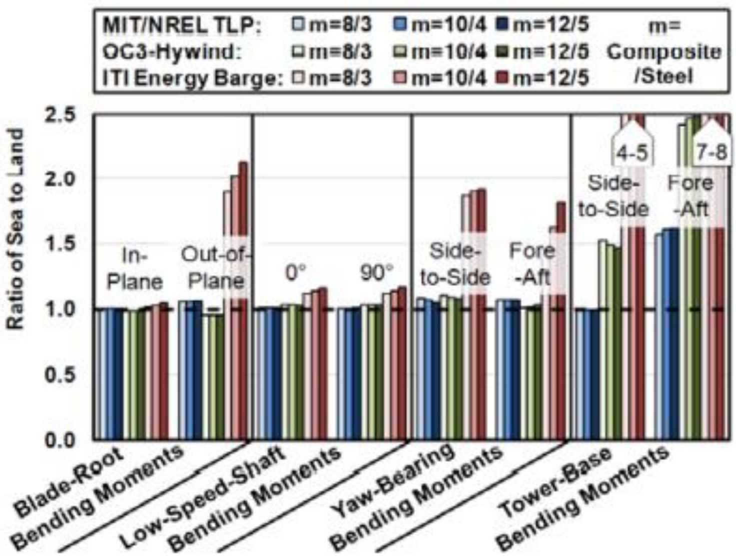

Figure 28: Sea-to-land ratios of fatigue loads for DLC 1.2 [13]

In [94] controllers for four different FOWT models are optimized as well as their influence on the dynamic responses is investigated. The results show that the tower base damage equivalent

loading (TBDEL) of the TLP is the lowest among all other concepts. In contrast to [13] and [81], the second highest loading is determined for the barge which is 10% higher compared to the tower loading of the TLP. The semi-submersible has the second highest TBDEL. The investigated spar buoy achieves the highest tower base equivalent loading among the concepts investigated.

Self-aligning platforms have the potential to use load-optimized towers. As mentioned in Section 2.2.2 the company Eolink claims that the pyramidal tower structure of their floating wind turbine is 40 % lighter than a single mast system. According to Eolink, this tower weight advantage can be achieved by distributing the loads more appropriately across all four masts which allows the steel thickness to be reduced. [68]

In [95] the dynamics of a self-aligning tetrahedral floating wind turbine platform is investigated and compared against single tower platforms. The nacelle of the downwind turbine is supported by three masts that transfer the loads into the floater. The findings of this study show that the rigid-body modes of the TetraFloat avoid the wave excitation frequencies. Next to that the accelerations at the nacelle are relatively low so that fatigue loads can possibly be reduced. The responses to wave excitation of the self-aligning platform are similar to those of the heavier DeepCWind semi-submersible. Overall, the floater weight of the investigated TetraFloat is below other floater designs offering a cost-saving potential.

3.2.3 Mooring System

The most important parameters, which are influenced by the choice of concept and affect the cost of the mooring system, are shown in the Figure 29. The procurement expenditures for the mooring system can be divided into the costs for the line, the anchor, and for additional components.

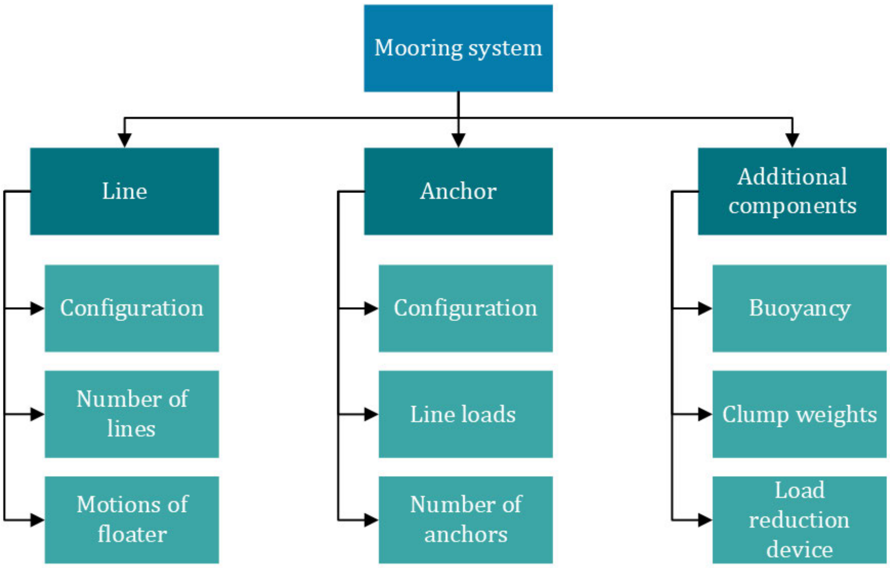

Figure 29: Parameters influencing the costs of the mooring system [author's illustration]

Line

In Figure 30 the line costs per meter and unit by mooring configuration are shown. Although the costs per meter of a catenary and semi-taut mooring system are lower than of a taut leg configuration, catenary and semi-taut systems tend to achieve higher line costs than taut leg moorings. The reason for this is the significantly longer mooring lines of the catenary and semi-taut system, which compensate the cost benefit per meter. [4] It should be mentioned that the line length of a semi-taut mooring is typically lower than a catenary line. As a result, the line costs for a semi-taut mooring are slightly lower than those of a catenary system. Since the configuration of the mooring system is affected by the floater typology (as mentioned in Table 2), the choice of floater thus affects the cost of the mooring system.

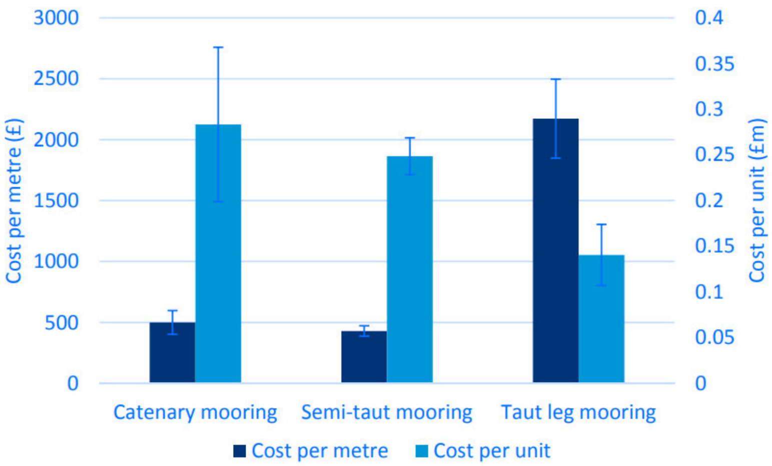

Figure 30: Mooring line costs per meter and per unit by configuration

The number of lines per FOWT can also affect the cost of the mooring system. Usually, TLP's require more mooring lines than the other typologies to decrease the risk of a line loss. [4] However, the individual design of the floater can also affect the required number of lines. In Figure 31 costs for a redundant and a nonredundant mooring system are compared with each other. For the shallow water case, a cost benefit can be achieved with the help of a nonredundant mooring system. However, this cost advantage should be compared with the costs which could result from an accidental line loss. For the deep water case, the cost difference between a three and a six-legged mooring system is nearly zero. [96] Since the number of lines is dependent on the floater typology and its design [4], the floater selection affects these costs.

Hybrid mooring systems which use synthetic mooring lines, clump weights, and buoyancy elements can lead to lower capital expenditures. Load-reducing technologies such as TFI or Exeter tether can also decrease the mooring system costs significantly. The cost-decreasing potential for hybrid and load reducing technologies is higher for shallower water since the snatch/snap loads do not play a significant role in deeper waters. [96]

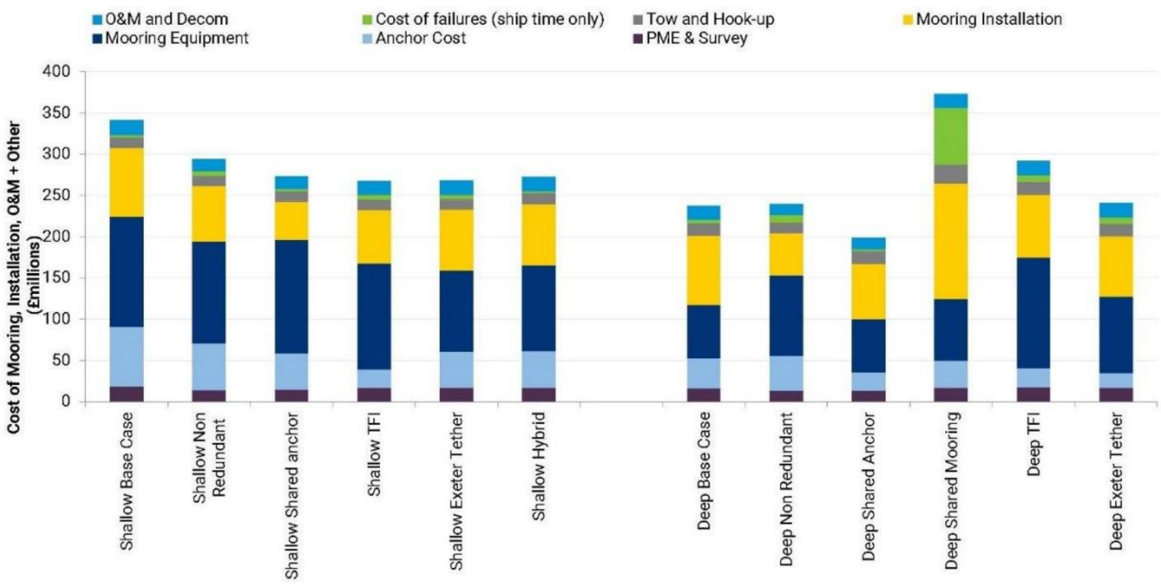

Figure 31: Total costs of mooring system for different mooring designs and water depths [96]

As the floater motions have a direct impact on the line loads and thus the dimensioning of the mooring system, the line costs can increase as the floaters motion susceptibility due to environmental influences increases. [97] The motions of the platform are dependent on the floater typology and also its design. [4]

Anchor

Depending on the anchor system requirements, different anchor typologies can be used to connect the mooring lines to the seabed (as mentioned in Table 3). The main factor impacting the anchor costs is its weight and its type. In Figure 32 the anchor weight and the associated costs are presented for different anchor types. Drag-embedment anchors are usually lighter and therefore cheaper than other anchor types. [96] Driven piles tend to be the most expensive anchor across all types. Usually, the anchor costs are the highest for the TLP largely attributed to the great vertical anchor loads and the anchor type. [4]

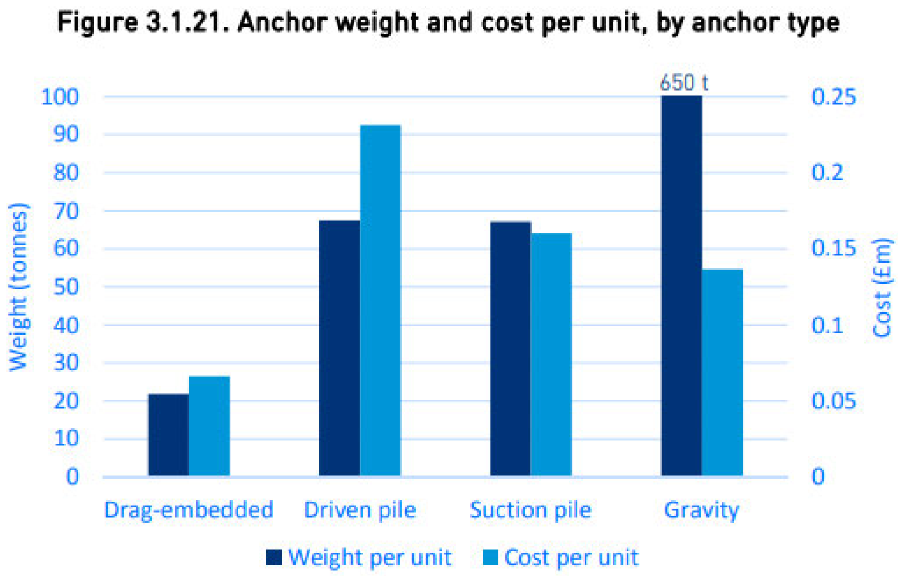

Figure 32: Anchor weight and costs per unit by anchor typology [4]

Similar to the number of mooring lines, the required quantity of anchors also influences the costs of the anchor. Figure 31 shows for the shallow water case a cost benefit for the nonredundant mooring configuration.

In Figure 29 additional cost parameters are presented. These parameters are not explained further here, due to their high variety and individuality.

3.2.4 Installation of floating wind turbine

The installation process of a floating wind turbine can be divided into three main parts. The first part is usually the installation of the mooring system. The second part includes the connection of the floater with the wind turbine including the tower. This part can be either done in port or offshore with e.g., floating cranes. In the third part, the floater is transported to the wind farm and connected to the pre-installed mooring system. In dependence on the platform type and the installation strategy, the transport of the FOWT can be performed by a wet tow with tug boats or with the help of barges or floating cranes with a storage area. [98]

According to [81] an important cost-influencing parameter of the installation is its applied strategy. Criteria that lead to different installation methods are the draft of the platform at the harbor and/or transit and the free-floating stability of the platform during towing. Depending on the installation method, different installation vessel types are required. Since the installations ships vary heavily in terms of day rates, the applied installation method mainly influences the installation costs. [81] The installation processes for the different floater typologies including their strengths and weaknesses are presented in the following.

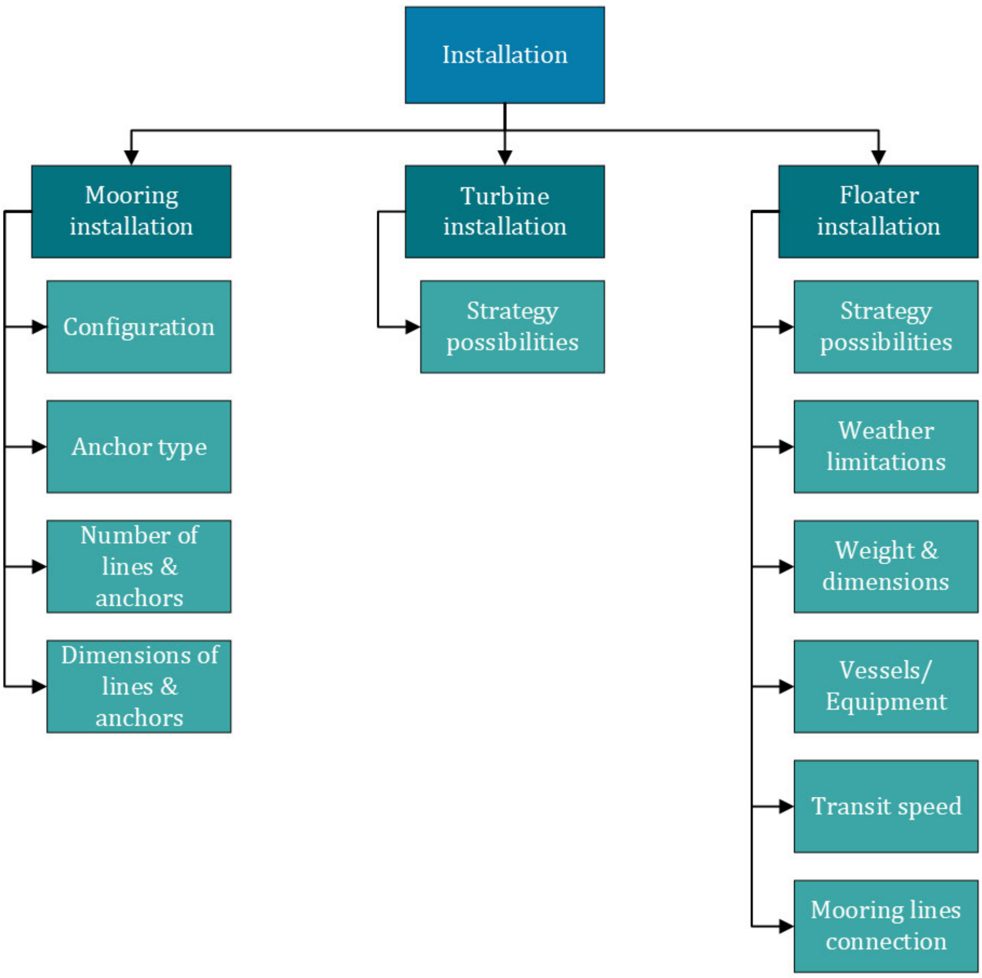

Figure 33: Parameters influencing the costs of the installation [author's illustration]

Next to the relatively small draft of barges and semi-submersibles compared to spars and TLP's, these typologies usually provide sufficient free-floating stability. These characteristics lead to the fact that barges and semi-submersibles can usually be assembled in port and towed to site with tugboats. If the water depth at the quayside is limited, a turbine integration at sheltered areas is also applicable. [4] [98] [81]

Figure 34: Towing operation of the WindFloat from Principle Power [99]

Since spar buoys are usually self-stable after the bottom end of the platform is ballasted, they can be towed out to the wind farm with simple barges and tug boats. Due to their high draft compared to waterplane area stabilized floater, usually, spar buoys cannot be fully assembled in port. [98] The installation of the tower and the rotor nacelle assembly takes place offshore, mostly in a sheltered deep water location due to the constrained wave height. [4] Finding a suitable installation site near the port can be challenging such that the installation of the turbine could take place offshore at site. [100], [84]

The different installation steps of the five floating wind turbines of the 30 MW wind farm Hywind Scotland are illustrated in [98]. In the first installation phase, the floater is towed out in a horizontal position to a sheltered deep water location. At this stage, issues might occur because to the low roll stability of the platform. [4] In the next installation step, the ballast water is filled into the bottom of the structure to upend the spar. After upending the platform, the water is pumped out and it is replaced by a solid ballast material. Finally, the tower including the RNA can be mated with the platform. The fully assembled floater can be towed upright from the sheltered area to the site using tugboats and vessels. [98]

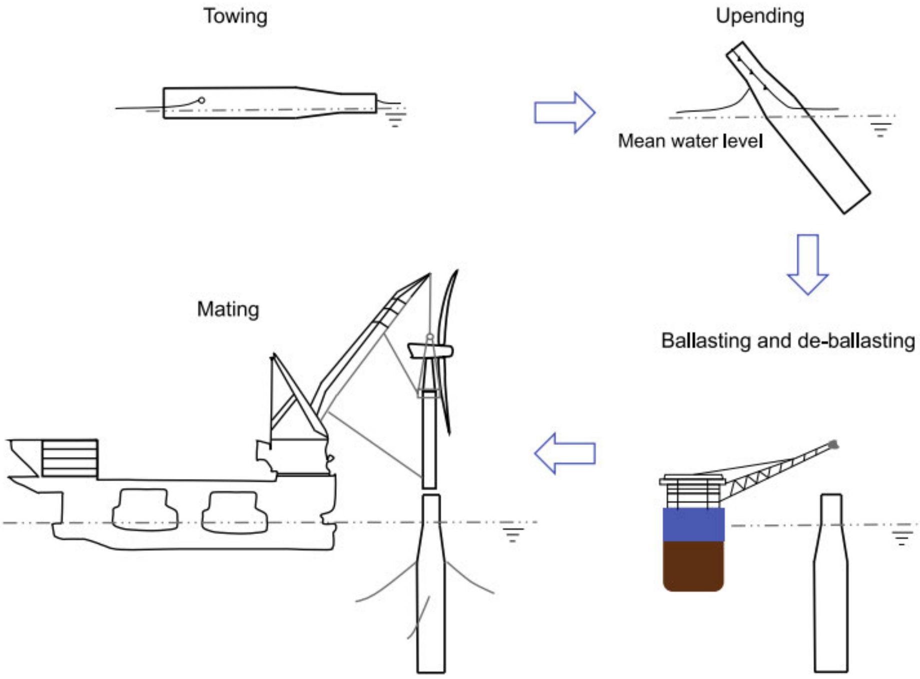

Figure 35: Typical installation process of a spar buoy [98]

A great cost driver of the installation of a spar buoy is the day rate for a heavy lifting floating crane. [81], [101] As a result innovative installation scenarios for ballast stabilized floaters aim to reduce the vessel requirements.

As mentioned earlier, some spars use a flexible keel. In port and during transport, this is attached close to the floater. In the wind farm, the ballast weight can be lowered and the motion responses of this structure are similar to a conventional spar buoy.

A different approach to reducing draft is taken by the Windcrete concept. This monolithic spar buoy can be lowered very deep at site, leading to a significant reduction of the hub height. This results in lower vessel requirements and allows an offshore installation of the RNA with smaller vessels. [59]

[102] investigated the suitability of a catamaran vessel for the installation of the spar. In this scenario, four towers with their mated RNAs are transported on a catamaran to the pre-moored floating support structure. The catamaran vessel is equipped with grippers than can lift the wind turbines on top of the floating substructure. [102]

The installation process of the TLP can vary significantly between concepts. Usually, due to the lack of the free-floating stability of the TLP, it must be transported either on barges or on floating cranes with storage from the port to the wind farm. [98], [81]

A more innovative installation approach for the TLP is investigated in [103] where a stabilizing floater/frame aids the transport and installation of the TLP. Due to the temporary installation frame, the TLP achieves higher floating stability allowing a towing out with tug boats. At the installation site, the buoyancy modules of the transport frame are ballasted with water and the pre-installed tendons can be connected to the TLP. Finally, the water in the buoys of the frame can be pumped out and the tendons gain tension. [98]

In [104] the installation process for the Gicon SOF is presented. Since the floater is placed on a floating gravity anchor it can be towed out fully assembled by tug boats. On site, the gravity anchor is ballasted, submerging the TLP to its final draft. [98]

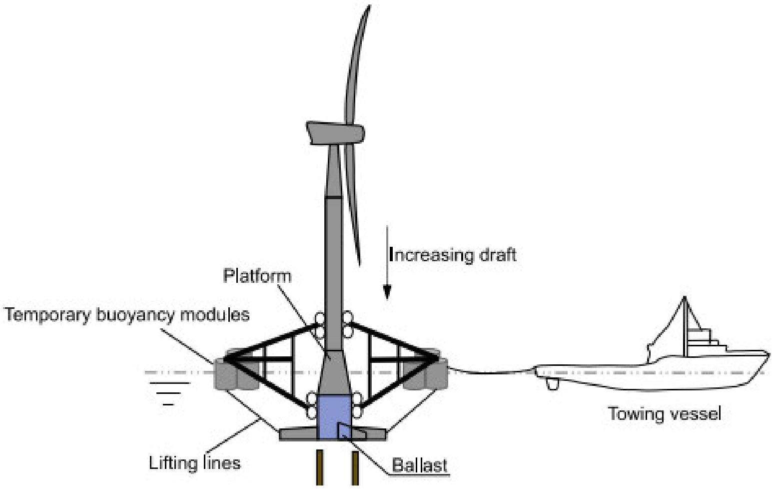

Figure 36: Installation frame for a TLP [98]

In [4] several installation strengths and weaknesses by typology are presented. The semi-submersible presents the most flexible solution among the other platform types. Due to the high draft of the spar buoy (conventional), the platform has weaknesses regarding the port assembly. The low stability of the TLP makes it more susceptible to harsher metocean conditions. Next to that, the TLP tends to require a higher installation time compared to the other floaters. However, this figure is only an indication, and the strengths and weaknesses can vary for different concepts within floater typologies.

Typology	Assembly (port vs offshore)	Draft requirements	Vessel requirements	Weather limitations	Time to install
Barge & semi-submersible	green	green	green	yellow	green
Spar	red	red	red	yellow	yellow
TLP	yellow	yellow	yellow	red	red

green	relatively advantageous
yellow	neutral
red	relatively disadvantageous

Figure 37: Installation strengths and weaknesses by floater typology [author's illustration adapted from [4]]

Figure 38 shows installation cost ratios between floater typologies determined in different studies. The percentage value of a concept indicates how well it performed in terms of installation costs compared to the other investigated concepts within this study. If a concept achieves 100% its installation costs are the highest among the other investigated floaters. The remaining percentages of the respective study reflect the cost ratios between the concepts. Since no study could be found which cost comparison includes installation costs for a barge this platform type is not presented in Figure 38. However, as the installation strategy for the barge is the same as for the semi-sub, [5] the installation costs should be similar.

The results from the literature review show a high variety regarding the cost ratios between the concepts. Especially the cost differences between TLP and spar buoy fluctuate significantly between the studies. Depending on the basic assumptions made in terms of installation method, vessel day rates, and installation time, the calculated costs for these two concepts can vary heavily. [4] In [81] and [105] it is assumed that the installation and the transport of the TLP are performed with the help of a floating crane with storage. The comparatively high vessel day rate leads to a cost-intensive installation for TLP. In contrast to this in [4] and [106] the underlying installation scenario for the TLP is that this platform can be towed out fully assembled to the wind farm by using tugboats. The still higher installation costs of the TLP compared to the spar buoy result from the longer installation time for the TLP.

Usually, the semi-submersible and thus the barge are the most cost-efficient designs in terms of installation among the other floater typologies. [100] The main reason for that is the small vessel requirements combined with a relatively short installation time. [4]

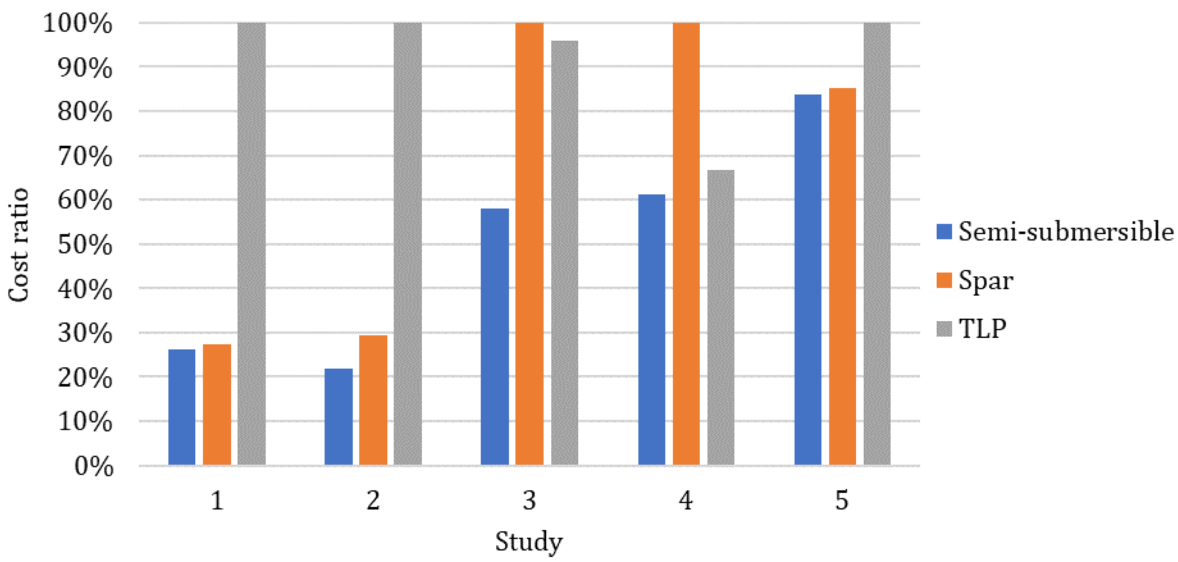

Figure 38: Installation costs relations between floater typologies identified in the literature (1= [105], 2= [81], 3= [4], 4= [106], 5= [107])

3.2.5 Operations and Maintenance

Floating wind turbines introduce new challenges and constraints from an O&M perspective for the wind industry. The most important reasons for that are increased distances between the wind farm to the port and the harsher environment. Another aspect is the wave sensitivity of the floating turbines, which poses difficulties for turbine accessibility. [108] According to [108] operations and maintenance is a key area of cost reduction for FOWT if it wants to compete against bottom-fixed offshore turbines. Figure 39shows parameters that depend on the floater typology and its design and can influence the cost of O&M. These parameters will be explained in more detail below.

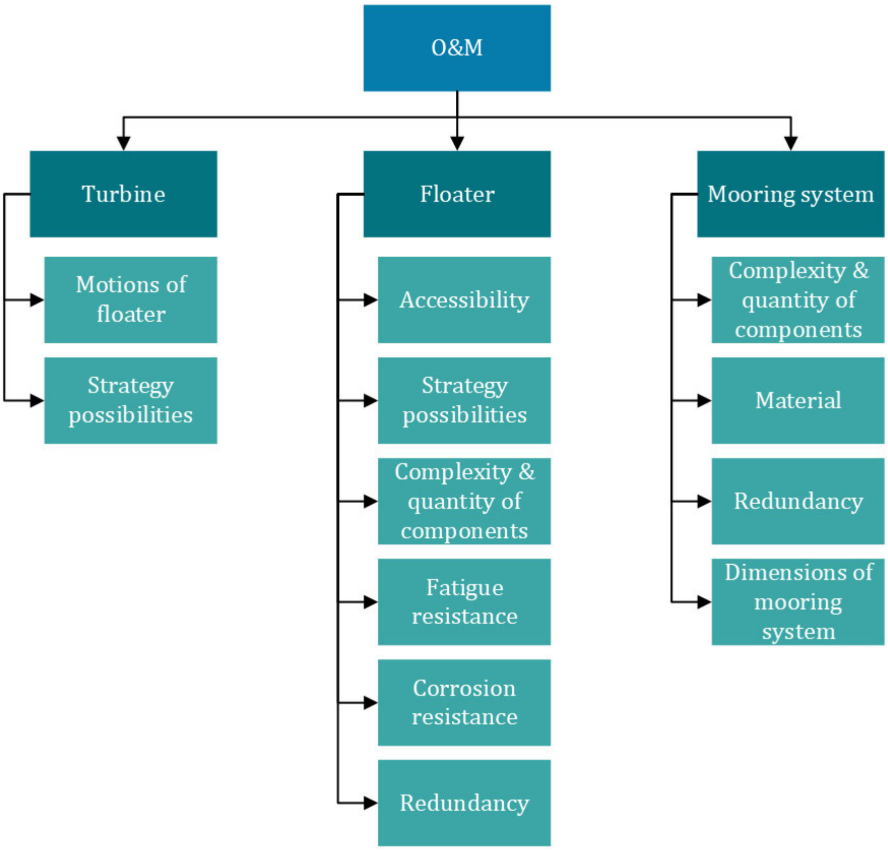

Figure 39: Parameters influencing the costs of the O&M [author's illustration]

A significant impact on the O&M can have the accessibility of the floating wind turbine. The motions of the floater can make it more challenging for the personnel to access the platform. Depending on the response characteristics of the floater typology this can lead to increased maintenance time and downtime. [108] A potential solution for this issue can be to tow the FOWT to a port for major maintenance operations. [83] This would lower the requirements for platform accessibility and the vessels. [109], [110] Figure 40 shows the suitability by floater typology for the tow-in maintenance. Due to their low draft and good stability during towing, barges and semi-submersibles are particularly well suited for a tow-in strategy. As a result of the high draft of the spar buoy, this platform cannot be maintained in ports so either sheltered areas must be used or the maintenance takes place at site. The instability of TLPs when disconnected from mooring lines leads to great challenges for the tow-in strategy. The stabilization frame which was mentioned before can enable the tow-to-port maintenance of TLP FOWT. But the connection and disconnection of the support frame for each maintenance in ports during the lifetime can be time-consuming and may not be cost-effective. [96]

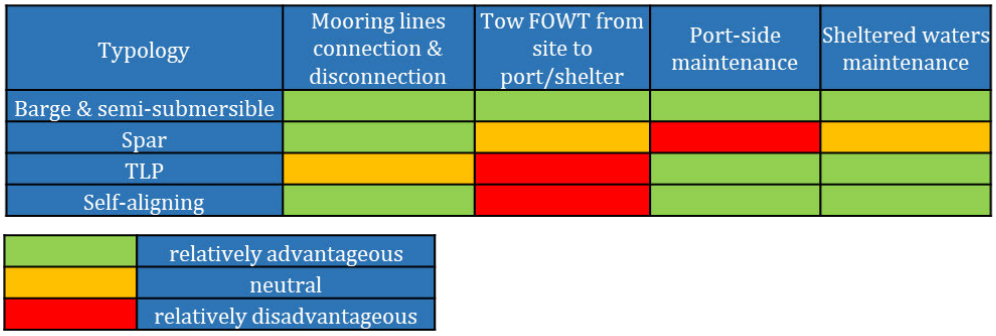

Figure 40: Maintenance strengths and weaknesses by floater typology [author's illustration adapted from [96]]

In [109] different O&M strategies are analyzed for a concrete semi-submersible (ActiveFloat) and a concrete spar buoy (Windcrete). One focus of the study is to determine the influence of the major component exchange strategy on the lifetime OPEX. The tow-to-shore strategy (tow-in) was compared with the offshore heavy lift scenario (F2F). As mentioned before for the tow-in strategy it is assumed that the platform is towed to the port where the major component exchange is performed. Due to its high draft, the tow-in strategy is a fictive scenario for the spar buoy. The F2F strategy requires a heavy lift crane vessel to exchange major components at the site. In Table 5 the OPEX results from [109] show that the tow-in strategy is the most economical solution for all sites for the maintenance of floating wind turbines. However, these cost differences between tow-in and F2F vary depending on the site conditions. For milder weather conditions like in Gran Canaria, the OPEX difference between these two strategies is relatively small. The weather conditions in Morro Bay are harsher than in Gran Canaria resulting in a higher OPEX difference between tow-in and F2F. Comparing the OPEX between the platforms for the same maintenance strategy for the case of Morro Bay, Windcrete achieves higher OPEX than ActiveFloat. This is a result of the harsher environment, in combination with the slightly more severe weather limits of the Windcrete structure. [109] However, it should be mentioned that the results are highly dependent on vessel costs. Lower vessel day rates for floating cranes could make the OPEX for the floating-to-floating scenario more attractive. [109]

Table 5: OPEX and lost production for different sites and strategies (data based on [109])

Site	Scenario	Floater type	OPEX [€/MW/yr]
Gran Canaria	Tow-in	ActiveFloat	77,2
		Windcrete	77,3
	F2F	ActiveFloat	84,4
		Windcrete	84,5
Morro Bay	Tow-in	ActiveFloat	77,8
		Windcrete	77,8
	F2F	ActiveFloat	98,7
		Windcrete	116,5

A part of the cost study from [106] is the determination of the costs for operations and maintenance of a bottom-fixed turbine and a floating wind turbine. For the FOWT two maintenance strategies are investigated – offshore site vs. tow-to-port maintenance. The results show that the tow-to-port strategy can save up to 35% in maintenance costs compared to the F2F strategy.

Looking at the factors influencing costs within the tow-to-port strategy, the connection and disconnection duration can play a significant role in economic efficiency. In [110] the potential benefit of a quick disconnection system (4-h duration) for the tow-to-shore maintenance is investigated and compared to a standard solution (24-h duration). The results show that the quick connection system can lower the expected average downtime between 20-30 % in comparison to the standard device.

Besides the opportunities of the tow-in maintenance, this strategy also brings challenges. Issues for this strategy can be the existing port infrastructure, including the port draught, the port availability, the crane capacity, sufficient channel width, and quayside length. [96], [84], [109] Another aspect that must be investigated is the allowable time and weather window for disconnection of the mooring system and the power cable. Dependent on the substructure type the stability during towing operation and the limits in terms of metocean conditions can also be an issue. Next to that, a time-consuming work could be the de-ballasting of the platform, which may be necessary for port access. [83], [96]

However, the typology can also have an impact on other cost-influencing parameters. Another parameter that can impact the OPEX is the used hull material of the floater. The choice of material affects, for example, the susceptibility to corrosion. Since concrete cannot corrode, platforms made out of concrete might have the advantage of lower maintenance requirements compared to steel structures. This can result in a reduction of OPEX and a longer lifetime. [101], [88] An extension of the lifetime of FOWT can lead to a cost reduction potential and could give concrete platforms an important cost advantage compared to other materials. [88]

Furthermore, the waterplane area of a floater can influence the O&M. The splash zone of the floater (area immediately above and below the mean water level [111]) must be inspected during maintenance. Since marine growth can lead to additional stress due to the added weight the submerged parts of the floater must be included for maintenance. If the substructure uses active ballast systems another aspect which will be inspected are internal pumps for signs of wear or failure. [5]

The influence of the mooring system on the OPEX is relatively small. In [96] a cost split was analyzed for a shallow and a deep-water case. The project lifetime was assumed to be 25 years and no removal or replacement, or mooring components were taken place. The results show that the influence of the O&M-related costs is low in comparison to other cost factors, like procurement of mooring and anchor equipment or the installation of the mooring system. For the shallow water case, the O&M and decommissioning cost share is less than 1 %, and for the deep-water case, it is about 5 %.

4 Assessments of FOWT concepts in literature

This chapter is intended to provide the reader with an overview of FOWT concept comparisons conducted in the literature. In Section 4.1, the results of qualitative and quantitative floater concept assessments are presented and summarized. In Section 4.2 assessments are pointed out that compare floater concepts in terms of their respective LCOE. Finally, Section 4.3 describes the perspectives from which concepts can be evaluated and compared.

4.1 Assessments based on qualitative and quantitative criteria

Weighted point analyses are intended to support the decision-making process for complex problems in a rational way. There are different assessment methods that vary in terms of quality of information and time required. [112] A weighted point analysis evaluates alternatives based on several quantitative and qualitative criteria, goals, or conditions. The criteria of the analyses are weighted to account for their influence on the overall score. Attention should be paid to the fact that the criteria are independent of each other. Furthermore, the inclusion of criteria that can lead to an exclusion of an alternative should be avoided. [113]

Table 6 shows the results of the assessments which were conducted in several studies. These assessments compare support structure concepts based on differently weighted criteria. In some studies, in addition to concepts for floating support structures, bottom-fixed foundations have also been investigated. The results in Table 6 show only the rankings between the support structures for floating wind turbines. The results for the bottom-fixed foundations are left out. Due to this, in some cases, the results in Table 6 do not reflect the absolute floater rankings from a respective study. The following is a brief overview of some of the basic assumptions and the results of the studies.

In [114] a systematic methodology for the evaluation of different bottom-fixed and floating offshore support structure concepts based on the TOPSIS (Technique for Order Preference by Similarity to Ideal Solution) is presented. Based on twelve weighted criteria, the barge foundation is the most advantageous floating support structure concept.

In 2014 [115] presented an extension of the TOPSIS method to explicitly consider stochastic inputs. That stochastic approach takes into account the uncertainty that arises from subjective inputs based on expert opinions. The result in Table 6 only presents the deterministic ranking. The semi-submersible achieves the highest score of all floating support structure concepts. In contrast to that the spar buoy, is the least favorable concept. This study also investigates how often a certain concept ranked in the first place under stochastic inputs. The results of this comparison show again that the semi-submersible is the concept that most often ends up in first place compared to the other floater typologies. The barge and the spar buoy achieve the same probability whereas the TLP has the lowest probability to end up in the first place.

In [116] different support structures are assessed with respect to their suitability for offshore wind farm deployment. With the help of a survey, ten floaters were evaluated based on ten weighted criteria. The results in Table 6 show the ranking for the four compared main concepts. Next to these main concepts, optimized/ advanced support structures were also assessed. The advanced spar buoy (reduced draft, vacillation fins, delta mooring connection, horizontal transportation methodology) achieves the highest score of all ten concepts. The advanced semi-submersible (braceless, wave-canceling geometry, inclined/shape-optimized columns, active ballast system) has the third highest potential for wind farm deployment. No advanced design for the barge is investigated and the standard barge type makes the fourth place in this assessment. The TLP is the worst-rated structure, followed by the advanced TLP (redundant mooring lines, gravity anchors).

In [117] the goal is to select an optimum support structure for a floating wind turbine that can be used for harnessing the potential that the Gulf of Guinea Offshore waters hold for renewable energy generation. To determine which of the three floating support structure concepts (spar buoy, semi-submersible, TLP) has the greatest potential for floating wind farm deployment, the concepts were assessed with the help of a modified TOPSIS analysis. The weighted vectors for the TOPSIS were obtained through a pairwise comparison. Based on this analysis the spar buoy performed best compared to the other two concepts. The semi-submersible was rated the worst in this assessment. The main reason for this is the high production costs of the semi-submersible compared to the other two concepts. The costs related to the production of the spar buoy are nearly 80% lower than these of the semi-sub. For the case of the TLP, the cost induced by the production are 60% lower in comparison to the semi-submersible.

[118] presented an independent assessment of current floater concepts for floating wind application. A total of 31 concepts were compared on the basis of 14 weighted criteria. The results show that the scores can vary significantly within a floater typology. For example, concepts of a low-ranked floater main typology may achieve a better score than a concept that belongs to a high-rated floater class.

Comparing the rankings from the literature review in Table 6, there is no clear trend in favor of any particular floater typology. Depending on the study, the potential and suitability of a particular support structure in terms of wind farm deployment is assessed differently. The criteria, their weighting, and also the evaluation of a respective concept result in a high variance in the results across the studies. Some of the assessments rank concepts based on different qualitative and quantitative criteria. A risk that is associated with the mixture of qualitative and quantitative criteria is that a clear separation between the criteria is more difficult. This can result in a property being weighted more than once. For example, concepts are often evaluated based on the LCOE and simultaneously on other qualitative criteria, such as installation or maintenance. Since aspects such as installation and maintenance are already included in the LCOE, this can lead to a double assessment of properties.

Table 6: Qualitative and quantitative assessments of floater concepts in the literature

Source	Barge	Semi-submersible	Spar buoy	TLP
[114]	**1**	3	4	2
[115][1]	2 (7)	**1** (5)	4 (9)	3 (8)
[116][2]	2	3	**1**	4
[117][3]	-	3	**1**	2
[118][4]	3	**1**	4	2

[1] Deterministic ranking of the solutions only for the floating wind support structures.

[2] Ranking inclusive the advanced concepts: Spar advanced=1; Spar-standard=2; Semi-sub advanced=3; Barge=4; Semi-sub standard=5; TLP advanced=9; TLP standard =10

[3] Modified TOPSIS

[4] Ranking according to average score by floater typology. Best concepts in different floater typologies: Barge=Damping Pool by Ideol; Semi-sub=Windfloat by Principle Power; Spar buoy=Hywind by Equinor; TLP=SBM (first generation of concept) by SBM

4.2 Assessments based on cost factors

A helpful measurement to compare different methods for energy production can be the LCOE which is mentioned in Section 3. Table 7 presents the results of the LCOE determined in different studies. If a concept reaches 100% it means that this concept achieves the highest costs compared to the other investigated concepts within this study. The percentages of the remaining concepts of this study indicate how high the costs are in relation to the most expensive concept. In the following, a short overview of the cost studies including its basic assumptions is given.

[107] investigated the costs of different floating and bottom fixed foundations as a part of the development of the floating TLB B and TLB X3 wind turbine concepts that were developed by the Norwegian University of Life Sciences and the Norwegian Institute for Energy Technology. The results show that both TLBs achieves the lowest LCOE compared to the other floating support structures. The SWAY platform, a single-point moored spar foundation, has a slightly higher LCOE compared to the TLBs. The second highest LCOE achieves the Spar (Hywind II) whose costs are 13 % lower compared to the LCOE from the most cost-intensive platform, the semi-submersible (WindFLoat).

2014 in the work [79] the LCOE of different floating and bottom-fixed foundations were calculated based on the work from [107]. The goal of this work was to implement revised and updated values in the calculation method from [107]. [79] calculated for all concepts slightly higher LCOE than [107]. Whereas the cost relations between the different support structure typologies stay nearly the same. The TLWT, a hybrid TLP which uses next to tendons also catenary mooring lines, was investigated as a part of this work. This platform type achieves nearly the same costs as the TLBs. The main reason for the relatively high costs for the semi-submersible in [107] and [79] is the heavy and complex platform resulting in an expensive support structure. In terms of O&M, no cost differences can be obtained for the investigated floaters. This is due to the same maintenance strategy which is applied to all platform types. Next to that, the same installation method is applied to all floaters which lead to comparatively small installation cost differences between the concepts.

Nilsson & Westin evaluated 2014 in [119] the LCOE for a floating wind farm which has a total capacity of 288 MW. The 48 turbines with each 6 MW were located at Utsira Nord wind farm at the coast of Norway. The LCOE for a semi-submersible, a spar, and a TLP are calculated in this study. Nilsson & Westin determined that in both cases (low and high estimate) the TLP is the most favorable platform in terms of LCOE. In both estimates, the highest Levelized Cost of Energy is calculated for the semi-submersible platform. The spar buoy lines up in the middle of the other two support structures. The main reason for the high LCOE of the semi-submersible is the expensive foundation compared to the other two platform types. The cost of the TLP platform is only one-seventh of the cost of the semi-sub platform. The Spar is half the price of the semi-submersible. The installation costs of the platforms and turbines are small compared to the costs of the platform. The OPEX are the same for all investigated platform types.

The objective of [104] is to identify cost reduction potentials for floating offshore wind turbines along the entire value chain. The main focus of this work was the investigation of the TLP platform SOF 2 from GICON, which is moored with the help of a gravity-based foundation. As already mentioned in Section 2.2.2, in the port, the anchor is attached to the bottom of the support structure and provides stability for the tow-out. In the wind farm, the anchor can be lowered to the seabed which saves effort and time for the floater and mooring installation. Next to that, [104] also investigated the LCOE for a semi-submersible, a spar, and a TLP platform. Since the determined values are based on the study from [119] the cost ratios are similar between these two studies.

One part of the report published by Carbon Trust in 2015 consisted of a cost analysis for different floating support structures typologies. Based on a fictive wind farm scenario floater designers submitted cost estimates for their particular platform. For each structure, the average of the reported costs was determined and compared with the others. As a result, the LCOE is nearly the same for all three platform types which were investigated. However, Figure 41 shows the respective cost data for the individual designs. The lowest, as well as the highest costs, were provided for the semi-submersible, resulting in the highest range of LCOE for this concept. The submitted LCOE for the TLP instead, are very close together. With the exception of one concept, the costs of the spar buoy designs are close to that of the TLP's.

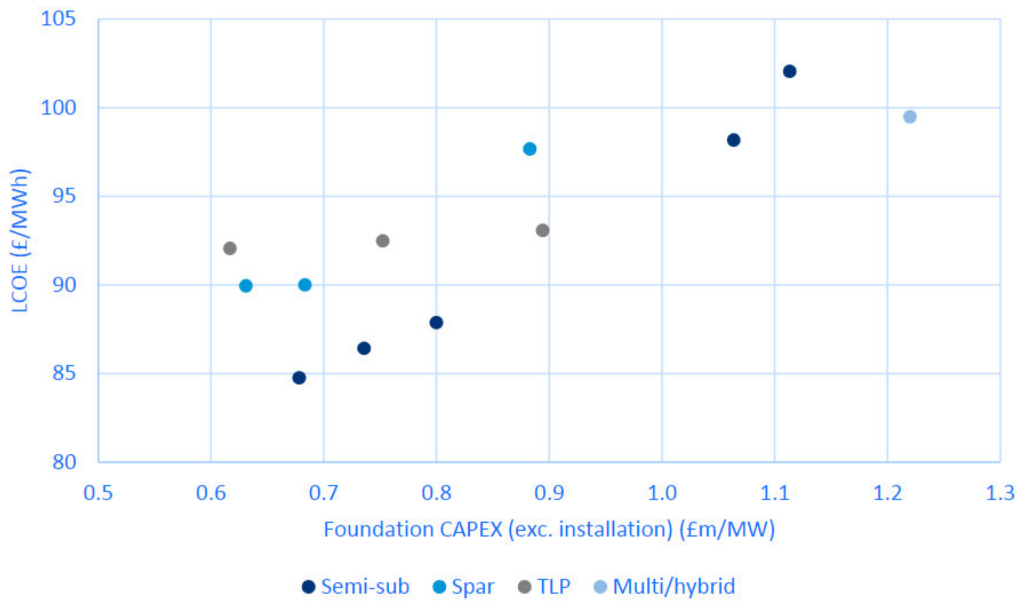

Figure 41: LCOE and CAPEX of commercial-scale floating wind projects [4]

In 2018 [120] calculated the LCOE for a concrete semi-submersible, a concrete spar, and a steel TLP, each for three different locations. For all sites, the semi-submersible is the least economic solution of the three investigated structures. If the water depth is sufficient, the spar buoy has the lowest LCOE compared to the other two platforms. In this work, the installation costs of the spar buoy are nearly the same as those for the semi-submersible. This is due to the special construction and installation method of the investigated Windcrete. [120]

The authors of [121] and [122] examined the costs for three platforms and two different locations. In [121] the investigated floating wind turbines were located near the coast of Portugal. For this site, the spar buoy achieves the lowest LCOE among the other concepts. In [122] the economic feasibility of offshore wind farms is assessed that are installed at the northern coast of Spain. The results show that the semi-submersible achieves the lowest lifetime costs of all three concepts.

[81] developed a life cycle cost model for floating offshore wind farms that can support in decision-making. The cost model determines the lowest cost for the semi-submersible. The TLP is the most expensive support structure, mainly due to its very high weight and cost-intensive installation.

The results of the cost studies in Table 7 do not indicate a cost trend in favor of one floater typology. Depending on the study, the most cost-effective typology differs. Furthermore, the bandwidth of fluctuation varies between those cost studies. For example, in [4] the LCOE of the floater typologies are close to each other, while in [119] the difference between the most expensive and least expensive concept is significantly larger. Another aspect that can be observed in Table 7 is that the economic efficiency of a concept can be influenced by the applied site conditions. [121] and [122] calculated LCOE for the same floaters but for two different locations. In Spain, the most economic concept is the semi-sub, whereas the site conditions of Portugal lead to the lowest LCOE for the spar buoy.

Table 7: Ratios of LCOE between floater typologies determined in cost studies

Source	Semi-submersible	Spar buoy	TLP
[107]	100%	87%	**83%**[1]
[79]	100%	87%	**84%**
[119] – low estimate	100%	87%	**84%**
[119] – high estimate	100%	82%	**74%**
[104]	100%	87%	**84%**
[4]	**99%**	100%	100%
[120] – site 1	100%	-[2]	**92%**
[120] – site 2	100%	**88%**	99%
[120] – site 3	100%	**86%**	97%
[123]	100%	**94%**	96%
[121] – coast of Portugal	93%	**89%**	100%
[122] – coast of Spain	**92%**	98%	100%
[81]	**89%**	92%	100%

[1] TLB platform

[2] No costs due to draft restrictions

4.3 Assessment perspectives and criteria

Separating the perspectives can help to perform a fairer assessment of concepts. As seen in Section 4.1 an important aspect in the evaluation of concepts based on qualitative and quantitative criteria is an appropriate weighting of these. Depending on the underlying requirements of a support structure concept, the importance of the dimensions may vary. For this purpose, Figure 42 shows the most important perspectives (or dimensions) for assessing floater typologies that could be identified in the literature review.

As already seen in Section 4.2 the **LCOE** can be an important indicator to compare floater concepts with each other. In Figure 42 parameters are pointed out that impact the LCOE and can be affected by the floater typology. As examined in the section 3 the floater typology and its individual design affect the expenses for the platform itself, the tower, the mooring system, the installation, and the operations and maintenance.

The wind and energy yield can vary between floater types and designs. An example of that is the self-aligning semi-submersible in [44] which is investigated in terms of its yaw drift. It is mentioned that high wind-rotor misalignments in combination with a high wind speed operation can cause an energy yield loss. Furthermore, some floater suppliers advertise an active ballasting system that can decrease the platform's pitch angle and thus increase the energy yield. [92]

Besides parameters of the LCOE, concepts may also be evaluated with each other based on **flexibility criteria**. A potential flexibility parameter could be the required infrastructure of the manufacturing and assembly facility of the platform. As mentioned in Section 3.2.1 there are several requirements for the infrastructure e.g., sufficient quay length, draught, cranes, wet storage area, etc. which can vary between FOWT concepts.

Another aspect that could be considered related to the infrastructure is the available vessels for the installation and maintenance of the FOWT. [5] Substructure concepts can furthermore be investigated in terms of limitations and restrictions for environmental site conditions. This assessment identifies differences regarding site conditions requirements of floater technologies and put them in relation to each other depending on their relative importance for the potential for offshore deployment.

In addition, time-related components can be included in the evaluation. Time efficiency in terms of the production duration of a unit can be a criterion when choosing a support structure concept. [89] The time efficiency in this category defines the required timespan for manufacturing, assembly, installation, or maintenance of a concept. For example, severe metocean limitations of a FOWT can lead to lengthy installation processes or long maintenance downtimes due to small allowable weather windows.

Due to the continuing trend of growing turbine capacity [124], it can be advantageous for a substructure if it is suited for turbine **upscaling**. This could decrease effort in the fields of planning, production, and operation for a new turbine size. Scalability also includes the potential for mass production of a floater design. **Adaptability** defines the skill to adjust to new conditions. In terms of floating wind turbines, adaptability can be helpful for changing infrastructure and site conditions.

With the help of the technological readiness level (**TRL**), the maturity of a particular technology can be measured and compared to other technologies. [125] One example is the study of [116] in which floater typologies are compared based on a two-dimensional scale -in addition to the score resulting from a TPOSIS analysis, the concepts are ranked according to their respective TRL.

The **environmental footprint** through the several lifecycle phases of a FOWT concept may also be considered when comparing different support structure technologies. Examples of important factors which should be investigated are the carbon footprint of the production and decommissioning, the noise impact of pile driving or hammering, and the disturbance of fishing activity due to the mooring system. [126], [4]

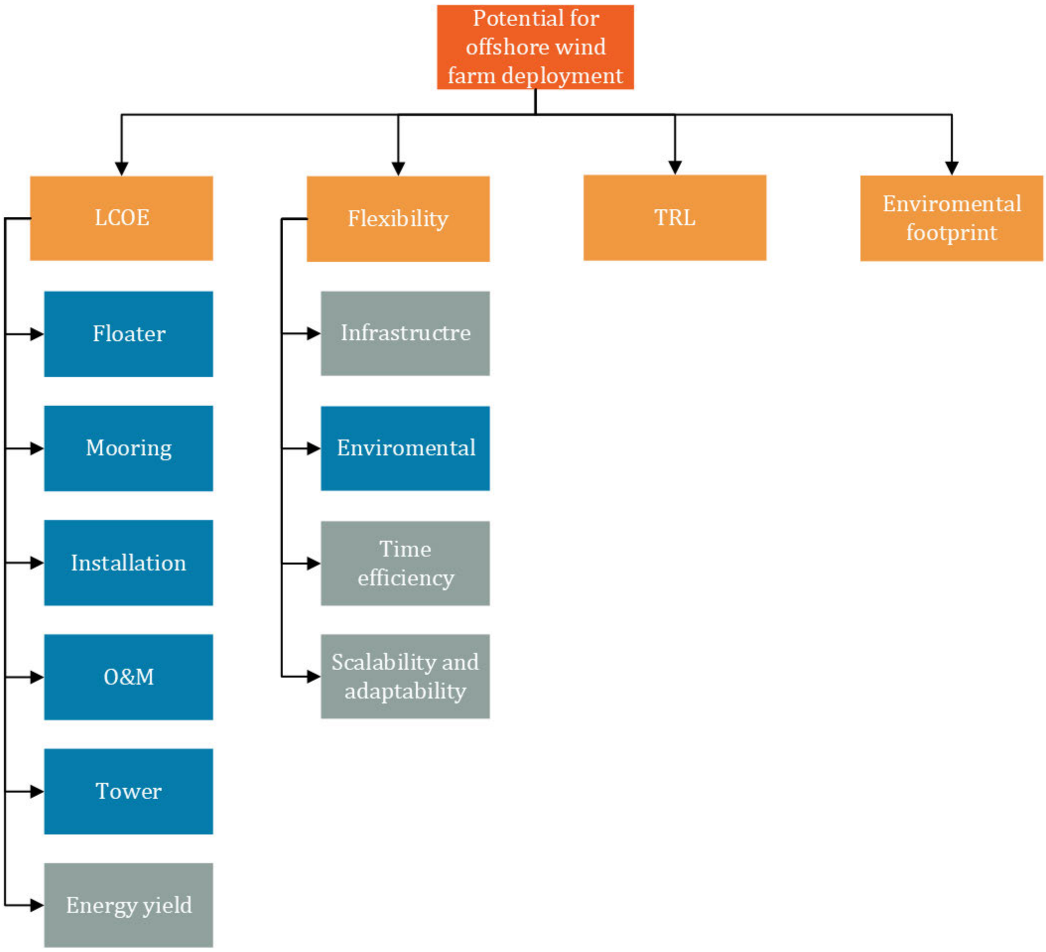

Figure 42: Perspectives and criteria for measuring the potential for offshore deployment of FOWT concepts [author's illustration]

5 Assessment of FOWT concepts

This chapter provides an assessment of floating wind support structure concepts. The introduction of the concepts (set of alternatives) is presented in Section 5.1. Since the mixture of evaluation perspectives can pose high challenges for a fair and rational assessment (see Section 4.3), the concepts are evaluated based on two separate dimensions. As the LCOE is a very important perspective for decision-making, the first dimension assesses the concepts in terms of life cycle cost criteria. (Section 5.2) Here, only those costs are to be considered which are influenced by the floater typology and its design. The second dimension compares the substructure concepts in terms of limitations and restrictions due to site conditions (Section 5.3). The investigated parameters in this dimension can be an exclusion criterion and should therefore not be mixed with the criteria in the cost comparison.

5.1 Set of alternatives

The set of alternatives for the assessment includes six generic concepts and 38 designs, that could be identified in the market research. Due to lack of data not all 52 of the commercial concepts which are mentioned in Section 2.2.2 are included in this assessment.

The six generic concepts are intended to represent a typical main case of a respective floater typology. Each of the 38 commercial market concepts is categorized into one of these main concept categories (superordinate/parent typology). To decrease the scope of this work and due to the lack of data, the score achieved by the respective generic superordinate typology in a category is adopted by the market concepts in some cases.

The categories of the generic floater typologies are presented in Figure 43. The investigated mix concepts combine properties of two generic main concepts. Overall, the assessment includes 5 barges, 20 semi-submersibles, 10 spars, 5 TLPs, and 12 mix concepts.

The commercial concepts including its underlying data can be found in Appendix G.

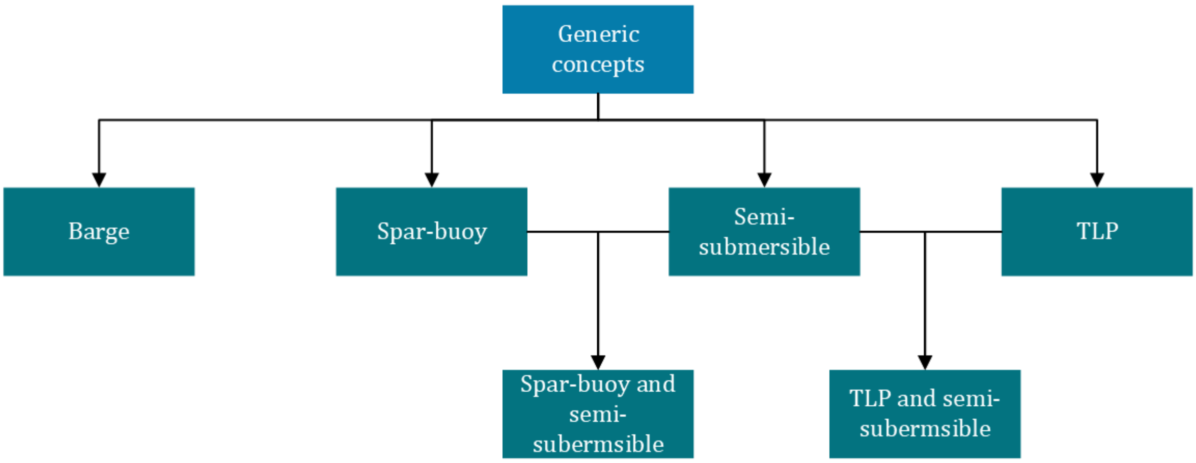

Figure 43: Overview generic concepts [author's illustration]

5.2 Cost assessment

As mentioned above the concepts are compared based on lifecycle costs that are influenced by the typology and the individual properties of a floating support structure. For this purpose, the concepts are assessed based on five weighted criteria. In the first part of the assessment (Section 5.2.1), the unweighted scores are determined for each concept in the categories floater, tower, mooring system, installation, and O&M. These categories form the most important capital expenditures of the LCOE, which can be evaluated separately for the different concepts and are affected by the floater typology. The calculation of the concept scores is based on the results of studies that have determined costs in these categories. Afterwards (Section 5.2.2) the weightings of the respective criteria are determined with the help of an underlying cost breakdown for a FOWT. The weighting of the criteria is intended to reflect the cost shares of the various categories.

5.2.1 Criteria

In the following, the set of criteria including its determination of unweighted scores is presented. An appropriate scoring of the respective concepts in each category, which reflects the relative difference between designs leads to high challenges for qualitative assessment methodologies as seen in Section 4.1. Therefore, based on the results of cost assessments for floating wind turbines, the score determination for each criterion is carried out in dependence on the expenses for the respective category. The underlying data for the individual designs are taken from public sources and can be seen in Appendix G.

Since the scores are oriented to the costs of a floating wind turbine, the goal for each concept is to achieve a low score. All concepts are measured against an underlying baseline design terminated as base case in the following. The normalized and unweighted score for a concept in a particular category is calculated as follows:

$$S_u = \frac{s}{s_{base\ case}} \tag{2}$$

Whereas s defines the respective unweighted score of a concept in a category and $s_{base\ case}$ is the unweighted score of the base case in a category.

In the following the score determination for each criterion is presented.

<u>Floater</u>

In the category floater the concepts are assessed based on their respective procurement and production effort which includes the financial effort for the raw material, as well as for the manufacturing. According to these assumptions the unweighted score for the floater $s_{floater}$ is determined as follows:

$$s_{floater} = s_{F,raw\ material} + s_{F,manufacturing} \tag{3}$$

Since the score for the raw material of a particular floater is dependent on the material type and its consumption/mass (see Section 3.2.1) it can be defined as:

$$s_{F,raw\ material} = \sum_{i=1}^{3} f_{F,material,i} * m_{F,i} \tag{4}$$

The factor $f_{F,material}$ indicates the price ratio between the different hull materials. Smaller factors indicate smaller unit prices, whereas higher factors indicate higher unit prices. The variable m_F defines the mass of the respective material. The included hull materials are steel, post-tensioned concrete, and solid ballast. Within one material type differences can occur in terms of material quality. However, for simplification, it is assumed that all support structures use the same steel, concrete, and ballast grade.

The volatility of the steel price leads to challenges in terms of finding a suitable ratio between the unit price for steel and concrete. An example is that the steel price fluctuated in the years from 2008-2012 between 250 €/ton to 1250 €/ton. At the same time, the unit price for concrete just fluctuated between +-3% in France. [87] However, the aim of this study is not a comparison between concrete and steel floaters for offshore deployment. Therefore, it is assumed that a steel floater is as expensive as the same floater consisting of concrete. Assuming that the solid material mass of a concrete floater is about four times higher than the hull mass of a steel floater [87], the unit price of steel is four times that unit price of post-tensioned concrete. The factor for the unit price for the ballast material is orientated to [127], where material unit prices for a 10 MW Tripod floating wind turbine are stated. In Table 8 the applied material factors are presented.

Table 8: Material cost factors

Material	Factor $f_{F,material}$
Steel	1,000
Post-tensioned concrete	0,250
Concrete ballast	0,070

In the literature, the masses for the investigated floater concepts are given for different turbine sizes. Consequently, the masses of the platforms are compared in terms of their scaled mass per megawatt. In [97] a foundation scaling for floating support structures is presented for turbine sizes in the range of 6 to 15 MW. The graph from Figure 44 shows that for an increasing turbine size the primary floater steel mass per megawatt decreases. Although different concepts and materials probably follow slightly different scaling trends, it is used for the mass scaling of all concepts. For some designs, the masses are specified for a turbine size smaller than 6 MW. For these cases, a trendline is used to calculate the particular scaling factors (dotted line in Figure 44).

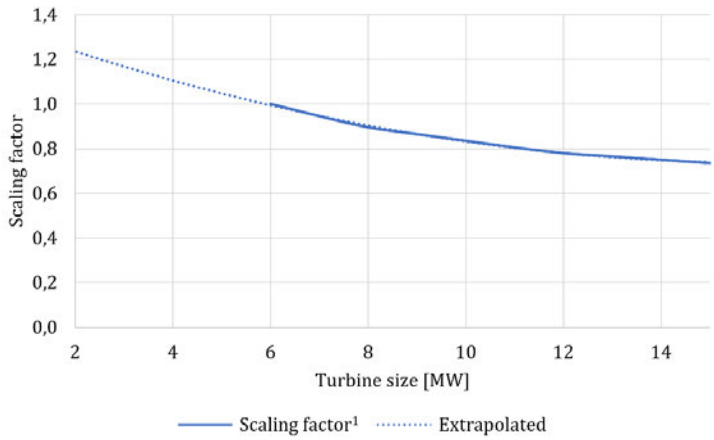

Figure 44: Scaling of primary steel mass per MW of floater (1= [97])

The manufacturing of the floater includes all necessary production steps on the way from the raw material to the assembled floating platform. It is heavily influenced by the complexity of the structure e.g., number of joints, quantity of parts, particular geometry of the parts, etc. In accordance with [107] the assembly score is determined by multiplying a complexity factor by the raw material costs:

$$s_{F,manufacturing} = f_{F,manufacturing} * s_{F,raw\ material} \tag{5}$$

Since the costs of a processed component depend on its complexity, the factor $f_{F,manufacturing}$ is intended to represent the variance in hull complexity between the different concepts. In [128] the unit price of the examined jacket is three to four times higher than that of the considered monopile. Assuming that the unit price for the raw steel is around 1.000 euros per ton (according to [107]), the factor for the processing complexity between a monopile and a jacket foundation is in the range of about three to five.

To simplify the assessment, each floater is classified into one of the five complexity classes which can be seen in Table 9. Due to the simple structure of a spar buoy, this platform type has the lowest complexity factor among all other concepts. On the other side support structures consisting of many smaller components and thus leading to a more complex geometry achieving a higher complexity factor. On the other side, semi-submersibles often show high structural complexity. It should be mentioned that in this assessment the mixture between spar buoy and semi-submersible leads to a slightly higher floater complexity than those of a conventional spar.

Table 9: Manufacturing factors by floater complexity

Cluster	Factor $f_{F,manufacturing}$	Example of structure
A	1,50	
B	1,75	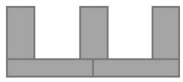
C	2,00	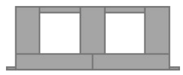
D	2,25	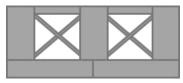
E	2,50	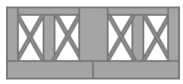

The factors B-D are determined with the help of a linear interpolation between the factors A and E.

Tower

The unweighted score for the tower is dependent on the platform typology and its respective tower design:

$$s_{tower} = s_{T,typology} * f_{T,design} \quad (6)$$

The tower score by floater typology $s_{T,typology}$ is dependent on the tower base bending moment of a particular substructure type. It is assumed that the cost score of the tower increases linearly with the tower bending moment. The applied tower scores by typology in Table 10 are orientated on the results mentioned in Section 3.2.2 .Further information for the tower factor can be found in the Appendix D.

Table 10: Tower factors by floater typology

Typology	Score $s_{T,typology}$
Barge	1,00
Semi-submersible	0,45
Spar and mix	0,50
TLP and mix	0,30

Self-aligning platforms offer the potential for using load optimized towers. As mentioned in Section 3.2.2 multi mast towers can reduce the tower weight compared to a single mast system. Taken into account that the unit price for a more complex innovative tower is higher than for cylindrical conventional tower, it is assumed that the tower costs of an innovative tower are 10 % less than these for a cylindrical tower. The factors for the single and muti mast tower are presented in Table 11.

Table 11: Tower factors by tower design

Tower design	Factor $f_{T,design}$
Single mast tower	1,0
Multi mast tower	0,9

Mooring system

The unweighted score for the mooring system is composed of the respective scores for the line and the anchor:

$$s_{mooring} = s_{M,line} + s_{M,anchor} \quad (7)$$

The score for the mooring line is dependent on the required number of lines and the platform typology:

$$s_{M,line} = f_{M,line} * n_{lines} \quad (8)$$

The line factor f_{line} is intended to reflect the line cost ratios between the different configurations. The line factors are orientated to the costs from [4] and are presented in Table 12. TLP's and its mixture concepts uses pre-stressed tendons, whereas the remaining platform types are moored with a catenary mooring line. It is assumed that due to its wave sensitivity the barge has a slightly higher line factor than the semi-submersible. According to [4] the spar buoy is advantageous in terms of line costs compared to the waterplane stabilized floater which also use catenary mooring systems. Due to the short mooring lines the TLP has the lowest mooring factor.

Table 12: Mooring configuration and line factors by typology

Platform type	Mooring configuration	Factor $f_{M,line}$
Barge	Catenary	1,00
Semi-submersible	Catenary	0,90
Spar and mix	Catenary	0,85
TLP and mix	Tendons	0,25

As for the score of the mooring line the anchor score is also dependent on the required quantity and its respective anchor factor:

$$s_{M,anchor} = f_{M,anchor} * n_{anchors} \tag{9}$$

Similar to the mooring line the anchor factor f_{anchor} represents the cost ratios between the applied anchor types. The factors are orientated to the results from [4] and are presented by floater typology and anchor type in Table 13. It is assumed that the anchor type within a platform typology stays the same. As in the study [4] a drag-embedment anchor is applied for barges, semi-submersibles, spars and its mixture concepts. Due to the vertical anchor loading of the TLP and its mixture concepts a driven pile is considered for these platform typologies. Some TLP's are also anchored to the seabed using gravity anchors which is slightly cheaper than a pile anchor but more expensive than a DEA. [4].

Table 13: Anchor type and factors by floater typology

Platform type	Anchor type	Factor $f_{M,anchor}$
Barge	Drag-embedment	0,28
Semi-submersible	Drag-embedment	0,25
Spar and mix	Drag-embedment	0,25
TLP and mix	Driven pile	0,50
	Gravity foundation	0,30

Installation

The unweighted score for the installation of a floater concept is dependent on the installation effort for the turbine, the floater, and the mooring system:

$$s_{installation} = s_{I,turbine} + s_{I,floater} + s_{I,mooring} \tag{10}$$

The scores for the installation of the turbine and the floater are dependent on the applied installation strategy (A-C). The respective installation strategy of a concept is dependent on its draft and tow-stability. For each floater typology the applied strategy including its installation vessels requirements for the port procedure, the transport of the platform to the wind farm, and the installation at sea are given in Table 14.

Table 14: Required vessels for different installation strategies (data based on [81])

<table>
<tr><th>Installation part</th><th>Strategy A</th><th>Strategy B</th><th>Strategy C</th></tr>
<tr><td>Port procedure</td><td>Onshore crane</td><td>Onshore crane</td><td>Onshore crane</td></tr>
<tr><td>Transport</td><td>Tug vessel</td><td>Tug and barge vessels</td><td rowspan="2">Floating crane with storage</td></tr>
<tr><td>Installation at sea</td><td>-</td><td>Floating crane without storage</td></tr>
</table>

The installation costs calculated in [81] are used for score determination for the installation of the floater and the turbine. The scores derived from the results of the cost study from [81] are shown in Table 15. The installation costs for both the floater and the turbine are the highest for strategy C because of the cost-intensive floating crane with storage. Strategy B requires a floating crane without storage which is not as cost-intensive as the installation vessel for strategy B resulting in lower installation costs both for the turbine and the floater. Strategy A achieves the lowest installation costs due to less cost-intensive vessels.

Table 15: Installation scores by installation strategy (data based on [81])

Draft	Tow stability	Installation Strategy	Score $s_{I,turbine}$	Score $s_{I,floater}$
Low	High	A	0,03	0,18
High	High	B	0,10	0,25
High	Low	C	0,30	1,00

The installation score of the mooring system is dependent on the quantity of the mooring lines and the anchors:

$$s_{I,mooring} = (n_{line} + n_{anchor}) * f_{I,mooring} \tag{11}$$

With $f_{I,mooring} = 0{,}03$.

In [81] it is assumed that the overall costs of the mooring system installation (lines and anchors) are directly dependent on the number of mooring lines and anchors while the mooring configuration does not influence the installation costs. As a result, the mooring costs increase with an increasing number of lines and anchors. Due to the lack of data, this approach is also used in this study to calculate the installation score for the mooring system. The installation factor $f_{I,mooring}$ represents the installation effort per line and anchor and relates this to the installation effort for the floater and the turbine.

Operations & maintenance

The unweighted score for the O&M is dependent on the applied maintenance strategy and the accessibility of the platform:

$$s_{O\&M} = s_{O\&M,strategy} * f_{O\&M,accessibility} \tag{12}$$

The draft, the tow stability, and the mooring system of a particular concept influences the choice of the applied maintenance strategy. As mentioned in Section 3.2.5 the OPEX in the study [109] are determined for two different typologies (semi-submersible and spar) and three different sites. The results of this study form the basis for the maintenance strategy scores. Since the cost ratios between the investigated platform types vary for different sites, the average cost ratio is applied for this comparison. The study [109] does not include TLP's but since the taut leg mooring of a TLP requires complex and time-consuming ballasting of the structure to disconnect the mooring lines it is assumed that this foundation type is not considered for a tow-in strategy. In Table 16 the maintenance score $s_{M,strategy}$ is presented by floater typology.

Table 16: O&M factors by typology and strategy (data based on [109])

Mooring configuration	Draft	Tow stability	Maintenance strategy	Score $s_{O\&M,strategy}$
Catenary	Low	High	Tow to shore	0,75
	High	High	Floating-to-floating	1,00
Taut-leg	-	-	Floating-to-floating	1,00

Usually, the motion characteristics of the TLP lead to an increased accessibility compared to other typologies [20]. As a result, the TLP achieves a slightly lower score for the accessibility of the FOWT compared to the spar buoy.

Table 17: Accessibility factors for spar buoy and TLP

Floater typology	Factor $f_{O\&M,accessibility}$
Spar & mix	1,00
TLP & mix	0,95

Since the mooring system has no significant influence on the OPEX (see Section 3.2.3) those costs are not included in the O&M score.

5.2.2 Weighting of criteria

The total score of a concept is the sum of the multiplied unweighted scores with their respective criteria weights:

$$S = \sum_{i=1}^{5} S_{u,i} * w_i \tag{13}$$

To reduce the subjectivity for the weighting of the criteria the weights are determined based on a cost breakdown of a floating wind turbine. Consequently, a criterion weighting depends on its respective cost share in the total LCOE. The Figure 45 shows the applied cost split for the weighting of the five criteria. This cost breakdown is adopted from [83] and is valid for a floating wind turbine mounted on a semi-submersible platform. Based on this base case semi-submersible all concepts are compared.

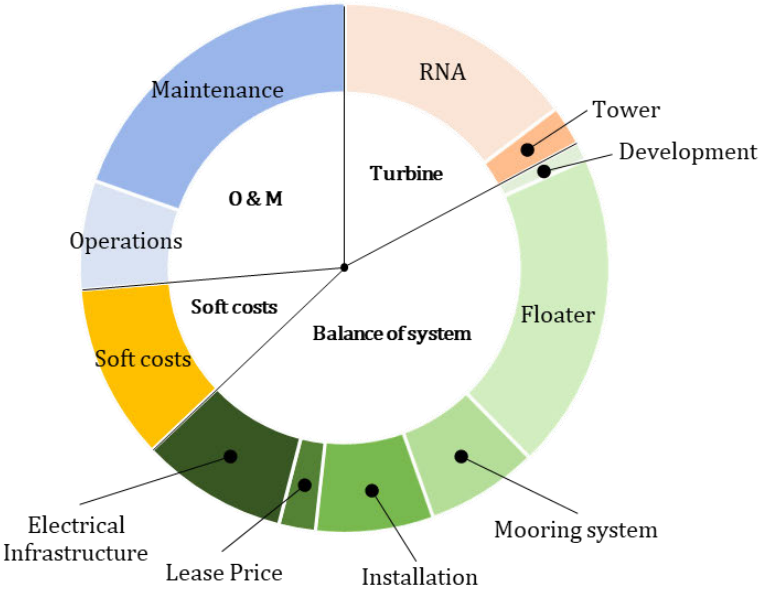

Figure 45: Base case cost breakdown of a FOWT [author's illustration, data based on [83]]

According to [83] the share of costs for the floater, the tower, the mooring system, the installation, and the O&M in the total LCOE is $cs_{total} = 61{,}2\ \%$.

Based on [83] the total cost share of the floater and its foundation is $cs_{floater\&foundation,total} =$ 27,1 % of the total LCOE of a FOWT. According to [4], the cost of the floater and foundation consists of $cs_{floater} = 73{,}9$ % of the cost of the floater and $cs_{mooring} = 26{,}1$% of the cost of the mooring system. Based on these assumptions the weightings for the floater and the mooring system are as follows:

$$w_{floater} = \frac{cs_{floater} * cs_{floater\&foundation,total}}{cs_{total}} = \frac{73{,}9\ \% * 27{,}1\ \%}{61{,}2\ \%} = 32{,}7\ \% \qquad (14)$$

$$w_{mooring} = \frac{cs_{mooring} * cs_{floater\&foundation,total}}{cs_{total}} = \frac{26{,}1\ \% * 27{,}1\ \%}{61{,}2\ \%} = 11{,}6\ \% \qquad (15)$$

[83] considered that the cost for the tower is $cs_{tower} = 14{,}0$ % of the total costs of the RNA including the tower. The total cost share of the RNA and the tower is $cs_{RNA\,\&\,tower,total} = 17{,}6$ %. Based on these assumptions the weighting for the tower can be calculated:

$$w_{tower} = \frac{cs_{tower} * cs_{RNA\,\&\,tower,total}}{cs_{total}} = \frac{14{,}0\ \% * 17{,}6\ \%}{61{,}2\ \%} = 4{,}0\ \% \qquad (16)$$

For the installation, [83] calculated a total cost share of $cs_{installation,total} = 4{,}1$ %. Based on this assumption the following weight is considered for the installation:

$$w_{installation} = \frac{cs_{installation,total}}{cs_{total}} = \frac{4{,}1\ \%}{61{,}2\ \%} = 6{,}7\ \% \qquad (17)$$

According to [83] the total cost share for the OPEX is $cs_{O\&M,total} = 27{,}5$ % and the weighting can be determined as follows:

$$w_{O\&M} = \frac{cs_{O\&M,total}}{cs_{total}} = \frac{27{,}5\ \%}{61{,}2\ \%} = 45{,}0\ \% \qquad (18)$$

An illustration of the individual criteria weights is presented in the Figure 46.

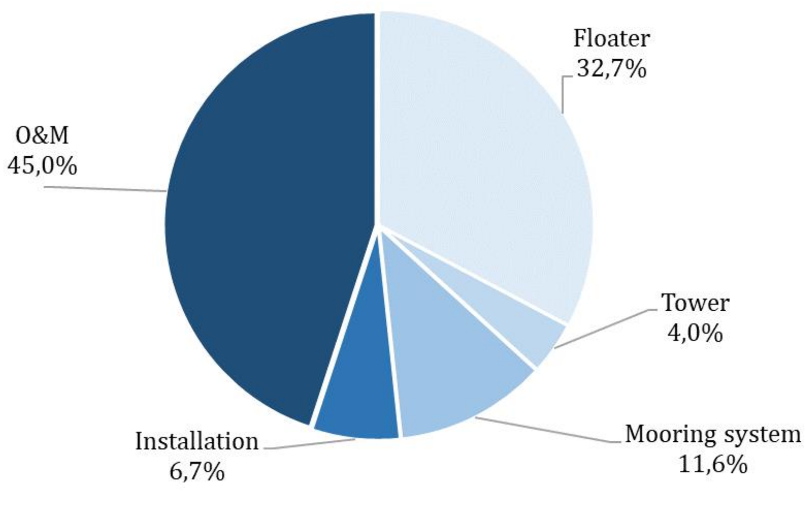

Figure 46: Criteria weightings [author's illustration]

5.2.3 Results

The results of the cost assessment are illustrated in Figure 47 and Figure 48 for the generic floater typologies. The results for the individual commercial concepts can be seen in Appendix H. The closer the graph of a typology is to the center of a criterion, the better this concept performs in this category. Overall, the illustrated results represent well the strengths and weaknesses of the respective concepts in the different categories.

It can be seen that no generic concept is able to achieve the lowest score in all categories. Each concept has advantages as well as disadvantages. As a result of its low structural weight, the TLP shows the best result among all other concepts in terms of the score for the floater. The spar buoy is able to achieve a low score for the floater as well but unlike the TLP this is a result of its simple cylindric geometry which leads to advantages in terms of substructure production. The relatively high mass in combination with its more complex structure results in a worse score for the semi-submersible compared to the TLP and the spar buoy. As it is assumed that the barge concept requires the highest hull mass among the other typologies, this concept performs worst in this category.

As mentioned in Section 3.2.2, the motion of the platform impacts the loads and thus the costs of the tower. The motion characteristics of the TLP are comparable to those of bottom-fixed structures resulting in small tower loads compared to the other investigated concepts. Consequently, the TLP achieves the best score for the tower among all other concepts Due to its wave sensitivity the semi-submersible achieves usually higher tower bending moments than the TLP and thus performs worse in this category. As the spar buoy is susceptible to large rotational movements, the tower bending moment is slightly higher than that of a semi-submersible. As a result, the tower score of the spar buoy is lower than that of the semi-submersible. Usually, the barge has the largest waterplane area compared to the other concepts, which makes the platform highly susceptible to waves. These wave-induced motions lead to comparatively high tower bending moments and thus the highest tower score.

Since the installation strategy as well as the number of lines and anchors is the same for the barge and the semi-submersible, both concepts achieve the same score in this category. Due to the port side assembly of the RNA and tower combined with the low towing requirements, the barge and the semi-submersible score the best in this category. The spar buoy can be towed by tug boats to the wind farm but requires a floating crane for mounting the tower and the RNA on the floater. This makes this platform type less suitable for a cost-effective installation compared to a barge and semi-submersible. In terms of installation effort, the TLP is behind the other structures. This is due to the cost-intensive floating crane with storage in combination with a long installation duration.

In terms of the mooring system, the scores between the typologies do not vary significantly. The semi-submersible, the spar buoy, and the TLP achieve nearly the same score. The relatively small loads on the catenary mooring system of the semi-submersible and the spar lead to low line costs per meter. However, this advantage is compensated by the long mooring line length of catenary systems compared to the tendons. Although the mooring line forces are higher for the tendons of the TLP than the line forces of catenary systems, its shorter length compensates this advantage which leads to an equality of costs. As mentioned before the barge has a high susceptibility to waves which must be compensated by the mooring system. Due to these higher line loads, the barge achieves a higher mooring score.

The O&M effort of a concept is heavily influenced by the applied strategy. It is assumed that the tow-in strategy which is considered for the barge and the semi-submersible is advantageous over the F2F strategy. That's why the barge and the semi-submersible performs the best in this category. The better accessibility of the TLP compared to the spar buoy causes the TLP to score slightly better than the spar buoy.

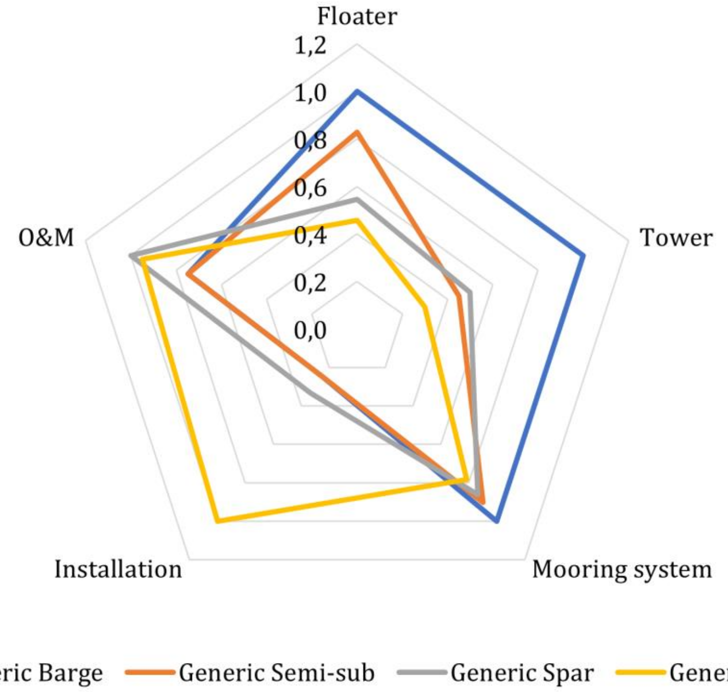

Figure 47: Results cost assessment of the four main generic concepts [author's illustration]

In Figure 48, the scores of the generic mix concepts are compared to their respective parent concept. The mixture between spar and semi-submersible is able to decrease its installation requirements and is thus on par with the semi-submersible. On the other side, it is assumed that the floater hull of the mixture concept is more complex than a conventional spar buoy, making the production of the substructure more cost-intensive than those of the generic spar buoy. The differences between the mixture and its parent typologies in the categories tower and mooring system are relatively low. As a F2F strategy is assumed for the O&M of the mixture concept, its score is the same as for the spar buoy in this category.

Due to the low draft and the high towing stability, the TLP mixture can benefit from a different installation strategy and thus decreasing the installation effort compared to the main TLP concept. As it is assumed that the weight of the mix concept increases compared to the TLP, the cost score for the floater increases as well. The mixture concept can benefit from the TLP's low tower bending moment and its lower mooring requirements. Since the O&M for the mixture is the same as for the generic TLP concept, their scores are the same.

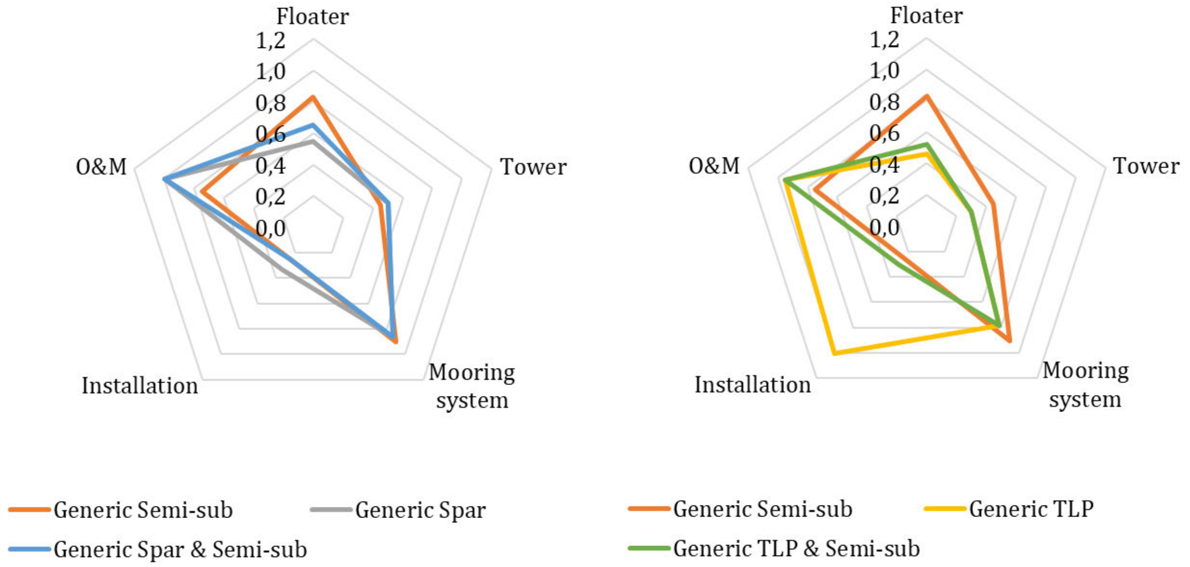

Figure 48: Results cost assessment of the main generic mix concepts [author's own illustration]

Figure 49 shows the score deviations of the generic concepts compared to the base case (semi-submersible) for the respective criteria. Next to that, the rhombus indicates for each concept the total score difference compared to the base case. The figure indicates which factors are decisive for the rankings of the different concepts.

The barge performs slightly worse in the categories floater, tower, and mooring system compared to the base case. Since the barge has no advantages over the semi-sub in any category, the sum of the disadvantages alone determines the total score difference.

The advantages of the spar buoy in terms of floater and mooring system are compensated by the disadvantages in the areas of installation and O&M whereby the operations and maintenance is the deciding factor. Overall, the spar buoy scores slightly worse than the semi-submersible.

The largest score difference in a category compared to the semi-submersible is achieved for the installation of the TLP. Combined with the higher maintenance effort these criteria are responsible for the poor ranking of the tension leg platform. The advantages in terms of floater and tower are not sufficient to compensate for these disadvantages.

The mixture between spar buoy and semi-submersible leads to advantages for the installation compared to the spar buoy. Since it is assumed that the concept can be towed out fully assembled it achieves a lower installation score compared to the spar buoy. However, the floating stability is achieved by the more expansive structure and the hanging counterweight which both lead to a more complex and thus more cost-intensive substructure.

The mixture between TLP and semi-sub scored the best among all other concepts. This is mainly attributed to the cost advantage for the floater. The main factor for the poor ranking of the TLP is its installation effort. It is assumed that the mixture between TLP and semi-submersible can also be towed out fully assembled reducing the vessel requirements.

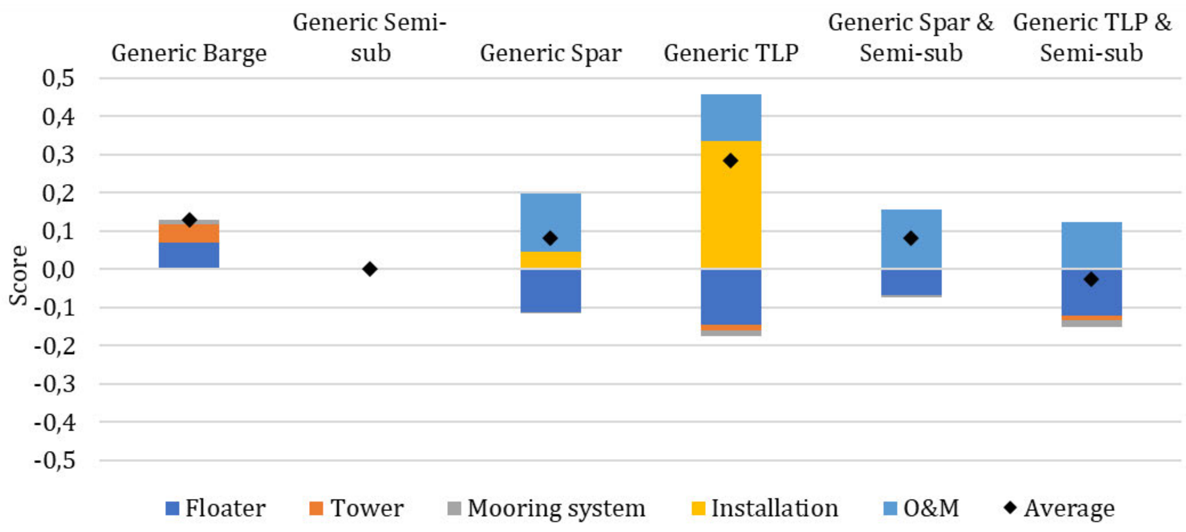

Figure 49: Score deviations of generic main concepts from generic base case semi-submersible [author's illustration]

The maximum score differences within the categories for the six generic floater types are presented in Figure 50. Due to the comparatively high expenditures for the installation of the TLP, the highest score difference can be seen for the category installation. As a result of the low hull mass of the TLP in combination with the high weighting of the criterion floater, the second highest score difference is achieved in the category. Although the criterion O&M has the highest weight among the other criteria, the score difference is not the largest for this criterion. This is due to the little unweighted score difference between the concepts in terms of O&M. Since the weight of the criterion tower is the lowest among the other concepts the score difference is the second lowest. Despite the three times higher weighting of the mooring system compared to the weighting of the tower, the score difference for the SKS is the lowest. The reason for that is the small bandwidth of the different mooring scores.

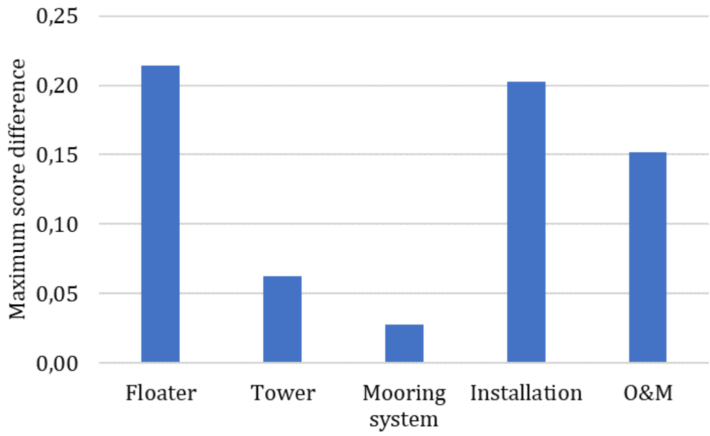

Figure 50: Maximum score differences between the categories determined for the main generic floaters [author's illustration]

The deviations for the market concepts are relatively similar to those of the main concepts. The biggest difference can be identified in terms of the criterion floater. Due to the high hull mass differences between the concepts, the score largely varies between the designs within this category.

5.3 Environmental flexibility assessment

The environmental flexibility assessment aims to compare the FOWT concepts in terms of their limitations and restrictions for specific site conditions. This comparison shall indicate the impact of different site conditions on the suitability for offshore wind farm deployment of a respective concept. For this purpose, the main generic concepts are assessed based on four weighted criteria. The criteria are selected on the basis on the site-specific restrictions which are identified in the literature review. The site conditions can affect the FOWT in terms of aspects like their dimensioning, durability, energy yield, and risk of failure. Furthermore, some conditions can lead to the fact that a concept cannot be deployed at this location. The most important limitations and restrictions that could be determined are water depth, waves, current including tidal hubs, and soil conditions. The concepts identified in the market receive the score that the respective generic floater typology achieves. An exception is made for a low draft spar buoy floater and a self-aligning mixture concept (TLP and semi-submersible) in terms of the score for the water depth. Differences because of hull materials are not included in this comparison due to the lack of data and the scope of this work.

The identification of the criteria weighting is carried out with the help of a pairwise comparison. For this purpose, two criteria are compared with each other in terms of their respective impact on the limitations and restrictions. The more important criterion of a head-to-head comparison receives one point. If two compared criteria have the same importance, then no criterion receives a point.

The number of pairwise comparisons is calculated as follows:

$$n_p = \frac{n^2 - 1}{2} \tag{19}$$

With $n =$ number of flexibility criteria.

After each possible head-to-head comparison is carried out the criteria are ranked in accordance with their respective number of points. Then the overall weighting of each criterion is determined:

$$w_F = \frac{w_{F,sum}}{s_{rankings}} * r_{inverse} \tag{20}$$

With $w_{F,sum}$ = sum of weights, $s_{rankings}$= sum of rankings, and $r_{inverse}$ = inversive ranking.

In Figure 51 the matrix for the pairwise comparison is presented whereas Table 18 shows the resulting criteria weights. As the water depth receives the most points, it is the highest weighted criterion among the others. Especially buoyancy stabilized platforms require a sufficient water depth for their operation. Too shallow water can be an exclusion criterion for the choice of a platform type.

High waves can be very challenging for floating platforms as they can result in large wave-induced motions. These more extreme platform motions can lead to increased structure loads. For example, wave-induced motions can influence the tower bending moment as well as the mooring line loads. Since they do not necessarily result in an exclusion of this structure for this specific site condition it receives a slightly lower weight than the criterion water depth.

Depending on the platform type the currents can also affect the operation of a FOWT. Risks associated with strong currents are high platform surge motions, loosening of tension in tendons, and wind-wave & current misalignments.

Due to the high variety of anchoring options, the soil conditions have the smallest weight among the other concepts. In dependence on the requirements, a suitable anchor can be selected for nearly any soil conditions. Some typologies may have a smaller bandwidth to choose from than others which could result in higher anchor expenses.

	Water depth (A)	Waves (B)	Current (C)	Soil conditions (D)
Water depth (A)		A	A	A
Waves (B)			B	B
Current (C)				C
Soil conditions (D)				

Figure 51: Pairwise comparison matrix for flexibility criteria [author's illustration]

Table 18: Weighting of flexibility criteria

Criterion	Weighting
Water depth	0,4
Waves	0,3
Current	0,2
Soil conditions	0,1

In Table 19 the results of the flexibility analysis are presented for the main floater typologies. In accordance with the cost assessment, small scores indicate a high potential whereas high scores indicate a low potential for offshore wind farm deployment. It is assumed that site limitations and restrictions can also lead to additional expenses for the FOWT as it could affect the lifecycle costs. The unweighted score by typology and category can be seen in Appendix I.

Since semi-submersible performs above average in all categories, it is the most flexible solution among the others.

As a result of the higher susceptibility to waves, the barge receives a higher score in this category compared to the semi-submersible. This leads to a slightly higher overall score compared to the semi-submersible.

The strongly tensioned tendons of a TLP require a constant water depth since otherwise the lines could be loosened. This leads to the fact that the TLP cannot be deployed in locations with strong tidal hubs and thus receives the highest score in this category compared to the other concepts.

Mainly due to the high draft requirements in combination with the high criterion weight of the water depth the spar buoy is the least flexible concept compared to the others. Next to that in the category current, the spar buoy achieves a higher score compared to the barge and the semi-submersible. This is due to the high current loads which can occur because of the long structure under the water surface. Another aspect is vortex-induced motions, which can lead to fatigue loads in the structure. As the slender spar buoy is less susceptible to waves compared to the buoyancy stabilized typologies it achieves a lower score than the barge and semi-submersible.

An issue with self-aligning wind turbines can result of a misalignment between wind and wave/current. This can result in a yaw error reducing the performance of the wind turbine. [44] That is why self-aligning platforms increase the score of its main floater typology in this category by 0,1 weighted points. The individual results for the commercial concepts can be seen in Appendix J.

Table 19: Weighted flexibility scores by category and floater typology

Concept	Water depth	Waves	Current and tidal hubs	Soil conditions	Standardized sum
Barge	0,40	1,20	0,20	0,10	1,19
Semi-submersible	0,40	0,90	0,20	0,10	1,00
Spar and mix	1,60	0,60	0,40	0,10	1,69
TLP and mix	0,80	0,30	0,80	0,30	1,38

5.4 Results

In Figure 52 the results for the two-dimensional weighted point analysis are illustrated. The horizontal axis indicates the score for the cost assessment, while the vertical axis shows the score of the flexibility analysis. The concepts that have the highest potential for offshore wind farm deployment are located in the lower-left corner of the figure. Consequently, concepts that are placed in the upper-right corner have the smallest potential. Steel concepts are marked with a cross, while concrete designs are illustrated with a point.

Comparing the results of the steel floaters with each other, the lowest cost scores and thus the lowest expenditures are achieved by self-aligning semi-submersible concepts. The combination of a lightweight substructure and a load-optimized tower design lead to cost advantages compared to the base case semi-submersible. As the energy yield of self-aligning platforms can be affected by wind-wave misalignments the flexibility score is slightly higher compared to the base case semi-submersible.

Driven by a high variance regarding weight and complexity within the investigated semi-submersible concepts the highest bandwidth in terms of the cost-specific scores is achieved for this floater typology. The best non-self-aligning semi-submersible concepts achieve cost scores in the range of 0,95. On the other side, the least ranked semi-submersible floater has a cost score that is 50% higher compared to the base case. This is a result of the high hull material weight of this concept.

The by far highest hull mass among all concepts is achieved by a low draft spar buoy design. This comparatively high platform weight results in a cost score of 2,09 which is nearly twice as much as the cost score for the generic spar buoy. As a result of its low draft, it is assumed that the installation strategy A can be applied which reduces the costs for installation compared to the generic spar buoy. Next to that, the low draft leads to a lower flexibility score than for the conventional spar buoy.

On average, combining the characteristics of a TLP and a semi-submersible can result in cost advantages, giving it a lower cost rating than either of its parent types. The reasons for that are the lightweight structure combined with low tower loads and a simple installation methodology. In terms of flexibility, however, these concepts perform slightly worse than the semi-submersible. Due to its reduced draft, one self-aligning design achieves a lower flexibility score compared to its generic floater typology. One self-aligning mixture concept achieves a lower flexibility score than the other concepts in this class. The reason for this is the shallow draft of the TLP&semi-sub mixture, which makes it applicable for shallower waters.

None of the investigated barges, TLP's, spar buoys, and their mixtures (spar and semi-submersible) achieve better cost scores than the base case. On the other side, the cost score bandwidth for these concepts is smaller than that of the semi-submersible concepts. The same phenome is also obtained in [4] (see Figure 26), in which developers of commercial concepts provided cost data for their floater technology.

On average the best performing concrete concepts in terms of the cost scores are again semi-submersibles. The two lowest cost scores among all concepts are achieved by semi-submersible designs. The self-aligning concrete semi-submersible can achieve a cost score of slightly above 0,7. The second best concrete semi-submersible performs better in terms of environmental flexibility as it does not rely on a self-aligning system. The best self-aligning barge achieves a cost score of about 0,85. The only investigated concrete spar receives a cost score of 1,14 which places it among the

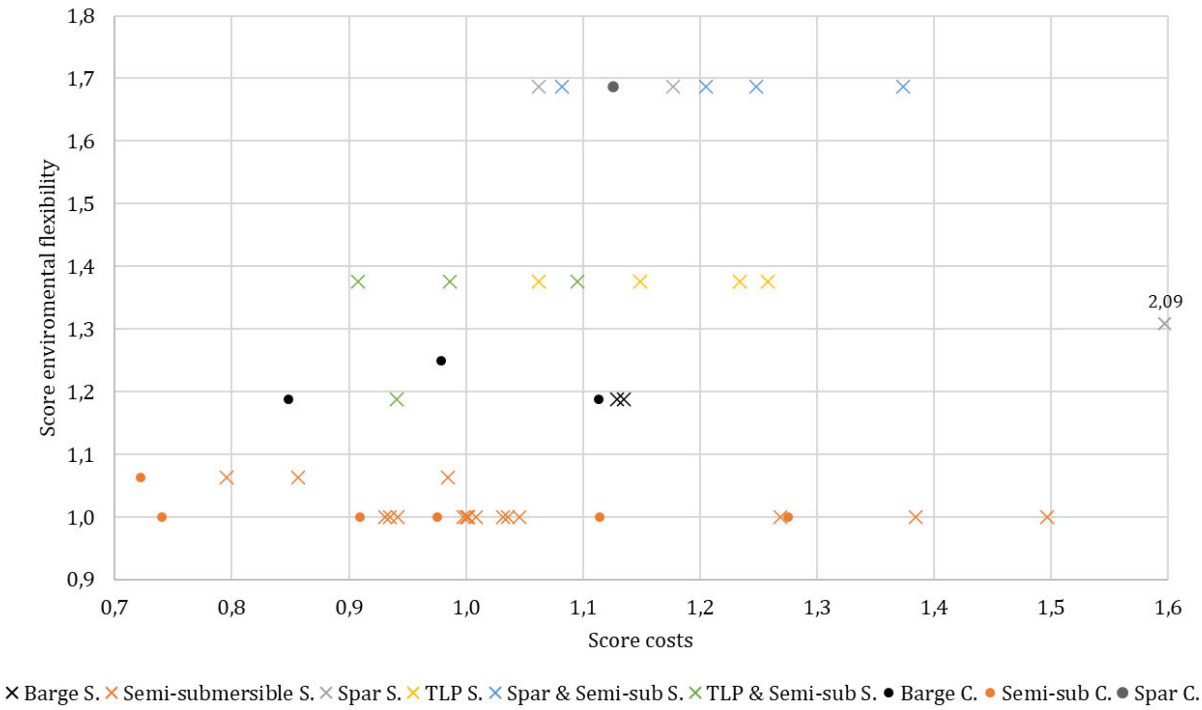

Figure 52: Results floater assessment S.=steel, C.=concrete [author's illustration]

5.5 Uncertainties

This section is intended to give a brief overview of the uncertainties associated with concept assessment. The aim is to draw attention to the difficulties and challenges that the evaluation of the designs entails.

In general, an assessment that fairly evaluates floater typologies and existing commercial concepts in the market in terms of their respective potential for offshore deployment poses high challenges for the comparison methodology. Due to the high individuality of the foundation concepts, it may be challenging to identify all parameters which affect the suitability of the platform for offshore wind farm deployment. Next to that, the lack of data for the several designs causes the designs to adopt the respective characteristics of their parent floater typology leading to a generalization of its properties. Usually, the characteristics of the designs are not directly identifiable to only one category but can range borderless between two or more main typologies or concepts. An example is the determination of the score for the tower which is mainly based on the motion behavior of the platform. Thereby the floater concepts adopt the respective scores achieved by their parent typology. However, the motion behavior within a floater typology can vary significantly and is highly dependent on the floater design and control. As a result, those simplifications lead to limitations in terms of fair comparability since some characteristics of certain floater designs could not be included. Another example is the score determination for the manufacturing of a substructure. As stated in several sources the costs for the manufacturing of a floater are based to a large extent on its applied manufacturing methods. Due to the lack of data, these production methods could not be included in this assessment. For this purpose, the concepts are categorized into five groups which classifies the substructures regarding their respective hull complexity. This may result in certain production-specific properties of concepts not being taken into account. Next to the manufacturing method, the grade of the floater hull material is an important factor that influences its unit price. Due to the lack of data, these aspects could not be included in the score calculation. Only the material and its consumption determine the raw material score of a concept. As a result, cost disparities due to different material qualities cannot be covered.

Next to that the score determination for the cost criteria is directly dependent on the underlying assumptions made in the respective cost study. Until today a lot of uncertainties are related to the determination of costs for a FOWT. As seen in Sections 3 and 4.2 this can result in significant cost differences between different cost assessment studies. A specific example is the vessel day rates for installation and O&M. Since, depending on the study, the cost ratios between the different types of ships may vary, the evaluations of the concepts are highly dependent on the underlying data Another risk associated with the determination of weightings is that a completeness of cost parameters for the respective categories is assumed. As the weightings are based on a cost breakdown for a FOWT it is considered that the included parameters in the score determination represent the whole expenses for a respective cost category. An exception of cost aspects within categories may result in an overweighting of criteria. An example is the composition of the score for the production of the substructure. It is composited of the costs for the raw material and the costs for the manufacturing. An aspect that is here not included due to the lack of data is the ease of handling a concept. Therefore, the differences between the concepts in terms of material effort and substructure complexity sum up to the overall score within the floater category.

As the pairwise comparison for the flexibility assessment is based on the (subjective) estimation of the author the individual weighting can differentiate between raters. Next that the level of intensity of a respective limitation is not covered in this assessment. This could affect the results of this comparison. A possibility for measuring the relative importance of a flexibility criterion is to investigate the site conditions of potential FOWTS locations. Depending on the probability of occurrence of each limitation or restriction the four criteria could be compared and weighted with each other. However, such an investigation would exceed the scope of this master thesis.

In addition to that, the scores in the flexibility categories can differentiate for the individual concepts within one floater typology. To reduce the effort of this assessment and due to the lack of data, the scores of the designs are only determined for the generic concepts. Depending on the superordinate generic concept, the market designs are evaluated and classified. For example, some concepts within a floater typology may be more susceptible to currents than others which would not be included in this assessment.

6 Numerical analysis of FOWT

In this chapter, a numerical analysis of a floating wind turbine is presented. The model is based on the results of the report [7] which investigates a steel version of the semi-submersible named VolturnUS by UMaine and the U.S. Department of Energy. As a first step, Section 6.1 is intended to provide a basic theory background for wave theory, wave loads, and RAOs. In the following Section 6.2, the general project information of the numerical simulation is described. The properties of the numerical model including its support structure, RNA as well as tower, and mooring system are presented in Section 6.3. The results of the simulation are summarized in Section 6.4.

6.1 Theory background

In this section the most important basic theory for the regular and irregular waves (Section 6.1.1), wave loads on floating structures (Section 6.1.2) as well as response amplitude operators (Section 6.1.3) is presented.

6.1.1 Wave theory

The following wave theory for regular and irregular ocean waves is from [129].

Regular waves

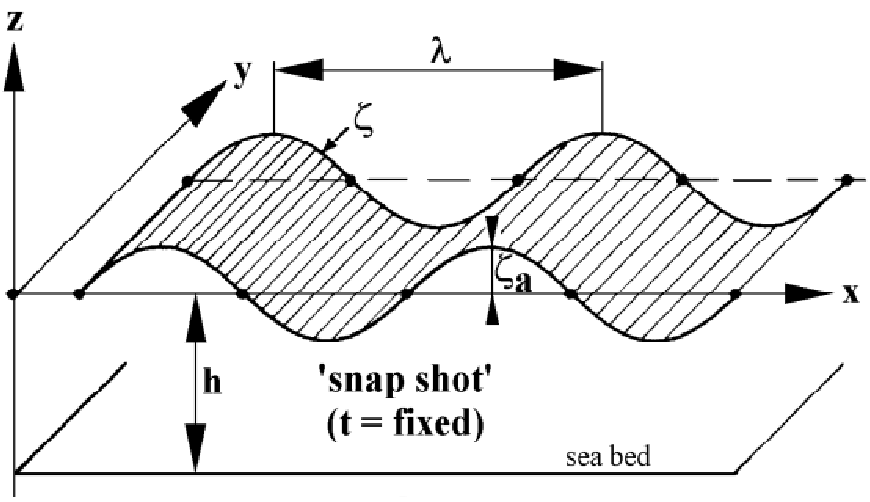

Figure 53: Harmonic wave definition [130]

With:

- λ = wavelength
- ζ_a = wave amplitude
- $H = 2 * \zeta_a$ = wave height
- h = water depth
- H/λ = wave steepness

A basic assumption for several wave theories is that the sea water is an incompressible, inviscid fluid and irrotational fluid. To describe the fluid velocity vector **V**(x,y,z,t)=(u,v,w) at time t at the point x=(x,y,z) in an Cartesian coordinate system, a velocity potential Φ can be used: [129, p. 13]

$$\mathbf{V} = \nabla\phi = \boldsymbol{i}\frac{\partial\phi}{\partial x} + \boldsymbol{j}\frac{\partial\phi}{\partial y} + \boldsymbol{k}\frac{\partial\phi}{\partial z} \tag{21}$$

Where $\boldsymbol{i}, \boldsymbol{j}$ and $\boldsymbol{k}$ are unit vectors along the x-, y-and z-axes. "The fluid is irrotational when the vorticity vector,

$$\omega = \nabla \times \mathbf{V} \tag{22}$$

is zero everywhere in the fluid." [129, p. 13] Because the fluid is incompressible $\nabla \times \mathbf{V} = 0$ and the velocity potential has to satisfy the Laplace equation, it can be written:

$$\frac{\partial^2\phi}{\partial x^2} + \frac{\partial^2\phi}{\partial y^2} + \frac{\partial^2\phi}{\partial z^2} = 0 \tag{23}$$

To find the velocity potential of irrotational, incompressible fluid motion, the Laplace equation must be solved with relevant boundary conditions. As this thesis does not present the mathematical forms of the boundary conditions, it is referred to [129]. The pressure is determined from the Bernoulli's equation. With the kinematic (no fluid enters or leaves the body surface) and the dynamic boundary condition (water pressure is the same as the constant atmospheric pressure on the free surface) and "when the velocity potential oscillates harmonically in time with circular frequency ω it can be written": [129, p. 17]

$$-\omega^2\phi + g\frac{\partial\phi}{\partial \mathrm{z}} = 0 \qquad \text{on: } z = 0 \tag{24}$$

Where g defines the acceleration of gravity.

For a horizontal sea bottom and an infinite horizontal free-surface the linear wave theory (Airy theory) can be derived for propagating waves. For that the Laplace equation is together used with the free-surface boundary conditions and the sea bottom condition,

$$\frac{\partial\phi}{\partial \mathrm{z}} = 0 \qquad \text{on: } z = -h \tag{25}$$

with h for the mean water depth.

The whole derivation of the linear wave theory is not presented here. For more information it is referred to [129]. However, the solution of velocity potential of the linear wave theory for an infinite water depth can be written as: [131, p. 47]

$$\phi = \frac{\mathrm{g}H}{2\omega}\frac{\cosh[k(z+h)]}{\cosh(kh)}\sin(kx - \omega t) \tag{26}$$

With $k = 2\pi/\lambda$

For an infinite water depth $z \to -\infty$ the velocity potential can be simplified to: [131, p. 47]

$$\phi = \frac{\mathrm{g}H}{2\omega}e^{kz}\sin(kx - \omega t) \tag{27}$$

Irregular waves

In an irregular sea state both, the wavelength, and the wave height vary continuously. By using a linear superposition of wave components, it is possible to represent an irregular sea surface. "The wave elevation of a long-crested irregular sea propagating along the positive x-axis can be written as the sum of a large number of wave components": [129, p. 23]

$$\zeta = \sum_{j=1}^{N} A_j \sin\left(\omega_j t - k_j x + \epsilon_j\right) \tag{28}$$

Where A_j defines the wave amplitude, ω_j represents the circular wave frequency, k_j is the wave number and ϵ_j are random phase angle of a wave component.

In Figure 54 an example can be seen how two regular waves can be added up to one irregular wave.

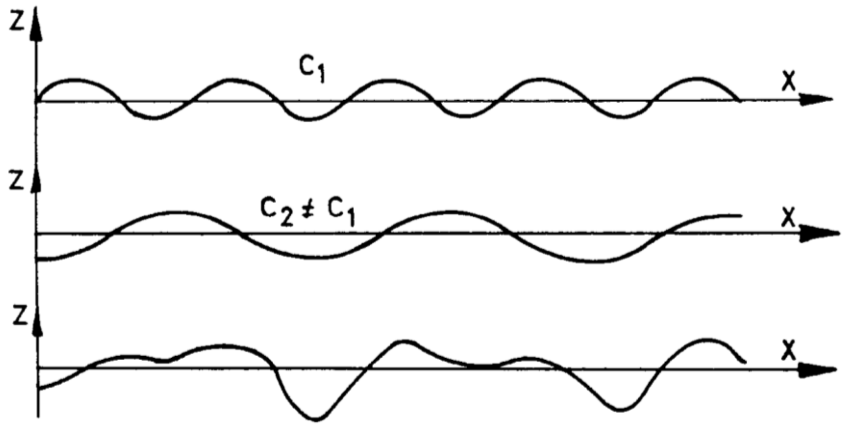

Figure 54: Superposition of two uni-directional harmonic waves [130]

The wave amplitude A_j can be described by a wave spectrum $S(\omega)$:

$$\frac{1}{2}\mathrm{A}_j^2 = S(\omega_j)\Delta\omega \tag{29}$$

Whereas $\Delta\omega$ defines a constant difference between succussive frequencies.

As a result of a wave measurement program in the North Sea between 1968 and 1969 the JONSWAP wave spectrum was evaluated. The JONSWAP wave spectrum defines the distribution of energy with frequency within ocean waves: [129]

$$S(\omega) = 155 \frac{H_{1/3}^2}{T_1^4 \omega^5} \exp\left(\frac{-944}{T_1^4 \omega^4}\right) 3{,}3^Y \tag{30}$$

$$Y = \exp\left(-\left(\frac{0{,}191\omega T_1 - 1}{2^{\frac{1}{2}}\sigma}\right)^2\right) \tag{31}$$

And

$$\sigma = 0{,}07 \qquad \text{for} \qquad \omega \leq 5{,}24/T_1 \tag{32}$$

$$\sigma = 0{,}09 \qquad \text{for} \qquad \omega > 5{,}24/T_1 \tag{33}$$

$H_{1/3}$ is called significant wave height and is defined as the average height of the one third largest waves. T_1 (0,834) is the mean wave period. [129] The peak enhancement factor γ describes ration between the maximum wave spectral density of the JONSWAP spectrum and the Pierson-Moskowitz spectrum. [132]

6.1.2 Wave loads on floating wind turbines

The loads acting on a floating structure can be divided into static and dynamic loads. Static loads are hydrostatic loads, gravitational loads, deck loads and current. The dynamic loads are time varying loads which occur due to waves and/or wind. Both the static and the dynamic loads must be considered in the design process of floating structures. [133] In the following the wave loads on floating structures shall be presented more in detail.

Equation of motion

In (34) the equation of motion for a rigid body can be expressed as: [129, p. 66]

$$\left(M_{jk} + A_{jk}\right)\ddot{\eta_k} + B_{jk}\dot{\eta_k} + C_{jk}\eta_k = F_{jk} \tag{34}$$

With:

M_{jk}=component of mass matrix

A_{jk}=component for added mass matrix

B_{jk}=component for damping matrix

C_{jk}=component of stiffness matrix

F =external excitation force vector

η, $\dot{\eta}$ and $\ddot{\eta}$ are the displacement, velocity and acceleration vectors. Each containing six DOF's, three translatory and three rotatory.

When written in matrix form the equation of motion is the following:

$$\big(M + A(\omega)\big)\ddot{\eta} + B(\omega)\dot{\eta} + C\eta = F \tag{35}$$

Response in regular waves

According to [129] and [130] the hydrodynamic problem in regular waves can be divided into two sub-problems. It is assumed a steady state condition which means that there are no transient effects present due to initial conditions:

A. Forces and moments when the structure is restrained from oscillating are called wave excitation loads. These loads can further be divided into the Froude-Kriloff and the diffraction forces and moments.
B. Forces and moments when the structure is oscillating with the wave excitation frequency are called radiation loads. In this case there are no incident waves, and the hydrodynamic loads are composed out of the added mass, the damping, and the restoring term.

Due to the linearity of the forces, the loads of A and B can be added to the total hydrodynamic forces (see Figure 55). [129]

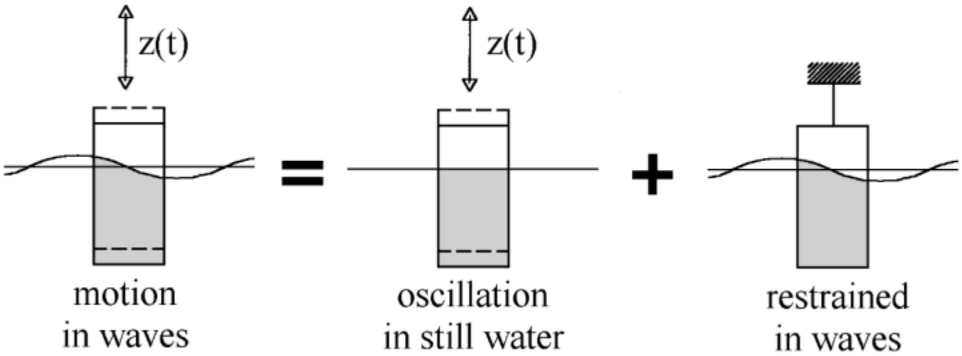

Figure 55: Hydrodynamic problem split into two subproblems [130]

The **added mass** and **damping** term take the appearance of an additional mass into account when an object is accelerated relative to a surrounding fluid. The forced motion of a structure generates outgoing waves, and it results in an oscillating fluid pressures on the body surface. By the integration of the fluid pressure forces over the body surface, the resulting forces can be determined.

When a floating platform is deflected, the **restoring force** brings the structure back to its equilibrium position. The restoring force follows from the hydrostatic and mass considerations for a particular body. The mooring system of a floating wind turbine can be a main contributor to the restoring forces (especially for TLP's).

As given in A, the exciting loads on a floating platform are the loads when the structure is restrained from oscillating and incident waves are acting on this body. By assuming regular and sinusoidal waves, the unsteady fluid pressure can be divided into two effects. The first effect is called the **Froude-Kriloff force**, which describes an unsteady pressure induced by undisturbed waves. The **diffraction force** describes the force which results from a changed pressure field.

Morison equation

The Morison equation is a semi-empirical equation which combines the linear inertia force and the drag force to calculate the horizontal force dF on a strip length dz acting on a vertical circular cylinder: [133]

$$dF = \rho \frac{\pi D^2}{4} dz C_M \dot{u} + \frac{\rho}{2} C_D D dz |u| u \tag{36}$$

The mass density of the water is ρ, the diameter of the cylinder is described with D, the undisturbed flow velocity is u and the acceleration is $\dot{u}$. The inertia/added mass coefficient C_M and the drag coefficient C_D are determined experimentally and are dependent on several factors such as the Reynolds number, the roughness number, the geometry of the body etc. [133]

The Morison model can be used for slender elements for which the dimensionless parameters such as the Keulegan-Carpenter number, the Reynolds number and the diameter-to-wavelength ratio remain within certain limits and the diffraction effect is less important. [133]

The **Keulegan-Carpenter number** KC determines the importance of the diffraction force on a structure and is defined in equation (37). u_0 is the water particle velocity amplitude, T is described as the period of the oscillation or as the wave period and D is the diameter of the considered cylinder: [133]

$$KC = \frac{u_0 T}{D} \quad (37)$$

Another parameter which is used to determine the importance of diffraction loads is the diffraction parameter: [133]

$$\frac{\pi D}{\lambda} \quad (38)$$

Whereas λ describes the wavelength. For a Keulegan-Carpenter number larger than 6 and diffraction parameter larger than 0,5 the Morison equation is applicable. [133]

Potential flow Theory

For a $KC < 6$ and $\pi D/\lambda < 0.5$ a diffraction and radiation theory should be used for the calculation of the wave forces acting on the offshore structure. The diffraction part within the potential flow theory considers the exciting forces which are acting on the restrained structure due to waves. The radiation part determines the added mass and the damping for a structure which is oscillating with the wave frequency as already mentioned. [133]

The potential flow theory is applicable for large volume structures that disturb the wave kinematics. A method to describe the potential function generated in the vicinity of the platform is the boundary element method (BEM). Limitations shows the potential flow theory in terms of determining the viscous drag loading from flow separation. To include the drag effect on smaller members of the offshore structure the drag term from the Morison equation can be used. [133], [129], [134]

6.1.3 Response amplitude operator

Response amplitude operators (RAO) are transfer functions which describe the response of a floating structure under the influence of waves. These frequency response functions are the ratio between an input parameter and an output parameter where linearity of wave excitation and system responses is assumed. With RAOs which can be determined either analytical, experimentally, or with the help of numerical simulations, motions for the six degrees of freedom can be predicted. [135]

In Figure 56 an example of the heave motion RAO for the OC4 floater is presented. This RAO describes the heave displacement per wave height over a range of different wave frequencies. Moreover, the differences between the experimentally determined RAOs and those identified by simulation can be seen.

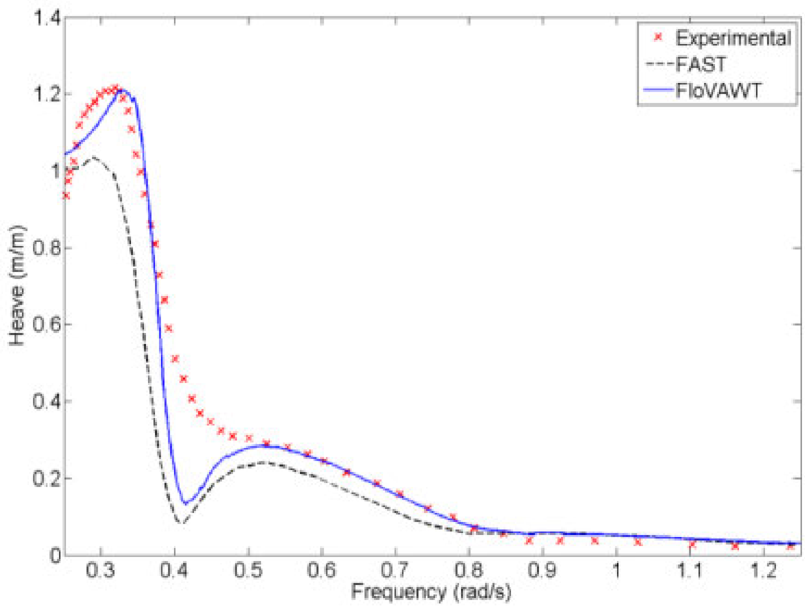

Figure 56: Heave motion RAO for the OC4 semi-submersible [136]

6.2 Project description

Three numerical models (BEM, BEM+Morison and Morison) shall be investigated that are based on the floating support structure VolturnsUS developed by NREL and presented in [7]. The diffraction, radiation, and hydrostatic loading of the BEM model(s) are calculated with coefficients from first-order RAOs which can be assessed over [137]. Next to diffraction and radiation loads, the BEM+Morison model also includes the drag term of the Morisons equation. The loads acting on the Morison model are calculated using the drag and inertia term of the Morison equation.

The simulation for each model is carried out with the tool Bladed by DNV. The investigated load case shall be comparable with the results obtained in the study from [7]. To reduce the simulation effort and to decouple the influence of the controller on the motion responses motion of the floater, an extreme load case (DLC 6.1) is considered for the simulation. The pitch angle of the rotor blades is kept constant at 82 degrees to keep the rotor permanently in a slow rotating motion. The FOWT is examined with respect to six wind and wave seeds, each of which is assumed to have a yaw error of 8°. The project information of the numerical simulation is presented in Table 20.

Table 20: General project information of numerical simulation

Parameter	Unit	Value
Number of seeds	-	6
Yaw error	degree	+8/ -8
Wind-wave-misalignment	degree	0
Simulation time	s	600
Wind model	-	3D turbulent wind
IEC turbulence	-	Edition 3 Class B
Wind speed	m/s	47,5
Wind shear exponent	-	0,14
Wave model	-	JONSWAP spectrum
Significant wave height	m	10,7
Wave peak period	s	14,2
Peak enhancement factor	-	2,75
Water depth	m	200

6.3 Numerical model

6.3.1 Support structure

The cylindrical members of the model are connected to each other at the outer nodes of the longitudinal axis (Figure 57). Since the simulation software Bladed is not able to model a rectangular cross-section, the pontoons of the floater are modelled with the help of an equivalent cylindric cross section. The diameter of the cylinder is selected such it has the same cross area as the pontoon from [7]:

$$d_p = \sqrt{\frac{4w_p h_p}{\pi}} = 10{,}56\,m \tag{39}$$

With w_p defined as the width of the pontoon (12,5 m), and h_p is the height of the pontoon (7,0 m).

The general structure of the numerical model can be seen in Figure 57. On the left side, the beam elements of the model are illustrated. The fairlead positions are presented with orange points. The right side of this Figure shows the cylindric members in accordance with their respective diameter. The darker illustrated elements in the right figure indicate that these parts are under the waterline when the structure is in equilibrium.

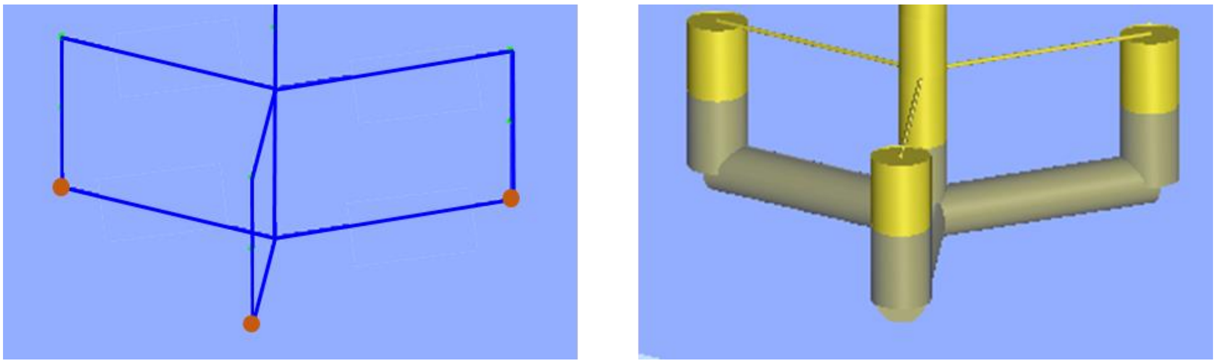

Figure 57: General numerical model of FOWT [author's illustration]

In Bladed the Morison loads on the members are applied as a trapezoidal distributed loading which varies linearly along the length of the member. Since in reality the variation is not totally linear the members are segmented into sub-members. The influence of the member segmentation can be found in the Appendix K.

The structure properties for the three numerical models are presented in Table 21. Since the structure members are connected at the intersection of their center axes, the length of the members is reduced compared to [7]. Due to the equivalent cylindrical pontoons the draft of the investigated numerical model is slightly higher compared to the model in [7]. As a result of the overlapping end parts of the members, the hull displacement of the Morison model is 3,7% higher compared to the hull displacement of the VolturnUS in [7]. To keep the draft of the longitudinal axis of the pontoons similar to those of the model in [7], the floater mass is increased to 18490 tons. Since the structure is modelled without ballast material the wall thicknesses of the floater components are adapted in order to reach the same center of gravity as the structure in [7]. The center of buoyancy of the Morison model is slightly higher compared to that of the BEM models. In the Appendix K the influence of a design variation for the Morison model is presented. However, the Morison model for the further comparison has the same structural properties as the BEM models (BEM, BEM+Morison).

Table 21: Properties of numerical models

Parameter	Unit	BEM models	Morison model
Center of gravity	m	-14,94	-14,94
Center of buoyancy	m	-13,63	-13,60
Platform mass		17754	18490
Draft	m	-21,78	-21,78
Length inner and outer columns	m	31,50	31,50
Length pontoons and struts	m	51,75	51,75
Diameter inner column	m	10,00	10,00
Diameter outer columns	m	12,50	12,50
Diameter pontoons	m	10,56	10,56
Diameter struts	m	0,91	0,91

Since for the Morison model, drag and inertia forces are applied and for the BEM+Morison model the drag force is included, the respective drag and inertia coefficients for the members must be defined. The coefficients for drag and inertia of the support structure members are determined according to the guideline [131]. The drag coefficient for the columns (inner and outer) is set to $C_{D,C} = 1{,}0$ whereas the drag coefficient for the pontoon is set to $C_{D,P} = 1{,}73$. The determination of the drag coefficients can be seen in the Appendix L.

The inertia coefficient is determined with the help of the Keulegan-Carpenter number. To determine the KC-number the orbital particle velocity of the wave needs to be calculated. According to [131, p. 38] the wavelength can be determined for deep waters as follows,

$$\lambda = \frac{gT^2}{2\pi} = 315\ m \tag{40}$$

if the deep water case can be applied,

$$h > \frac{\lambda}{2} \tag{41}$$

with h = water depth,

$$200\ m > \frac{315\ m}{2} \tag{42}$$

As the deep water case criterion is fulfilled the horizontal particle velocity can be calculated with:

$$u_h = \frac{\pi H}{T} e^{kz} cos\ (kx - \omega t) \tag{43}$$

With the wave height $H = 10{,}7\ m$, the wave peak period $T = 14{,}2\ s$, the z-position $z = 0$ and $cos = 1$ ($x = 0$ and $t = 0$), the particle velocity is:

$$u_h \approx 2{,}4 \frac{m}{s} \tag{44}$$

As the vertical particle velocity is zero for the case that the horizontal particle velocity reaches its maximum, the maximum orbital particle velocity can be calculated the following:

$$v_m = \sqrt{u_v^2 + u_h^2} = \sqrt{u_h^2} = 2{,}4 \frac{m}{s} \tag{45}$$

With the maximum orbital particle velocity and according to Formula (37), the KC numbers for the columns are determined to $KC_{IC} = 3{,}4$ and $KC_{OC} = 2{,}7$. With the help of Figure 58 the inertia coefficient for the inner and outer columns is $C_{M,IC} \approx C_{M,OC} \approx 2{,}0$. The inertia coefficient for the pontoons is determined according to [131] where for non-circular cylinders the coefficient can be obtained by multiplying the C_M with the theoretical value of C_{M0} for $KC = 0$. Since the KC is low, it is assumed that the inertia coefficient for the pontoons is $C_{M,P} = 2{,}0 * 2{,}0 = 4{,}0$.

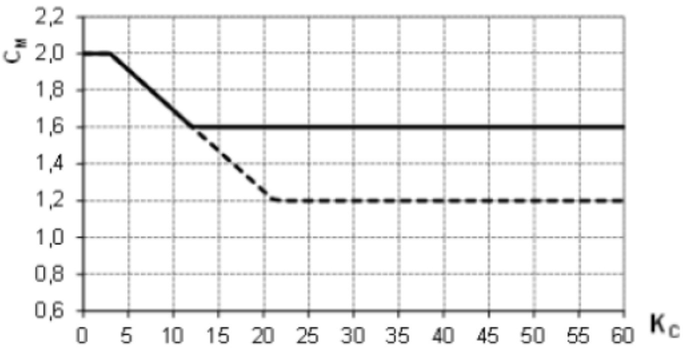

Figure 58: Added mass coefficients of KC-number for smooth (solid line) and rough (dotted line) cylinder [131]

6.3.2 Wind turbine generator and tower

The 15 MW wind turbine used for the simulation is the International Energy Agency (IEA)-15-240-RWT which was jointly designed by NREL, DTU and UMaine. The most important design parameters are presented in Table 22. The tower was redesigned for the VolturnUS floater in [7] increasing the mass from 987 ton to 1263 ton.

Table 22: Properties of turbine and tower

Parameter	Unit	Value
Power rating	MW	15
Turbine class	-	IEC Class 1B
Specific rating	W/m^2	332
Rotor orientation	-	Upwind
Number of blades	-	3
Rotor diameter	m	240
Hub height	m	150
Blade mass	ton	65
Rotor nacelle assembly mass	ton	1017
Tower mass	ton	1263

6.3.3 Mooring system

The mooring system of the VolturnUS is a three-legged catenary steel chain configuration. The properties of the mooring system are provided in Table 23.

Table 23: Properties of mooring system

Parameter	Unit	Value
Configuration	-	Catenary
Number of lines	-	3
Line material	-	Steel chain studless
Grade	-	R3
Chain diameter	mm	185
Weight of line	kg/m	685
Water depth	m	200
Fairlead depth	m	16,5
Anchor radial spacing	m	837,6
Fairlead radial spacing	m	51,8
Line length	m	850

6.4 Results

A free decay test for each of the three numerical models is performed for surge and pitch. An initial support structure displacement of 10 meters for surge and 10 degrees for pitch is applied for the tests. The decay simulations are carried out for no wind and waves.

The results of the surge decay test in Figure 59 show large differences between the BEM model compared to the models which include the Morison drag. After 5000 seconds the amplitude of the BEM model is still around 70% of the initial offset. The BEM+Morison model shows the lowest surge displacements among the other concepts.

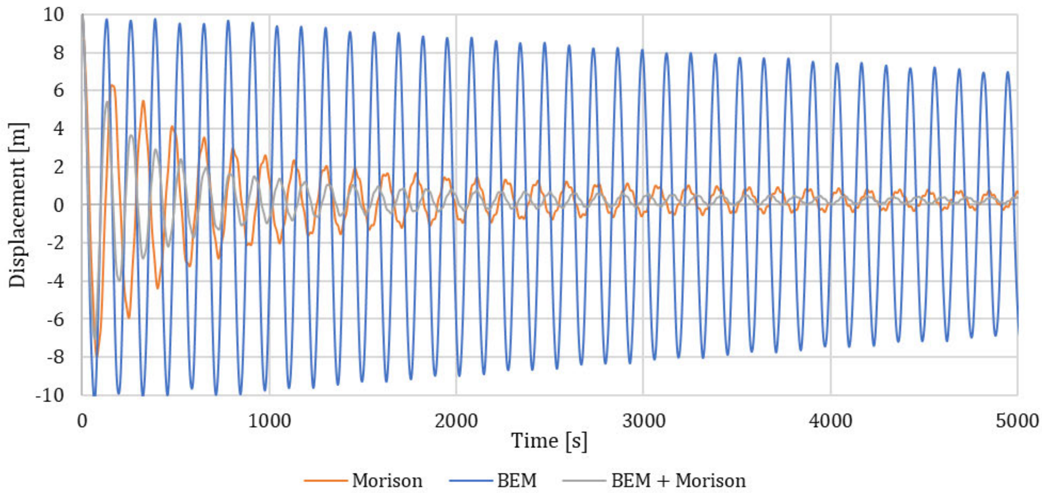

Figure 59: Surge decay test [author's illustration]

In Figure 60 the results for the pitch decay test are presented. As for the surge decay the BEM model has the highest amplitudes at the end of the simulation time among the investigated models. The BEM+Morison model achieves slightly lower amplitudes compared to the Morison model. Since the center of gravity of the RNA is in front of the tower axis, the FOWT is slightly tilted forward when it is in equilibrium. As a result, the negative pitch amplitudes are larger than the positive ones. In contrast the amplitudes of the pitch decay test in [7] are symmetrical.

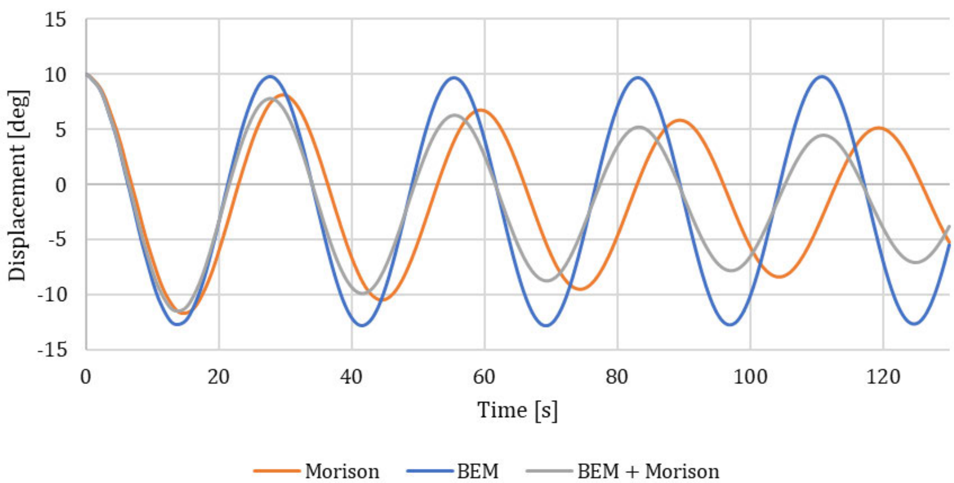

Figure 60: Pitch decay test [author's illustration]

Figure 61 shows the resulting maximum nacelle accelerations and substructure displacements in compared to the results of the model investigated in [7].

All three investigated models show a higher susceptibility for large side-side accelerations than the model in [7].With a ratio of over 2,1 the BEM model has the highest side-side accelerations among the other concepts.

The responses of the BEM+Morison and the Morison models are lower compared to those of the BEM model. Especially for the heave and pitch motions the models that include Morison drag show decreased responses.

The ratios of the BEM model for the fore-aft and vertical accelerations as well as the heave and pitch motions are closely to the 1,0 indicating similar results to the model of NREL.

Since the pontoon has no rectangular cross section and its drag and inertia coefficients for the vertical and horizontal direction are the same, the replication of the response characteristics of the NREL floater leads to some limitations.

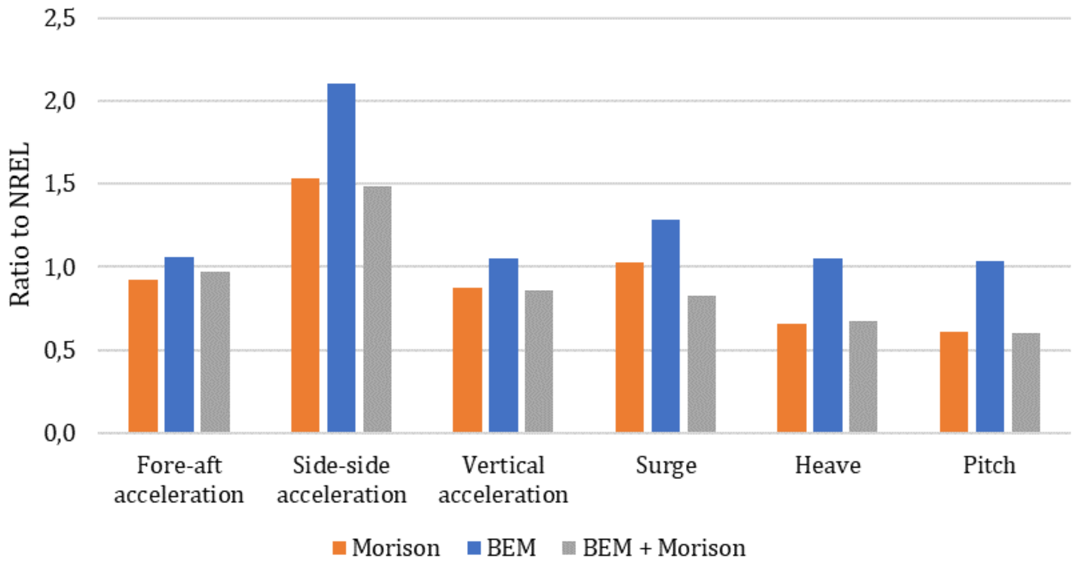

Figure 61: Nacelle acceleration and floater displacement ratios of numerical models compared to FOWT of NREL [author's illustration], results from NREL based on [7]

As mentioned in Section 2.3 the first natural tower frequency in [76] is lower compared to the frequencies determined in the NREL study [77]. This observation could also be made for the models studied here. The fore-aft and side-side accelerations of the numerical models are in the range of 0,40-0,45, Hz, which is about 10% lower than those of NREL.

7 Conclusion

7.1 Assessment of FOWT concepts

In the last years, the number of designs increased rapidly, and more than 50 concepts could be identified on the market. With the help of the stabilization principle, the concepts can be categorized into four main floater typologies. The market research revealed (see Section 2.1.1) that all these four main floater typologies are represented in the market. However, with a share of over 60%, the typology with the highest number of commercial designs is the semi-submersible. This wide distribution in the market is probably due to the independence of water depth (low draft) combined with a simplified installation (free-floating stability). Furthermore, most of the self-aligning structures are based on a semi-submersible platform. This is probably due to its long lever arm supporting the moment for the self-rotation of the structure while applying a less complex mooring system. Next to its high number of commercial concepts the semi-submersible has the highest capacity of operating and upcoming FOWTs among all other concepts.

The two-dimensional weighted point analysis assessed FOWT designs with regard to their potential for offshore wind farm deployment. The first step of this analysis included a cost assessment which evaluates concepts in dependence on their respective lifecycle cost differences. The selection of criteria including its score calculation was determined by an extensive literature review presented in Section 4. To better assess the importance of the criteria, their weighting is orientated on the cost share of the LCOE of a floating wind turbine. The score determination for the individual concepts in the different categories is based on the results of the cost assessment identified in the literature. The second dimension assesses the floater concepts with regard to their limitations and restrictions in terms of site conditions. Four weighted criteria were used to measure the respective environmental flexibility of a concept. In the final step, the results of both assessments are combined and illustrated in a plot.

Overall, the results of the assessment reflect well the strengths and weaknesses of the respective typologies identified in the market research. The concept with the highest percentage of commercial designs is also the typology that performs best on average in the two-dimensional assessment. Especially self-aligning semi-submersibles provide a high potential for offshore wind farm deployment. The combination of a small hull mass, a load-optimized tower, and efficient installation and maintenance methods lead to the lowest cost scores among the other designs. Slight disadvantages could be determined in terms of the flexibility as the weathervane effect can result in yaw-misalignments. Potential solutions for reducing the risk of a lower energy yield can be a specialized tower geometry that increases the drag-effect of the structure or a multi-rotor turbine that could counteract with individual rotor pitch. It should be mentioned that the advantages in terms of a shorter connection duration of the mooring lines and cables is not included for self-aligners. This could lead to further maintenance advantages as the downtime of the wind turbine can be reduced.

The floater designs in the category TLP performed on average worse than semi-submersibles. The main reason for this is the high installation costs compared to the other floater typologies.

The combination of two typologies can result in increasing strengths while eliminating weaknesses. The concept that benefits most from a combination of two typologies is the mixture of TLP and semi-submersible. This platform type can be installed similarly to low draft floaters and thus reducing the installation costs significantly. As a result, these designs perform above average. Furthermore, a gravity anchor which is for example used in the SOF concept could further lower the installation costs of the mooring system.

In contrast, the combination of semi-sub and spar leads to a reduction in the overall rating compared to its parent typologies. The installation advantages of the semi-sub are offset by disadvantages in the manufacturing of the floater. However, exceptions can be found here as well.

It is noticeable that concrete floaters perform well in the overall comparison and are mostly placed ahead of the steel concept in a respective typology. Especially the concrete barges and the semi-submersibles achieve a good cost score.

Furthermore, it can be observed that there are no TLP concepts made of concrete. Flexibility in the choice of materials can be advantageous as you can compensate for fluctuations in market prices. It is possible that the stabilization principle of the TLP causes that it cannot be made of concrete, which leads to minor limitations in the flexibility of material selection.

Although there is a trend in favor of the self-aligning semi-submersibles, there are other concepts that receive a similarly good rating. This also reflects the general opinion of the market - most likely, even in the long term, not only one design will prevail. With a more maturing market, the number of concepts will probably decrease due to the economics of scale. The concept that meets the project-specific requirements for infrastructure and environmental flexibility while achieving the lowest LCOE costs will be favored. [138]

7.2 Numerical analysis of FOWT

The numerical analysis of the steel semi-submersible is based on results of the support structure investigated in "IEA Wind TCP Task 37: Definition of the IEA Wind 15-Megawatt Offshore Reference Wind Turbine by NREL [7]. Three numerical model variants are investigated in terms of an extreme load case and the resulting nacelle accelerations and support structure displacements are compared with each other. The lowest damping for the decay test among all models occurred for the BEM model. This results in relatively high accelerations and motions compared to the other two models. The BEM+Morison model and the Morison model show relatively similar response characteristics to each other. An exception is determined for the surge displacement where the Morison-only model shows a higher offset.

Furthermore, the results of the numerical simulation are compared with those of the report by NREL. The BEM model shows similar results in terms of fore-aft and vertical nacelle accelerations as well as heave and pitch displacements. The side-side nacelle accelerations and the surge displacements are larger compared to the NREL results. The two models which include the drag force achieve lower vertical nacelle accelerations as well as lower heave and pitch displacement than the NREL model.

Since Bladed is not able to model rectangular cross sections, the pontoon is a cylindrical member with an equivalent diameter. This may partially lead to some of the obtained differences between the models which use a drag and/or inertia force compared to the results determined by NREL. To represent the aspect ratio of the pontoons and thus achieve better results, the coefficients could be adjusted according to the ratio between the diameter of the equivalent cylindric member and the respective side length of the rectangular pontoon.

Next to that, the center of gravity of the overall floating wind turbine could be centered to achieve more similar results to those determined in the study from NREL. The pitch motions are comparatively small compared to NREL's floater which can be caused by the forward inclination of the model in equilibrium.

The hydrodynamic loading of the BEM models is calculated with first-order RAOs which could cause s small surge displacement error. Second-order RAOs may increase the surge offset since they can result in additional drift forces for low wave frequencies. [139]

Two-bladed wind turbines offer great potential for use in FOWT projects. Cost advantages compared to conventional turbines can probably be achieved in all life cycle phases. In addition, they offer greater flexibility in terms of site conditions as they are more resistant to higher wind speeds.

Bibliography

[1] J. Lee and F. Zhao, "Global Offshore Wind Report 2021," GWEC - Global Wind Energy Council, 2021.

[2] B. Neddermann, T. Neumann, T. Habekost, H. Bredmose, A. Pegalajar-Jurado, V. Arramounet, S. Doole, C. Lourie, F. Borisade, M.-A. Schwarzkopf, S. Potestio and L. Ramirez, "D7.1 Preliminary market assessment and development needs," Corewind.eu, 2021.

[3] M. Hannon, E. Topham, J. Dixon, D. McMillan and M. Collu, "Offshore wind, ready to float? Global and UK trends in the floating offshore wind market," University of Strathclyde, Glasgow, 2019.

[4] R. James and M. Costa Ros, "Floating Offshore Wind: Market and Technology Review," Carbon Trust, 2015.

[5] L. Eatough, "FLOATING OFFSHORE WIND TECHNOLOGY AND OPERATIONS REVIEW," Catapult, 2021.

[6] Global Wind Energy Council and Aegir Insights, "Floating Offshore Wind - A Global Opportunityy," Global Wind Energy Council, 2022.

[7] C. Allen, A. Viselli, H. Dagher, A. Goupee, E. Gaertner, N. Abbas, M. Hall and G. Barter, "Definition of the UMaine VolturnUS-S Reference Platform Developed for the IEA Wind 15-Megawatt Offshore Reference Wind Turbine," National Renewable Energy Laboratory, 2020.

[8] E. Uzunoglu, E. Oguz and C. Guedes Soares, "An Overview of Platform Types Used in Floating Wind Energy," 2021.

[9] K. Longridge, "FLOATING WIND: WHAT ARE THE MOORING OPTIONS? - A Q&A WITH KENT LONGRIDGE," 2020. [Online]. Available: https://acteon.com/blog/floating-wind-mooring-options/. [Accessed 26 03 2022].

[10] DNV, "DNVGL-ST-0119 Floating wind turbine structures," 2021.

[11] A. Maximiano, "D5.4 Benchmark of PivotBuoy Compared to Other Floating Systems," 2021.

[12] DNV, "DNV-RP-F205: Global Performance Analysis of Deepwarer Floating Structures," 2004.

[13] J. Jonkman and D. Matha, "A Quantitative Comparison of the Responses of Three Floating Platforms," NREL, 2009.

[14] S. Bashetty and S. Ozcelik, "Review on Dynamics of Offshore Floating Wind Turbine Platforms," *Energies,* vol. 14, no. 6026, 2021.

[15] J. Deign, "So, What Exactly Is Floating Offshore Wind?," 2020. [Online]. Available: https://www.greentechmedia.com/articles/read/so-what-exactly-floating-offshore-wind. [Accessed 26 05 2020].

[16] Vryhof, "Vryhof Manual: the ultimate anchoring and mooring guide," 2018. [Online]. Available: https://insights.vryhof.com/download-the-vryhof-manual. [Accessed 28 06 2022].

[17] D. Timmington and L. Efthimiou, "Mooring Systems for Floating Offshore Wind: Integrity Management Concepts, Risks and Mitigation," World Forum Offshore Wind e.V., 2022.

[18] IRENA, "RENEWABLE CAPACITY STATISTICS 2022," International Renewable Energy Agency, Abu Dhabi, 2022.

[19] DNV, "ENERGY TRANSITION OUTLOOK 2021," 2021.

[20] M. Harvey, S. Strivens, H. Evans, A. Morris, F. Wendet, D. Matha, S. Phillips, G. Hawkes, J. Sowman, B. Borgarino, F. Lemmer, H. Robic and S. Raach, "Phase IV - Summary Report," Carbon Trust, 2022.

[21] CATAPULT, "INTERNATIONAL MARKET OPPORTUNITTIES," 2022.

[22] Blue H Engineering BV, "Historical development," 2022. [Online]. Available: http://www.bluehengineering.com/tablet/historical-development.html. [Accessed 08 03 2022].

[23] J. Madslien, "BBC NEWS | Business | Floating challenge for offshore wind turbine," 2009a. [Online]. Available: http://news.bbc.co.uk/1/hi/business/8235456.stm. [Accessed 27 02 2022].

[24] J. Madslien, "BBC NEWS | Business | Floating wind turbine launched," 2009b. [Online]. Available: http://news.bbc.co.uk/2/hi/business/8085551.stm. [Accessed 2022 27 02].

[25] Equinor ASA, "Hywind Scotland," 2022. [Online]. Available: https://www.equinor.com/energy/hywind-scotland. [Accessed 01 03 2022].

[26] Equinor ASA, "Hywind Tampen," 2021. [Online]. Available: https://www.equinor.com/energy/hywind-tampen. [Accessed 04 03 2022].

[27] Principle Power Inc., "Projects - Principle Power, Inc.," 2022. [Online]. Available: https://www.principlepower.com/projects. [Accessed 04 03 2022].

[28] Inocean AS, "Inocean – SWAY Offshore Wind Turbine," 2022. [Online]. Available: https://www.inocean.no/projects/sway-offshore-wind-turbine/#:~:text=The%20SWAY%C2%AE%20system%20is%20a%20floating%20spar%20wind,both%20for%20tension%20leg%20moorings%20and%20slack%20moorings.. [Accessed 28 3 2022].

[29] Advanced Structures & Composite Center, "Volturnus-A Concrete Semi-Submersible Floating Wind Platform Produced with Proven Industrialized Concrete Construction Methods," 2022. [Online]. Available: https://composites.umaine.edu/volturnus/. [Accessed 25 06 2022].

[30] JPLOURDE, "What is VolturnUS?," 2017. [Online]. Available: https://maineaquaventus.com/index.php/faqs/what-is-volturnus/. [Accessed 15 03 2022].

[31] H. Yoshimoto, T. Natsume, J. Sugino, H. Kakuya, R. Harries, A. Alexandre and D. McCowen, "EERA DeepWind - Offshore Wind R&D Digital Conference - 2019 Conference," 2019. [Online]. Available: https://www.sintef.no/projectweb/eera-deepwind/eera-deepwind-conference/previous-conferences/2019-conference/. [Accessed 12 08 2022].

[32] National Wind Watch, "National Wind Watch | Authorization Required," 2021. [Online]. Available: https://www.wind-watch.org/news/2021/03/06/failure-of-worlds-1st-offshore-floating-wind-farm-in-fukushima-disappoints-3-11-survivors/. [Accessed 07 03 2022].

[33] K. Radtke, "Setback for Japanese Offshore Wind Efforts | windfair," 2018. [Online]. Available: https://w3.windfair.net/wind-energy/news/29116-wind-turbine-floater-japan-coast-capacity-factor-yield-turbine-lower. [Accessed 17 03 2022].

[34] Toda Corporation, "haenkaze.com – – The First Grid Connected Floating Wind Turbine in Japan –," 2022a. [Online]. Available: https://haenkaze.com/en/. [Accessed 17 03 2022].

[35] Toda Corporation, "Sakiyama 2MW Floating Offshore Wind Turbine – haenkaze.com," 2022b. [Online]. Available: https://haenkaze.com/en/about-en/about-facility-en/. [Accessed 15 03 2022].

[36] BW Ideol, "FRANCE'S FIRST OFFSHORE WIND TURBINE AND BW IDEOL'S FIRST DEMONSTRATOR," 2022. [Online]. Available: https://www.bw-ideol.com/en/floatgen-demonstrator. [Accessed 12 03 2022].

[37] BW Ideol, "BW IDEOL'S SECOND DEMONSTRATOR HIBIKI," 2022. [Online]. Available: https://www.bw-ideol.com/en/japanese-demonstrator. [Accessed 21 03 2022].

[38] Saitec Offshore, "DemoSATH - Demonstration Project.," 2022a. [Online]. Available: https://saitec-offshore.com/projects/demosath/. [Accessed 12 03 2022].

[39] Stiesdal A/S, "The TetraSpar full-scale demonstration project," 2021. [Online]. Available: https://www.stiesdal.com/offshore/the-tetraspar-full-scale-demonstration-project/. [Accessed 23 02 2022].

[40] D. Snieckus, "Is this floating wind turbine the start of an offshore energy revolution in China?," 2021. [Online]. Available: https://www.rechargenews.com/wind/is-this-floating-wind-turbine-the-start-of-an-offshore-energy-revolution-in-china-/2-1-1038516. [Accessed 28 06 2022].

[41] Stiesdal, "Tetra Floating offshore foundations," 2021. [Online]. Available: https://www.stiesdal.com/offshore/. [Accessed 19 04 2022].

[42] Gazelle Wind Power, "LIGHT, AGILE, FAST," 2022. [Online]. Available: https://gazellewindpower.com/technology/. [Accessed 19 05 2022].

[43] Gazelle Wind Power, "How Does It Work? - Gazelle's Unique Floating Offshore Wind Platform," 2022b. [Online]. Available: https://www.youtube.com/watch?v=_wGsqwC61uQ. [Accessed 26 04 2022].

[44] A. Manjock and S. Netzband, "Drift stability of HyStOH semi-submersible supported by airfoil shaped structures," *Journal of Physics: Conference Series,* 2019.

[45] EDF Renewables UK, "Blyth 2 Floating Offshore Windfarm is a planned new generating facility located 14km off the Northumberland coastline," 2022. [Online]. Available: https://www.edf-re.uk/our-sites/blyth-2/. [Accessed 25 07 2022].

[46] Saitec Offshore, "SATH TECHNOLOGY," 2022. [Online]. Available: https://saitec-offshore.com/sath/. [Accessed 23 5 2022].

[47] Landbø and Trond, "EERA DeepWind'2018 Conference 17-19 January 2018," 2018. [Online]. Available: https://www.sintef.no/en/search/?flow=reports&querytext=deepwind#search. [Accessed 16 08 2022].

[48] Dr.techn. Olav Olsen AS, "RENEWABLE ENERGY," 2022. [Online]. Available: https://www.olavolsen.no/en/business-areas/renewable-energy. [Accessed 07 04 2022].

[49] D. Snieckus, "Global energy heavyweights buy into US' flagship floating wind power pilot," 05 08 2020. [Online]. Available: https://www.rechargenews.com/wind/global-energy-heavyweights-buy-into-us-flagship-floating-wind-power-pilot/2-1-853183. [Accessed 07 04 2022].

[50] Principle Power, "The WindFloat® advantage: Performance - Principle Power, Inc.," 2012. [Online]. Available: https://www.principlepower.com/windfloat/advantage/performance. [Accessed 23 5 2022].

[51] Stiesdal A/S, "Stiesdal Offshore," 2022. [Online]. Available: https://www.stiesdal.com/offshore/. [Accessed 23 5 2022].

[52] M. Foster, "Work starts on Fukushima floating project," 25 06 2012. [Online]. Available: https://www.windpowermonthly.com/article/1187536/work-starts-fukushima-floating-project. [Accessed 24 06 2022].

[53] Green Architecture and Building Report, "7 WindFloat," 2022. [Online]. Available: https://www.gabreport.com/wind-turbines-ride-the-wave-to-renewable-energy-future/7-windfloat. [Accessed 16 06 2022].

[54] World Energy News, "Japan: Experimental Floating Wind Farm Project," 11 11 2013. [Online]. Available: https://www.worldenergynews.com/news/japan-experimental-floating-wind-farm-project-596264. [Accessed 15 08 2022].

[55] Clovers AS, "Floating Wind Turbines," 2022. [Online]. Available: https://www.clovers.no/floating-wind/. [Accessed 25 5 2022].

[56] OCERGY – Sustainable Offshore Solutions, "OCG WInd," 2022. [Online]. Available: https://ocg-wind.com/. [Accessed 24 2 2022].

[57] Mareal, "XCF," 2022. [Online]. Available: https://www.mareal.eu/en/research-and-development/xcf. [Accessed 08 16 2022].

[58] Nautilus Floating Solutions, S.L., "We Design offshore Wind Floating Solutions," 2022. [Online]. Available: https://www.nautilusfs.com/. [Accessed 03 08 2022].

[59] Windcrete, "Construction & Installation," 2022. [Online]. Available: https://www.windcrete.com/construction-installation/. [Accessed 04 02 2022].

[60] Stinger Keel – Floating Energy Systems, "The Stinger Keel," 2012. [Online]. Available: https://floatingenergysystems.com/stinger-keel/. [Accessed 09 3 2022].

[61] C. Molins and A. Campos, "A Monolithic Concrete Platform for Floating Offshore Wind Turbines," 2016. [Online]. Available: https://www.windtech-international.com/editorial-features/windcrete. [Accessed 27 08 2022].

[62] SBM Offshore, "SBM Offshore launches Float4WindTM," 2022. [Online]. Available: https://www.sbmoffshore.com/newsroom/news-events/sbm-offshore-launches-float4windtm. [Accessed 3 5 2022].

[63] "PELAFLEX - Our structurally efficient floating platform," 2022. [Online]. Available: https://www.marinepowersystems.co.uk/pelaflex/. [Accessed 05 07 2022].

[64] PELASTAR, "PELASTAR," 2022. [Online]. Available: https://pelastar.com/. [Accessed 21 05 2022].

[65] PELASTAR, "INSTALLATION," 2022. [Online]. Available: https://pelastar.com/?page_id=55. [Accessed 21 05 2022].

[66] GICON, "TECHNOLOGICAL INNOVATIONS," 2022. [Online]. Available: http://www.gicon-sof.de/en/technical-solution.html. [Accessed 26 07 2022].

[67] X1 Wind, "Technology," 2022. [Online]. Available: https://www.x1wind.com/technology/. [Accessed 12 04 2022].

[68] Eolink, "AN INNOVATIVE CONCEPT," 2022. [Online]. Available: https://eolink.fr/en/article-structure-en. [Accessed 07 08 2022].

[69] Aerodyn Engineering GmbH, "SCD nezzy," Aerodyn, 2022. [Online]. Available: https://aerodyn-engineering.com/products/nezzy-technology/nezzy/?L=1%22. [Accessed 16 08 2022].

[70] E. Ferraro, "X1 Wind's PivotBuoy: Innovative floating platform to help scale offshore wind energy," 2020. [Online]. Available: https://www.compasslist.com/insights/x1-winds-pivotbuoy-innovative-floating-platform-to-help-scale-offshore-wind-energy. [Accessed 27 08 2022].

[71] D. Hautmann, "Siegfriedsens Seeungeheuer," 2021. [Online]. Available: https://energiewinde.orsted.de/trends-technik/floating-wind-nezzy2-aerodyn-doppel-rotor-offshore-windenergie-trend. [Accessed 05 04 2022].

[72] C. Micrea, "eawind's Unique Floating Offshore Wind Energy System To Be Deployed in European Waters," 2022. [Online]. Available: https://www.autoevolution.com/news/seawind-s-unique-floating-offshore-wind-energy-system-to-be-deployed-in-european-waters-182376.html. [Accessed 05 05 2022].

[73] V. Schorbach, "Pendelendanschläge bei Zweiblatt-Windenergieanlagen," Wuppertal, 2015.

[74] P. Fairley, "Two-Bladed Wind Turbines Make a Comeback," 2014. [Online]. Available: https://www.technologyreview.com/2014/06/30/13044/two-bladed-wind-turbines-make-a-comeback/. [Accessed 31 08 2022].

[75] m. Jakubowski, "Why two blades are better than three for floating wind turbines," LinkedIn, 2018. [Online]. Available: https://www.linkedin.com/pulse/why-two-blades-better-than-three-floating-wind-martin-jakubowski#:~:text=The%20benefit%20of%20a%20two-bladed%20teetering%20hinge%20turbine,placed%20between%20the%20hub%20and%20the%20main%20shaft.. [Accessed 05 04 2022].

[76] T. Kim, A. Natarajan, A. Lovera, E. Julan, C. Peyrard, M. Capaldo, G. Huwart, P. Bozonnet and M. Guiton, "A comprehensive code-to-code comparison study with the modified IEA15MW-UMaine Floating Wind Turbine for H2020 HIPERWIND project," *Journal of Physics: Conference Series,* vol. 2265, 2022.

[77] E. Hau, Windkraftanlagen - Grundlagen, Technik, Einsatz, Wirtschaftlichkeit, Krailling: Springer Vieweg, 2016.

[78] P. Colin, "THREE BLADES OR TWO BLADES?," 2014. [Online]. Available: https://www.mywindpowersystem.com/2014/07/03/three-blades-or-two-blades/. [Accessed 31 08 2022].

[79] A. Myhr, C. Bjerkseter, A. Agotnes and T. A. Nygaard, "Levelised cost of energy for offshore floating wind turbines in a life cycle perspective," 2014.

[80] C. E. Inc, "Levelized Cost of Energy (LCOE)," 2022. [Online]. Available: https://corporatefinanceinstitute.com/resources/knowledge/finance/levelized-cost-of-energy-lcoe/. [Accessed 18 04 2022].

[81] C. Maienza, A. Avossa, F. Ricciardelli, D. Coiro, G. Troise and C. Georgakis, "A life cycle cost model for floating offshore wind farms," *Applied Energy,* 2020.

[82] BVG Associates, "Wind farm costs – Guide to an offshore wind farm," 2022. [Online]. Available: https://guidetoanoffshorewindfarm.com/wind-farm-costs. [Accessed 15 04 2022].

[83] T. Stehly and P. Duffy, "2020 Cost of Wind Energy Review," Golden, CO: National Renewable Energy Laboratory, 2021.

[84] R. James, W.-Y. Weng, C. Spradbery, J. Jones, D. Matha, A. Mitzlaff, R. V. Ahilan, M. Frampton and M. Lopes, "Phase I Summary Report - Key findings from Electrical Systems, Mooring Systems, and Infrastructure & Logistics studies," Carbon Trust, 2018.

[85] K. Davis, "How Deep can the Monopile go in Offshore Wind?," 2019. [Online]. Available: https://www.empireengineering.co.uk/how-deep-can-the-monopile-go-in-offshore-wind/. [Accessed 19 04 2022].

[86] A. Martinez and G. Iglesias, "Mapping of the levelised cost of energy for floating offshore wind in the European Atlantic," 2021.

[87] T. Choisnet, B. Geschier, G. Vetrano and I. S.A., "INITIAL COMPARISON OF CONCRETE AND STEEL HULLS IN THE CASE OF IDEOL'S SQUARE RING FLOATING SUBSTRUCTURE," 2016.

[88] R. Ebenhoch, D. Matha, S. Marathe, P. Cortes Munoz and C. Molins, "Comparative Levelized Cost of Energy Analysis," *Energy Procedia,* vol. 80, pp. 108-122, 2015.

[89] R. Torr, "Strategic Infrastructure and Supply Chain Development," CATAPULT - Offshore Renewable Energy, 2022.

[90] NOV, "Tri-Floater Floating Offshore Wind Turbine Foundation," 2022. [Online]. Available: https://www.nov.com/products/tri-floater-floating-offshore-wind-turbine-foundation#:~:text=The%20GustoMSC%20Tri-Floater%20is%20a%20triangular%20semi-submersible%20with,optimized%20for%20local%20environmental%20conditions%20and%20supply%20chain.. [Accessed 10 08 2022].

[91] F. Borisade, J. Bhat, R. Scheffler, M.-A. Schwarzkopf and D. Matha, "Deliverable D7.10 - Recommendations for platform design under considerations of O&M, logistics, manufacturing and decommissioning," Ramboll, 2019.

[92] Principle Power Inc., "Performance," 2022a. [Online]. Available: https://www.principlepower.com/windfloat/advantage/performance. [Accessed 10 08 2022].

[93] A. N. Robertson, J. M. Jonkman, M. D. Masciola, P. Molta, A. J. Goupee, A. J. Coulling, I. Prowell and J. Browning, "Summary of Conclusions and Recommendations Drawn from the DeepCWind Scaled Floating Offshore Wind System Test Campaign," France, 2013.

[94] D. Zalkind, N. J. Abbas, J. Jasa, A. Wright and P. Fleming, "Floating wind turbine control optimization," *J. Phys.: Conf. Ser. 2265 042021,* 2022.

[95] M. Simpson, T. Davenne and S. Garvey, "DYNAMIC RESPONSE OF A TETRAHEDRAL FLOATING WIND TURBINE PLATFORM," 2016.

[96] S. Strivens, H. Evans, E. Northridge, M. Harvey, T. Camp and N. Terry, "Phase III summary report: Floating Wind Joint Industry Project," Carbon Trust, 2021.

[97] D. K. Spearman, S. Strivens, D. Matha, N. Cosack, A. Macleay, J. Regelink, D. Patel and T. Walsh, "Floating Wind Joint Industry Project – Phase 2 summary report," Carbon Trust, 2020.

[98] Z. Jiang, "Installation of offshore wind turbines: A technical review," *Renewable and Sustainable Energy Reviews ,* vol. 139, 2020.

[99] reNEWS Ltd, "Principle Power secures US grant for deepwater floater," 2019. [Online]. Available: https://renews.biz/56494/principle-power-wins-us-grant-for-deepwater-floater-rd/. [Accessed 11 04 2022].

[100] R. C. Ramachandran, C. Desmond, F. Judge, J.-J. Serraris and J. Murphy, "Floating offshore wind turbines: Installation, operation, maintenance and decommissioning challenges and opportunities," 2021.

[101] Windcrete, "Cost reduction," 2022b. [Online]. Available: https://www.windcrete.com/cost-reduction/. [Accessed 07 25 2022].

[102] Z. Jiang, L. Li, Z. Gao, K. H. Halse and P. C. Sandvik, "Dynamic response analysis of a catamaran installation vessel during the positioning of a wind turbine assembly onto a spar foundation," *Marine Structures,* vol. 61, pp. 1-24, 2018.

[103] P. Sclavounos, S. Lee, J. DiPietro, G. Potenza, P. Caramuscio and G. and De Michele, "FLOATING OFFSHORE WIND TURBINES: TENSION LEG PLATFORM AND TAUGHT LEG BUOY CONCEPTS SUPPOTING 3-5 MW WIND TURBINES," Warsaw, 2010.

[104] M. Kausche, Wirtschaftlichkeit schwimmender Offshore WindenergieanlagenWirtschaftlich-technische Untersuchungen und Kostensenkungspotenziale, Freiberg: Springer Gabler, 2018.

[105] L. Castro-Santos, A. Filgueira-Vizoso, I. Lamas-Galdo and L. Carral-Couce, "Methodology to calculate the installation costs of offshore wind farms located in deep waters," *Journal of Cleaner Production,* vol. 170, pp. 1124-1135, 2017.

[106] G. Katsouris and A. Marina, "Cost Modelling of Floating Wind Farms," 2016.

[107] C. Bjerkseter, Agotnes and Anders, "Levelised costs of energy for offshore floating wind turbine concepts," 2013.

[108] J. McMorland, M. Collu, D. McMillan, Carroll and J., "Operation and maintenance for floating wind turbines: A review," *Renewable and Sustainable Energy Reviews,* vol. 163, 2022.

[109] Ramboll, "D4.2 Floating Wind O&M Strategies Assessment," 2021.

[110] A. Maximiano and P. X1 Wind, "D6.4: Optimal maintenance strategies for single point mooring systems," PivotBuoy, 2019.

[111] Mark Tool, "What is the Splash Zone and How to Protect It?," 2022. [Online]. Available: https://www.marktool.com/what-is-the-splash-zone-and-how-to-protect-it/. [Accessed 2022 08 30].

[112] J. Feldhusen and K.-H. Grote, Pahl/Beitz Konstruktionslehre - Methoden und Anwendung erfolgreicher Produktentwicklung, Aachen: Springer Vieweg, 2013.

[113] W. authors, "Nutzwertanalyse," 2022. [Online]. Available: https://de.wikipedia.org/wiki/Nutzwertanalyse#%C3%84hnliche_Methoden. [Accessed 01 05 2022].

[114] A. Kolios, M. Collu, A. Chahardehi, F. P. Brennan and M. H. Patel, "A Multi-Criteria Decision Making Method to Compare Support Structures for Offshore Wind Turbines," in *ewec2010*, 2010.

[115] A. Kolios, A. Rodriguez-Tsouroukdissian and K. Salonitis, " Multi-criteria decision analysis of offshore wind turbines support structures under stochastic inputs, Ships and Offshore Structures," 2014.

[116] M. Leimeister, A. Kolios and M. Collu, "Critical review of floating support structures foroffshore wind farm deployment," *Journal of Physics: Conference Series,* 2018.

[117] J. J. Habuh-Rajan, T. A. Briggs and E. O. Diemuodeke, "COMPARATIVE ANALYSIS OF FLOATING OFFSHORE WIND TURBINE FOUNDATION FOR RENEWABLE ENERGY GENERATION," *European Journal of Mechanical Engineering Research,* vol. 7, no. 1, pp. 22-50, 2020.

[118] G. Singhal, A. Connolly, M. Laranjinha, C. McKinnon and A. Mortimer, *Independent Assessment of Current Floater Concepts for Floating Wind Application,* Houston: SNAME, 2021.

[119] D. Nilsson and A. Westin, "Floating wind power in Norway - Analysis of future opportunities and challenges," 2014.

[120] M. Lerch, d. P. Gil, Mikel, C. Molins Borrell and G. Benveniste, "Sensitivity analysis on the levelized cost of energy for1floating offshore wind farms," *Sustainable Energy Technologies and Assessments,* vol. 30, pp. 77-90, 2018.

[121] L. Castro-Santos, D. Silva, A. Rute Bento, N. Salvacao and C. Guedes Soares, "Economic feasibility of floating offshore wind farms in Portugal," *Ocean Engineering,* vol. 207, 2019.

[122] L. Castro-Santos, A. Rute Bento, D. Silva, N. Salvacao and C. Guedes Soares, "Economic Feasibility of Floating Offshore Wind Farms in the North of Spain," *Marine Science and Engineering,* vol. 8, no. 58, pp. 1-18, 2020.

[123] S. Heidari, "ECONOMIC MODELLING OF FLOATING OFFSHORE WIND POWER," 2017.

[124] Union of Concerned Scientists, "How Wind Energy Works," 2013. [Online]. Available: https://www.ucsusa.org/resources/how-wind-energy-works. [Accessed 14 08 2022].

[125] Tzinis and Irene, "Technology Readiness Level," 2012. [Online]. Available: https://www.nasa.gov/directorates/heo/scan/engineering/technology/technology_readiness_level. [Accessed 23 07 2022].

[126] H. Farr, B. Ruttenberg, R. K. Walter, Y.-H. Wang and C. White, "Potential environmental effects of deepwater floating offshore wind energy facilities," Ocean & Coastal Management, 2021.

[127] J. Azcona, F. Vittori, U. Schmidt, F. Savenije, G. Kapogiannis, X. Karvelas, D. Manolas and S. Voutsinas, "Design Solutions for 10MW Floating Offshore Wind Turbines," Innwind.EU, 2017.

[128] W. de Vries, "Final report WP 4.2 Support Structure Concepts for Deep Water Sites: Deliverable D4.2.8 (WP4: Offshore Foundations and Support Structures)," UpWind – Integrated Wind Turbine Design, 2011.

[129] O. M. Faltinsen, Sea Loads on Ships and Offshore Structures, Cambridge, 1990, p. 23.

[130] J. M. J. Journée and W. W. Massie, OFFSHORE HYDROMECHANICS, Delft University of Technology, 2001.

[131] DNV, "DNV-RP-C205 - Environmental Conditions and Environmental Loads," DNV, 2014.

[132] WikiWaves, "Ocean-Wave Spectra," 2022. [Online]. Available: https://wikiwaves.org/Ocean-Wave_Spectra. [Accessed 27 05 2022].

[133] S. K. Chakrabarti, Handbook of Offshore Engineering, 2005.

[134] Flexcom, "Potential Flow Theory and Morison's Equation," 2022. [Online]. Available: https://flexcom.fea.solutions/potential-flow-theory-and-mori.html. [Accessed 18 04 2022].

[135] I. Ibinabo and D. T. Tamunodukobipi, "Determination of the Response Amplitude Operator(s) of an FPSO," *Scientific Research Publishing,* vol. 11, pp. 541-556, 2019.

[136] M. Collu, M. Borg, A. Shires, F. N. Rizzo and E. Lupi, "FLOVAWT: FURTHER PROGRESSES ON THE DEVELOPMENT OF A COUPLED MODEL OF DYNAMICS FOR FLOATING OFFSHORE VAWTS," in *ASME 2014 33rd International Conference on Ocean, Offshore and Arctic Engineering*, 2014.

[137] M. Hall and G. Barter, "IEA-15-240-RWT/OpenFAST/IEA-15-240-RWT-UMaineSemi/HydroData/," 2022. [Online]. Available: https://github.com/mattEhall/IEA-15-240-RWT/tree/develop/OpenFAST/IEA-15-240-RWT-UMaineSemi/HydroData. [Accessed 15 06 2022].

[138] W. Musial, P. Breiter and J. Nunemaker, "Cost of Floating Offshore Wind Energy Using New England Aqua Ventus Concrete Semisubmersible Technology," National Renewable Energy Laboratory, 2020.

[139] Z. Chuang, S. Liu and Y. LuGao, "Influence of second order wave excitation loads on coupled response of an offshore floating wind turbine," *International Journal of Naval Architecture and Ocean Engineering,* vol. 12, pp. 367-375, 2020.

[140] A. Robertson, J. M. Jonkman, A. J. Goupee, P. Molta, A. J. Coullin, I. Prowell, J. Browning and M. D. Masciola, "Summary of Conclusions and Recommendations Drawn From the DeepCWind Scaled Floating Offshore Wind System Test Campaign," Nantes, 2013.

[141] M. T. Islam, "Design, Numerical Modelling and Analysis of a Semi-submersible Floater Supporting the DTU 10MW Wind Turbine," 2016.

[142] X. Tian, "Design, Numerical Modelling and Analysis of TLP Floater Supporting the DTU 10MW Wind Turbine," 2016.

[143] W. Xue, "Design, numerical modelling and analysis of a spar floater supporting the DTU 10MW wind turbine," 2016.

[144] S. Pontow, D. Kaufer, R. Shirzahdeh and M. Kühn, "Deliverable D4.36 Design Solution for a Support Structure Concept for future 20MW," Innwind.EU, 2017.

[145] Studyflix, "Biegelinie," 2022. [Online]. Available: https://studyflix.de/ingenieurwissenschaften/biegelinie-1099. [Accessed 02 05 2022].

[146] Q. F. W. Energy, "Floating Wind Designs of the World," Quest Floating Wind Energy, 2022. [Online]. Available: https://questfwe.com/pbi-fwdi/. [Accessed 16 03 2022].

[147] M. Youssef Mahfouz, M. Salari, S. Hernández, F. Vigara, C. Molins, P. Trubat, H. Bredmose and A. Pegalajar-Jurado, "Public design and FAST models of the two 15MW floater-turbine concepts," Corewind, 2020.

[148] C. Technology, "CEFRONT FLOATING WIND," 2022. [Online]. Available: https://www.cefront.com/wind. [Accessed 27 04 2022].

[149] M. Abdel-Maksoud, A. Düster, A. Bockstedte, G. Haake, S. Siegfriedsen and J. Cruse, "Konzept einer selbstausrichtenden schwimmenden Windkraftanlage," 2020.

[150] A. Manjock and S. Netzband, "Drift stability of HyStOH semi-submersible supported by airfoil shaped structures," *Journal of Physics: Conference Series,* vol. 1222, 2019.

[151] Sener, "HiveWind - Semi-submersible floating steel platform for offshore wind turbines," 2022. [Online]. Available: https://www.energy.sener/project/hivewind-semisubmersible-floating-steel-platform-offshore-wind-turbines#:~:text=HiveWind%20is%20a%20semi-submersible%20floating%20steel%20platform%20for,marketed%20by%20SENER%20Renewable%20Investments%20and%20Nervi%C3%B3n%. [Accessed 18 04 2022].

[152] J. Galván, M. J. Sánchez-Lara, I. Mendikoa, G. Pérez-Morán, V. Nava and R. Rodríguez-Arias, "NAUTILUS-DTU10 MW Floating Offshore Wind Turbine at Gulf of Maine: Public numerical models of an actively ballasted semisubmersible," *Journal of Physics: Conference Series,* vol. 1102, 2018.

[153] H. S. Andersen, E. Dufseth, J. G. Straume, M. H. Madsen, L. Laukeland and T. Landbø, "D1.2 Concept Description Report," FLAGSHIP, 2021.

[154] R. Damiani and M. Franchi, "An innovative second-order design method for the structural optimization of the SpiderFLOAT offshore wind Platform," *Ocean Engineering,* vol. 228, 2021.

[155] WISON, "Wison Delivers China's First Floating Wind Platform," 2021. [Online]. Available: https://www.wison.com/en/read_page/1033. [Accessed 21 04 2022].

[156] P. Technology, "Fukushima Floating Offshore Wind Farm," 2015. [Online]. Available: https://www.power-technology.com/projects/fukushima-floating-offshore-wind-farm/#:~:text=The%20Fukushima%20floating%20offshore%20wind%20farm%20demonstration%20project,caused%20by%20the%20earthquake%20and%20tsunami%20in%202011.. [Accessed 23 04 2022].

[157] Equinor, "World’s first floating wind farm has started production," 2017. [Online]. Available: https://www.equinor.com/en/news/archive/worlds-first-floating-wind-farm-started-production. [Accessed 13 04 2022].

[158] A. Ghigo, L. Cottura, R. Caradonna, G. Bracco and G. Mattiazzo, "Platform Optimization and Cost Analysis in a Floating Offshore Wind Farm," *Journal of Marine Science and Engineering,* vol. 8, 2020.

[159] N. Repalle, Y. Arikan and M. Campbell, "Technical paper - Offshore Wind Energy for Australia, A Case Study with a Floating 15MW Turbine," 2021. [Online]. Available: https://2hoffshore.com/technical-papers/. [Accessed 26 04 2022].

[160] M. Borg, M. Walkusch Jensen, S. Urquhart, M. Thøtt Andersen, J. Bjerg Thomsen and H. Stiesdal, "Technical Definition of the TetraSpar Demonstrator Floating Wind Turbine Foundation," *Energies,* vol. 13, 2020.

[161] W. L. Hurley and C. J. Nordstrom, "PelaStar Cost of Energy: A cost study of the PelaStar floating foundation system in UK waters," Glosten, 2014.

[162] J. Amate, G. D. Sánchez and G. González, "Development of a Semi-submersible Barge for the installation of a TLP floating substructure. TLPWIND® case study.," *Journal of Physics: Conference Series 749,* 2016.

[163] A. Janisch, "Kostenfaktoren im Stahlbau – was kostet ein Kg Stahlbau 2022?," 2022. [Online]. Available: https://jactio.com/kostenfaktoren-im-stahlbau/#Wie_ist_die_Kostenverteilung_im_Stahlbau. [Accessed 08 04 2022].

[164] H. S. Andersen, E. Dufseth, J. G. Straume, M. H. Madsen, L. Laukeland and T. Landbø, "D1.2 Concept Description Report," FLoAtinG offSHore wInd oPtimization for commercialization, 2021.

[165] P. Breiter, W. Musial, P. Duffy, A. Cooperman, M. Shields, D. Heimiller and M. Optis, "The Cost of Floating Offshore Wind Energy in California Between 2019 and 2032," Golden, CO: National Renewable Energy Laboratory, 2020.

[166] Stiesdal A/S, "The TetraSpar full-scale demonstration project," 2022. [Online]. Available: https://www.stiesdal.com/offshore/the-tetraspar-full-scale-demonstration-project/. [Accessed 7 3 2022].

[167] Offshore WIND, "Germans Developing Self-Aligning Floating Wind Turbine," 2020. [Online]. Available: https://ips-baltics.com/useful/germans-developing-self-aligning-floating-wind-turbine/. [Accessed 2 4 2022].

[168] Ørsted, "Siegfriedsens Seeungeheuer," 2021. [Online]. Available: https://energiewinde.orsted.de/trends-technik/floating-wind-nezzy2-aerodyn-doppel-rotor-offshore-windenergie-trend. [Accessed 19 04 2022].

[169] Principle Power Inc., "Installation," 2022c. [Online]. Available: https://www.principlepower.com/windfloat/advantage/installation. [Accessed 12 08 2022].

[170] Bluewater, "Floating offshore wind turbine," 2022. [Online]. Available: https://www.bluewater.com/our-solutions/renewable-energy-solutions/floating-offshore-wind-turbine/. [Accessed 14 08 2022].

[171] BW Ideol, "FRANCE'S FIRST OFFSHORE WIND TURBINE AND BW IDEOL'S FIRST DEMONSTRATOR," 2022a. [Online]. Available: https://www.bw-ideol.com/en/floatgen-demonstrator. [Accessed 12 03 2022].

[172] L. Castro-Santos, S. F. González and V. Diaz-Casas, "Methodology to calculate mooring and anchoring costs of floating offshore wind devices," in *International Conference on Renewable Energies and Power Quality*, 2013.

[173] A. Kolios, V. Mytilinou, E. Lozano-Minguez and K. Salonitis, "A Comparative Study of Multiple-Criteria Decision-Making Methods under Stochastic Inputs," *Energies,* vol. 9, pp. 1-21, 2016.

[174] T. Duarte, A. J. Sarmento and J. Jonkman, "Effects of Second-Order Hydrodynamic Forces on Floating Offshore Wind Turbines," in *32nd ASME Wind Energy Symposium*, Maryland, 2014.

[175] J. V. Taboada, "Comparative Analysis Review on Floating Offshore Wind Foundations (FOWF)," in *54th Naval Engineering and Maritime Industry Congress*, Ferrol, 2015.

[176] H. Weihrich, "The TOWS matrix—a tool for situational analysis," *Lon Range Planning,* vol. 15, pp. 54-66, 1982.

Appendencies

A. Commercial concepts identified in the market research

Technical Developer	Concept Name	Substructure Type	Picture	Hull material	Self-aligning
IDEOL	Damping Pool Steel	Barge		Concrete or steel	no
Beridi	Triwind Floater	Barge		Concrete	no
Saitec	Sath	Barge		Concrete	yes
Cefront Technologies	CEFRONT FLOATING WIND	Semi-Sub		Steel	no
Doris Group	Nerewind	Semi-Sub		Steel	no
Equinor	WindSemi	Semi-Sub		Steel	no
GustoMSC/ NOV	Tri-Floater	Semi-Sub		Steel	no
Mareal	XCF	Semi-Sub		Concrete	no
Mitsubishi Heavy Industries	V-shape semi-sub	Semi-Sub		Steel	no
Mitsui Eng. & Shipbuilding	Compact semi-sub	Semi-Sub		Steel	no
Nautica Windpower	Sealift	Semi-Sub		Steel	no
Nautilus Floating Solutions	Nautilus	Semi-Sub		Steel	no
Naval Energies (Naval Group)	Sea Reed	Semi-Sub		Steel	no
Ocergy	OCG-Wind	Semi-Sub		Steel	no
Olav Olsen	OO-STAR	Semi-Sub		Concrete	no
Principle Power	WindFloat	Semi-Sub		Steel	no
Seawind	Seawind 6	Semi-Sub		Concrete	no
Stockhouse et al. (NREL?)	SpiderFLOAT	Semi-Sub		Concrete	no
University of Maine & DeepCwind	Volturn US	Semi-Sub	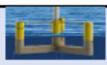	Concrete or steel	no
Saipem (Naval Energies)	Star1	Semi-Sub		Concrete	no
Saipem (Naval Energies)	X-Base	Semi-Sub		Steel	no
Stiesdal	Tetrasub	Semi-Sub		Steel	no
Dolfines	TrussFloat	Semi-Sub	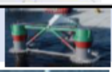	Steel	no
Wison Offshore & Marine	Three Gorges - TH Floater	Semi-Sub		Steel	no
InOcean	INO 12MW	Semi-Sub		Steel	no
Clovers	MOLO	Semi-Sub		Steel	no

Appendencies

Technical Developer	Concept Name	Substructure Type	Picture	Hull material	Self-aligning
Bassoe Technology	D-Floater/ T-Floater	Semi-Sub	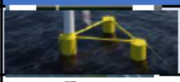	Steel	no
SENER group	Hive	Semi-Sub		Steel	no
Aerodyn	Nezzy	Semi-Sub		Concrete	yes
Eolink	Eolink Floater	Semi-Sub		Steel	yes
HyStOH	HyStOH self-aligner	Semi-Sub	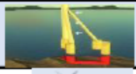	Steel	yes
TetraFloat	TetraFloat	Semi-Sub		Steel	yes
Fred. Olsen 1848	Brunel	Semi-Sub		Steel	yes
Catalunya University	WindCrete	Spar		Concrete	no
Equinor	Hywind Scotland	Spar		Steel	no
Japan Marine United Corporation	Advanced spar	Spar		Steel	no
Inocean	SWAY	Spar		Steel	yes
Toda Corporation	Hybrid Spar	Spar		Concrete and steel	no
Daewoo Engineering & Construction;	Mspar	Spar & Semi-Sub		Steel	no
Saipem (Naval Energies)	Hexafloat	Spar & Semi-Sub		Steel	no
Stiesdal	Tetraspar	Spar & Semi-Sub		Steel	no
Floating Energy Systems	Stingerkeel	Spar & Semi-Sub		Steel	no
Telwind Project (Esteyco etc.)	Telwind	Spar & Semi-Sub		Concrete	no
Stiesdal	TetraTLP	TLP		Steel	no
Glosten	PelaStar	TLP		Steel	no
SBM	Float4WindTM	TLP	 	Steel	no
Marine Power Systems	Pelaflex	TLP	 	Steel	no
Gazelle Wind Power	Gazelle Floater	TLP & Semi-Sub		Steel	no
Blue H Engineering	Blue H TLP	TLP & Semi-Sub		Steel	no
GICON	SOF	TLP & Semi-Sub		Steel	no
ECO TLP	ECO TLP	TLP & Semi-Sub		Concrete	no
X1 Wind	X1 Wind	TLP & Semi-Sub		Steel	yes

B. Floater weights by typology

Source	Ballast status	Turbine size [MW]	Barge [ton]	Semi-submersible [ton]	Spar buoy [ton]	TLP [ton]
[140]	Ballasted	5	5450	-	7466	8600
[4]	Unballasted	6	-	1918	1404	1039
[4]	Ballasted	6	-	6011	8311	1055
[141], [142], [143]	Unballasted	10	-	1689	1232	3667
[141], [142], [143]	Ballasted	10	-	6367	12100	8123
[94]	Ballasted	15	12419	16517	24925	4662

C. Unit prices for different materials and components

Source	Component	Material	Costs [euro/ton]
[144]	TP	Steel	5000
	Jacket	Steel	4800
	Pile	Steel	1200
[128]	Monopile	Steel	2000
	Jacket	Steel	4000-6000
	Conical tower Sections	Steel	2000-3000
[87]	Damping pool floater	Steel	4000
	Damping pool floater	Concrete	520

D. Tower bending moment

With the tower bending moment the bending stress of a tube can be determined the following: [145]

$$\sigma_b = \frac{M_b}{W} = \frac{M_b}{\frac{I}{a_{max}}} = \frac{M_b}{\frac{D_a^4 - D_i^4}{a_{max}}}$$

Where σ_b is the bending stress, W is defined as the resistance moment, I is the moment of inertia, a_{max} is the maximal distance between neutral fiber and the edge fiber, D_a is the outer diameter of the pile and $D_i$is here defined as the inner pile diameter.

Assuming that the bending stress remains constant for different bending moments and that the outer diameter of the pile is not changed, we can determine the inner diameter of the tower the following:

$$D_i = \sqrt[4]{D_a^4 - \frac{a_{max} * M_b}{\sigma_b}}$$

In [7] the tower dimensions for the VolturnUS floater are presented. For a constant outer diameter of 10 meters and an initial wall thickness of 0,083 meters the mass increase for different bending moment ratios is the following (ratio between diameter and wall thickness):

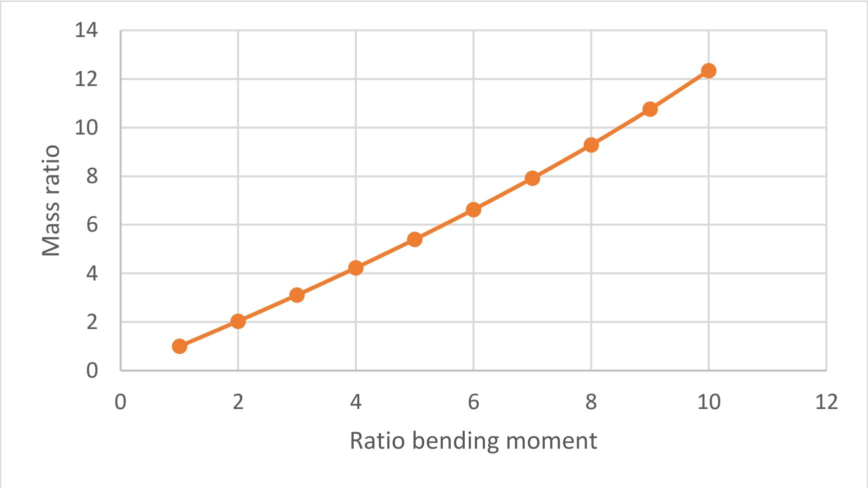

Assuming that next to the wall thickness also the outer diameter is increased, the ratio between mass increase and bending moment increase is nearly the same and linear. This assumptions leads to the fact that the tower bending moment ratio has a direct and linear impact on the mass ratio of the tower.

E. Installation cost ratios identified in studies

Study	Semi-submersible	Spar buoy	TPL
[105]	26 %	27 %	100 %
[81]	22 %	29 %	100 %
[4]	58 %	100 %	96 %
[106]	61 %	100 %	67 %

F. Detailed installation scores based on [81]

Draft	Tow stability	Installation Strategy	$s_{I,turbine}$	$s_{I,floater}$
low	high	A	0,0265	0,1839
	Low	-		
high	high	B	0,0962	0,2483
	low	C	0,2987	1,0000

G. Underlying data of concepts for cost assessment

***Note: Yellow is base case concept*

Technical Developer	Concept Name	Substructure Type	Picture	Primary hull material	Scaled steel mass	Scaled concrete mass	Scaled ballast mass	Factor floater assembly	Score tower by typology	Factor tower design	Factor mooring line	Number of lines	Factor anchor typology	Number of anchors	Score inst. turbine	Score inst. floater	Score inst. mooring system	Score maint. strategy	Factor maint. accessibility	Source
IDEOL	Damping Pool Concrete	Barge		Concrete	0	1146	0	1,75	3,33	1,00	1,00	4,00	0,28	4,00	0,03	0,18	0,24	0,75	1,00	1
IDEOL	Damping Pool Steel	Barge		Steel	306	0	0	1,75	3,33	1,00	1,00	4,00	0,28	4,00	0,03	0,18	0,24	0,75	1,00	1
-	Generic Barge	Barge	-	Steel	347	0	0	1,75	3,33	1,00	1,00	3,00	0,28	3,00	0,03	0,18	0,18	0,75	1,00	Estimated
Saitec	Sath	Barge		Concrete	30	605	0	2,25	3,33	1,00	1,00	3,00	0,28	3,00	0,03	0,18	0,18	0,75	1,00	2
Beridi	Triwind Floater	Barge	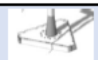	Concrete	0	400	0	1,75	3,33	1,00	1,00	3,00	0,28	3,00	0,03	0,18	0,18	0,75	1,00	2
COBRA & ESTEYCO	Activefloat	Semi-Sub		Concrete	0	2121	0	1,75	1,50	1,00	0,90	3,00	0,25	3,00	0,03	0,18	0,18	0,75	1,00	3
Cefront Technologies	CEFRONT FLOATING WIND	Semi-Sub		Steel	227	0	0	1,75	1,50	1,00	0,90	3,00	0,25	3,00	0,03	0,18	0,18	0,75	1,00	4
HyStOH	HyStOH self-aligner	Semi-Sub		Steel	278	0	0	1,75	1,50	0,90	0,90	3,00	0,25	3,00	0,03	0,18	0,18	0,75	1,00	5, 6
Eolink	Eolink Floater	Semi-Sub		Steel	151	0	0	2,00	1,50	0,90	0,90	3,00	0,25	3,00	0,03	0,18	0,18	0,75	1,00	7
-	Generic Semi-Sub	Semi-Sub	-	Steel	264	0	0	2,00	1,50	1,00	0,90	3,00	0,25	3,00	0,03	0,18	0,18	0,75	1,00	8
Sener	HiveWind	Semi-Sub		Steel	212	0	0	2,00	1,50	1,00	0,90	3,00	0,25	3,00	0,03	0,18	0,18	0,75	1,00	9
Nautilus	Nautilus	Semi-Sub		Steel	241	0	389	2,00	1,50	1,00	0,90	4,00	0,25	4,00	0,03	0,18	0,24	0,75	1,00	10
Doris Group	Nerewind	Semi-Sub		Steel	378	0	0	2,50	1,50	1,00	0,90	4,00	0,25	4,00	0,03	0,18	0,24	0,75	1,00	2
Aerodyn	Nezzy	Semi-Sub		Concrete	0	154	51	2,25	1,50	0,90	0,90	3,00	0,25	3,00	0,03	0,18	0,18	0,75	1,00	2

Technical Developer	Concept Name	Substructure Type	Picture	Primary hull material	Scaled steel mass	Scaled concrete mass	Scaled ballast mass	Factor floater assembly	Score tower by typology	Factor tower design	Factor mooring line	Number of lines	Factor anchor typology	Number of anchors	Score inst. turbine	Score inst. floater	Score inst. mooring system	Score maint. strategy	Factor maint. accessibility	Source
Ocergy	OCG-Wind	Semi-Sub		Steel	200	0	0	2,25	1,50	1,00	0,90	3,00	0,25	3,00	0,03	0,18	0,18	0,75	1,00	2
Olav Olsen	OO-STAR	Semi-Sub		Concrete	0	1516	377	1,75	1,50	1,00	0,90	3,00	0,25	3,00	0,03	0,18	0,18	0,75	1,00	11
Seawind	Seawind 6	Semi-Sub		Concrete	0	834	0	1,75	1,50	1,00	0,90	3,00	0,25	3,00	0,03	0,18	0,18	0,75	1,00	2
Stockhouse et al. (NREL?)	SpiderFLOAT	Semi-Sub		Concrete	0	200	0	2,25	1,50	1,00	0,90	3,00	0,25	3,00	0,03	0,18	0,18	0,75	1,00	12
TetraFloat Ltd	TetraFloat	Semi-Sub		Steel	94	0	0	2,25	1,50	0,90	0,90	3,00	0,25	3,00	0,03	0,18	0,18	0,75	1,00	13
Stiesdal	Tetrasub	Semi-Sub		Steel	250	50	0	2,00	1,50	1,00	0,90	3,00	0,25	3,00	0,03	0,18	0,18	0,75	1,00	2
Wison Offshore & Marine Co.,	Three Gorges - TH	Semi-Sub	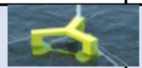	Steel	665	0	0	2,00	1,50	1,00	0,90	3,00	0,25	3,00	0,03	0,18	0,18	0,75	1,00	2, 14
GustoMSC/ NOV	Tri-Floater	Semi-Sub		Steel	245	0	0	2,25	1,50	1,00	0,90	3,00	0,25	3,00	0,03	0,18	0,18	0,75	1,00	2
Dolfines	TrussFloat	Semi-Sub	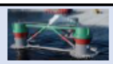	Steel	250	0	0	2,25	1,50	1,00	0,90	3,00	0,25	3,00	0,03	0,18	0,18	0,75	1,00	2
University of Maine & DeepCwind	Volturn US	Semi-Sub		Steel	296	0	192	2,00	1,50	1,00	0,90	3,00	0,25	3,00	0,03	0,18	0,18	0,75	1,00	15
Mitsubishi Heavy Industries	V-shape semi-sub	Semi-Sub		Steel	626	0	0	1,75	1,50	1,00	0,90	3,00	0,25	3,00	0,03	0,18	0,18	0,75	1,00	2, 16
Principle Power	WindFloat	Semi-Sub		Steel	270	0	0	2,25	1,50	1,00	0,90	3,00	0,25	3,00	0,03	0,18	0,18	0,75	1,00	2
Equinor	WindSemi	Semi-Sub		Steel	265	0	0	2,00	1,50	1,00	0,90	3,00	0,25	3,00	0,03	0,18	0,18	0,75	1,00	2
Mareal	XCF	Semi-Sub		Concrete	0	757	0	2,25	1,50	1,00	0,90	4,00	0,25	4,00	0,03	0,18	0,24	0,75	1,00	2

Technical Developer	Concept Name	Substructure Type	Picture	Primary hull material	Scaled steel mass	Scaled concrete mass	Scaled ballast mass	Factor floater assembly	Score tower by typology	Factor tower design	Factor mooring line	Number of lines	Factor anchor typology	Number of anchors	Score inst. turbine	Score inst. floater	Score inst. mooring system	Score maint. strategy	Factor maint. accessibility	Source
Japan Marine United Corporation	Advanced spar	Spar		Steel	1112	0	0	1,75	1,67	1,00	0,85	3,00	0,25	3,00	0,03	0,18	0,18	1,00	1,00	2, 16
Carbon trust	Generic Spar	Spar		Steel	208	0	0	1,50	1,67	1,00	0,85	3,00	0,25	3,00	0,10	0,25	0,18	1,00	1,00	8
Equinor	Hywind Scotland	Spar		Steel	320	0	0	1,50	1,67	1,00	0,85	3,00	0,25	3,00	0,10	0,25	0,18	1,00	1,00	17
Catalunya University	WindCrete	Spar		Concrete	0	869	1897	1,50	1,67	1,00	0,85	3,00	0,25	3,00	0,10	0,25	0,18	1,00	1,00	3
-	Generic Spar & Semi-Sub	Spar & Semi-Sub	-	Steel	208	0	0	2,00	1,67	1,00	0,85	3,00	0,25	3,00	0,03	0,18	0,18	1,00	1,00	Estimated
Saipem (Naval Energies)	Hexafloat	Spar & Semi-Sub		Steel	169	0	454	2,25	1,67	1,00	0,85	6,00	0,25	6,00	0,03	0,18	0,36	1,00	1,00	18
Floating Energy Systems	Stingerkeel	Spar & Semi-Sub		Steel	333	189	0	2,50	1,67	1,00	0,85	3,00	0,25	3,00	0,03	0,18	0,18	1,00	1,00	2, 19
Stiesdal	Tetraspar	Spar & Semi-Sub		Steel	342	0	0	2,00	1,67	1,00	0,85	3,00	0,25	3,00	0,03	0,18	0,18	1,00	1,00	20
SBM	Float4WindTM	TLP	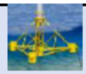	Steel	184	0	0	2,50	1,00	1,00	0,25	6,00	0,50	3,00	0,30	1,00	0,27	1,00	0,95	2
Carbon trust	Generic TLP	TLP	-	Steel	146	0	0	2,00	1,00	1,00	0,25	6,00	0,50	3,00	0,30	1,00	0,27	1,00	0,95	8
Marine Power	Pelaflex	TLP		Steel	227	0	0	2,00	1,00	1,00	0,25	6,00	0,50	3,00	0,03	0,18	0,27	1,00	0,95	21
Glosten	PelaStar	TLP		Steel	209	0	0	2,00	1,00	1,00	0,25	5,00	0,50	5,00	0,30	1,00	0,30	1,00	0,95	22
Gazelle Wind Power	Gazelle Floater	TLP & Semi-Sub		Steel	200	0	0	2,00	1,00	1,00	0,25	6,00	0,50	6,00	0,03	0,18	0,36	1,00	0,95	2
-	Generic TLP & Semi-Sub	TLP & Semi-Sub	-	Steel	153	0	0	2,25	1,00	1,00	0,25	6,00	0,50	3,00	0,03	0,18	0,27	1,00	0,95	Estimated

Technical Developer	Concept Name	Substructure Type	Picture	Primary hull material	Scaled steel mass	Scaled concrete mass	Scaled ballast mass	Factor floater assembly	Score tower by typology	Factor tower design	Factor mooring line	Number of lines	Factor anchor typology	Number of anchors	Score inst. turbine	Score inst. floater	Score inst. mooring system	Score maint. strategy	Factor maint. accessibility	Source
GICON	SOF	TLP & Semi-Sub		Steel	28	389	0	2,00	1,00	1,00	0,25	8,00	0,30	4,00	0,03	0,18	0,06	1,00	0,95	23
X1 Wind	X1 Wind	TLP & Semi-Sub		Steel	258	0	0	2,25	1,00	0,90	0,25	3,00	0,50	3,00	0,03	0,18	0,18	0,75	0,95	2, 24

Sources for concept assessment:

Source number	Source
1	[87]
2	[146]
3	[147]
4	[148]
5	[149]
6	[150]
7	[68]
8	[4]
9	[151]
10	[152]
11	[153]
12	[154]
13	[95]
14	[155]
15	[7]
16	[156]
17	[157]
18	[158]
19	[159]
20	[160]
21	[63]
22	[161]
23	[104]
24	[11]

H. Weighted concept scores for cost assessment

Concept Name	Floater	Tower	Mooring system	Installation	Maintenance	Overall score
Damping Pool Concrete	0,33	0,09	0,17	0,08	0,45	1,11
Damping Pool Steel	0,35	0,09	0,17	0,08	0,45	1,13
Generic Barge	0,39	0,09	0,13	0,07	0,45	1,13
Sath	0,24	0,09	0,13	0,07	0,45	0,98
Triwind Floater	0,11	0,09	0,13	0,07	0,45	0,85
Activefloat	0,60	0,04	0,12	0,07	0,45	1,28
CEFRONT FLOATING WIND	0,26	0,04	0,12	0,07	0,45	0,93
HyStOH self-aligner	0,32	0,04	0,12	0,07	0,45	0,98
Eolink Floater	0,19	0,04	0,12	0,07	0,45	0,86
Generic Semi-Sub	0,33	0,04	0,12	0,07	0,45	1,00
HiveWind	0,26	0,04	0,12	0,07	0,45	0,94
Nautilus	0,31	0,04	0,15	0,08	0,45	1,03
Nerewind	0,55	0,04	0,15	0,08	0,45	1,27
Nezzy	0,05	0,04	0,12	0,07	0,45	0,72
OCG-Wind	0,27	0,04	0,12	0,07	0,45	0,94
OO-STAR	0,44	0,04	0,12	0,07	0,45	1,11
Seawind 6	0,24	0,04	0,12	0,07	0,45	0,91
SpiderFLOAT	0,07	0,04	0,12	0,07	0,45	0,74
TetraFloat	0,13	0,04	0,12	0,07	0,45	0,80
Tetrasub	0,33	0,04	0,12	0,07	0,45	1,00
Three Gorges - TH Floater	0,82	0,04	0,12	0,07	0,45	1,50
Tri-Floater	0,33	0,04	0,12	0,07	0,45	1,00
TrussFloat	0,34	0,04	0,12	0,07	0,45	1,01
Volturn US	0,37	0,04	0,12	0,07	0,45	1,05
V-shape semi-sub	0,71	0,04	0,12	0,07	0,45	1,38
WindFloat	0,36	0,04	0,12	0,07	0,45	1,04
WindSemi	0,33	0,04	0,12	0,07	0,45	1,00
XCF	0,25	0,04	0,15	0,08	0,45	0,98
Advanced spar	1,26	0,04	0,11	0,07	0,60	2,09
Generic Spar	0,22	0,04	0,11	0,09	0,60	1,06
Hywind Scotland	0,33	0,04	0,11	0,09	0,60	1,18
WindCrete	0,28	0,04	0,11	0,09	0,60	1,13
Generic Spar & Semi-Sub	0,26	0,04	0,11	0,07	0,60	1,08
Hexafloat	0,24	0,04	0,22	0,10	0,60	1,21
Stingerkeel	0,55	0,04	0,11	0,07	0,60	1,37
Tetraspar	0,42	0,04	0,11	0,07	0,60	1,25
Float4WindTM	0,27	0,03	0,10	0,27	0,57	1,23
Generic TLP	0,18	0,03	0,10	0,27	0,57	1,15
Pelaflex	0,28	0,03	0,10	0,08	0,57	1,06
PelaStar	0,26	0,03	0,13	0,27	0,57	1,26
Gazelle Floater	0,25	0,03	0,15	0,10	0,57	1,09
Generic TLP & Semi-Sub	0,21	0,03	0,10	0,08	0,57	0,99
SOF	0,16	0,03	0,11	0,05	0,57	0,91
X1 Wind	0,35	0,02	0,08	0,07	0,43	0,94

I. Unweighted scores for flexibility assessment by floater typology

Floater typology	Water depth	Waves	Current	Soil conditions
Barge	1	4	1	1
Semi-submersible	1	3	1	1
Spar and mix	4	2	2	1
TLP and mix	2	1	4	3

J. Weighted concept scores for flexibility assessment

Concept Name	Substructure Type	Self-aligning	Water depth	Waves	Current	Soil conditions	Sum normalized
Damping Pool Concrete	Barge	no	0,40	1,20	0,20	0,10	1,19
Damping Pool Steel	Barge	no	0,40	1,20	0,20	0,10	1,19
Generic Barge	Barge	no	0,40	1,20	0,20	0,10	1,19
Sath	Barge	yes	0,40	1,20	0,30	0,10	1,25
Triwind Floater	Barge	no	0,40	1,20	0,20	0,10	1,19
Activefloat	Semi-Sub	no	0,40	0,90	0,20	0,10	1,00
CEFRONT FLOATING WIND	Semi-Sub	no	0,40	0,90	0,20	0,10	1,00
HyStOH self-aligner	Semi-Sub	yes	0,40	0,90	0,30	0,10	1,06
Eolink Floater	Semi-Sub	yes	0,40	0,90	0,30	0,10	1,06
Generic Semi-Sub	Semi-Sub	no	0,40	0,90	0,20	0,10	1,00
HiveWind	Semi-Sub	no	0,40	0,90	0,20	0,10	1,00
Nautilus	Semi-Sub	no	0,40	0,90	0,20	0,10	1,00
Nerewind	Semi-Sub	no	0,40	0,90	0,20	0,10	1,00
Nezzy	Semi-Sub	yes	0,40	0,90	0,30	0,10	1,06
OCG-Wind	Semi-Sub	no	0,40	0,90	0,20	0,10	1,00
OO-STAR	Semi-Sub	no	0,40	0,90	0,20	0,10	1,00
Seawind 6	Semi-Sub	no	0,40	0,90	0,20	0,10	1,00
SpiderFLOAT	Semi-Sub	no	0,40	0,90	0,20	0,10	1,00
TetraFloat	Semi-Sub	yes	0,40	0,90	0,30	0,10	1,06
Tetrasub	Semi-Sub	no	0,40	0,90	0,20	0,10	1,00
Three Gorges - TH Floater	Semi-Sub	no	0,40	0,90	0,20	0,10	1,00
Tri-Floater	Semi-Sub	no	0,40	0,90	0,20	0,10	1,00
TrussFloat	Semi-Sub	no	0,40	0,90	0,20	0,10	1,00
Volturn US	Semi-Sub	no	0,40	0,90	0,20	0,10	1,00
V-shape semi-sub	Semi-Sub	no	0,40	0,90	0,20	0,10	1,00
WindFloat	Semi-Sub	no	0,40	0,90	0,20	0,10	1,00
WindSemi	Semi-Sub	no	0,40	0,90	0,20	0,10	1,00
XCF	Semi-Sub	no	0,40	0,90	0,20	0,10	1,00
Advanced spar	Spar	no	1,00	0,60	0,40	0,10	1,31
Generic Spar	Spar	no	1,60	0,60	0,40	0,10	1,69
Hywind Scotland	Spar	no	1,60	0,60	0,40	0,10	1,69
WindCrete	Spar	no	1,60	0,60	0,40	0,10	1,69
Generic Spar & Semi-Sub	Spar & Semi-Sub	no	1,60	0,60	0,40	0,10	1,69
Hexafloat	Spar & Semi-Sub	no	1,60	0,60	0,40	0,10	1,69
Stingerkeel	Spar & Semi-Sub	no	1,60	0,60	0,40	0,10	1,69
Tetraspar	Spar & Semi-Sub	no	1,60	0,60	0,40	0,10	1,69
Float4WindTM	TLP	no	0,80	0,30	0,80	0,30	1,38
Generic TLP	TLP	no	0,80	0,30	0,80	0,30	1,38
Pelaflex	TLP	no	0,80	0,30	0,80	0,30	1,38
PelaStar	TLP	no	0,80	0,30	0,80	0,30	1,38
Gazelle Floater	TLP & Semi-Sub	no	0,80	0,30	0,80	0,30	1,38
Generic TLP & Semi-Sub	TLP & Semi-Sub	no	0,80	0,30	0,80	0,30	1,38
SOF	TLP & Semi-Sub	no	0,80	0,30	0,80	0,30	1,38
X1 Wind	TLP & Semi-Sub	yes	0,40	0,30	0,90	0,30	1,19

K. Numerical model

Segmentation of elements

In the part it is investigated how the fineness of the segmentation of the members affects the motion behavior of the platform. For this purpose, three models which differentiate in terms of their segmentation are compared with each other based on an extreme wind and wave scenario. The models are illustrated in the Figure below. In the first step only the columns are segmented more finely whereas in the second step also, the pontoons are segmented into smaller sub-members.

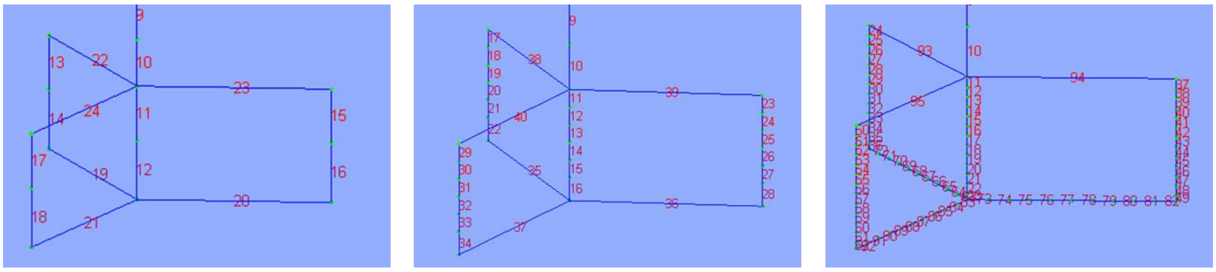

The results in the figure below show that the segmentation of the structure leads to differences in terms of nacelle accelerations and platform motions. For this reason, the segmentation of the model C is used for the BEM+Morison and the Morison model further investigations.

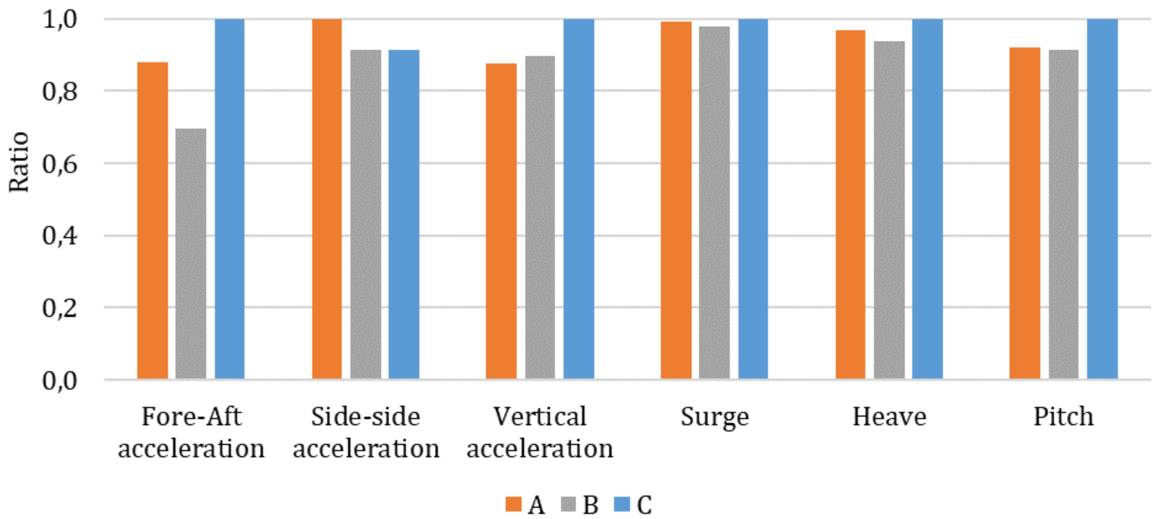

Variation of hull geometry of the Morison model

Four different Morison models are investigated which vary in terms of draft and structure geometry. The properties for those models can be seen in the Table below:

Parameter	Unit	1.2	**2.1**	2.2	3.2
Center of gravity	m	-14,94	**-14,94**	-14,94	-14,94
Center of buoyancy	m	-13,63	**-13,60**	-13,63	-13,63
Hull displacement	m^3	20127	**20955**	20975	20239
Length inner columns (inner and outer)	m	26,00	**31,50**	31,55	36,50
Length pontoons and struts	m	58,00	**51,75**	51,75	40,50
Diameter inner column	m	10,00	**10,00**	10,00	10,00
Diameter outer columns	m	12,50	**12,50**	12,50	12,50
Diameter pontoons	m	10,56	**10,56**	10,56	10,56
Diameter struts	m	0,91	**0,91**	0,91	0,91
Wall thickness columns and struts	mm	31,7	**37,8**	39,0	31,4
Wall thickness pontoons	mm	380,1	**438,2**	437,4	544,6

The figure below shows the nacelle accelerations and substructure displacements of the Morison models for the investigated extreme load case DLC 6.1. In terms of the fore-aft acceleration the variant 1.2 and especially the variant 3.2 show reduced motions compared to the variants 2.1 and 2.2. Since the differences between the models 2.1 and 2.2 are relatively small, and the reduced center of buoyancy of the variant 2.1 has a small impact on the overall response characteristics, the model 2.1 is selected for further investigations presented in 6.3 and 6.4. This also ensures better comparability of the three models (BEM, BEM+Morison, Morison).

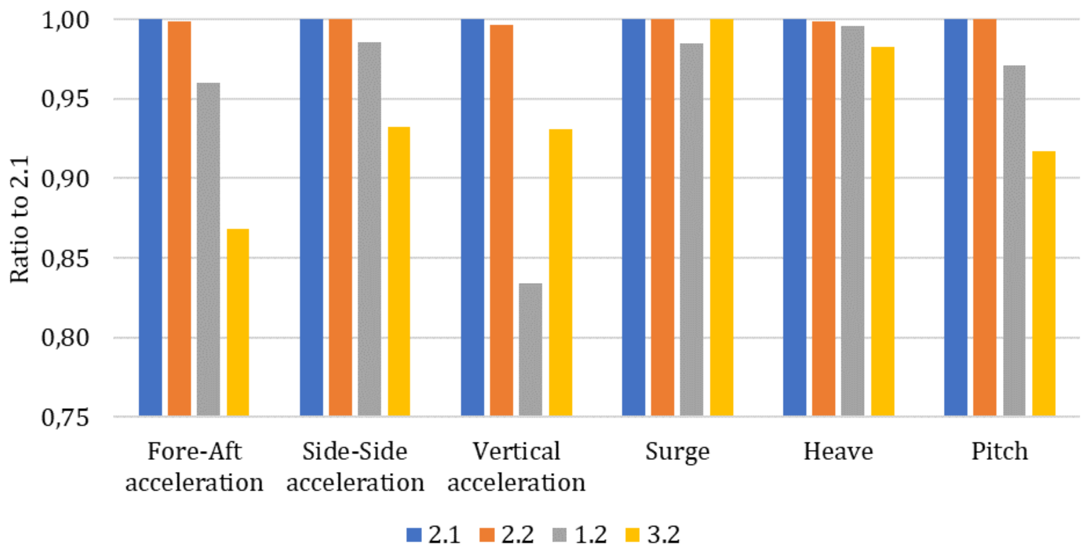

L. Drag coefficients from [131]

4. Rectangle with rounded corners	L/D	R/D	C_D	L/D	R/D	C_D
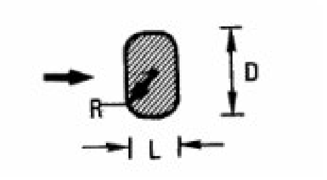	0.5	0 0.021 0.083 0.250	2.5 2.2 1.9 1.6	2.0	0 0.042 0.167 0.50	1.6 1.4 0.7 0.4
	1.0	0 0.021 0.167 0.333	2.2 2.0 1.2 1.0	6.0	0 0.5	0.89 0.29

14. Ellipse	D/L	C_D (R_e ~10^5)
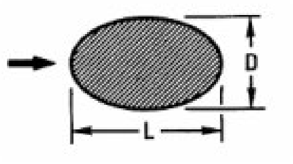	0.125 0.25 0.50 1.00 2.0	0.22 0.3 0.6 1.0 1.6

The drag coefficient for the pontoons is calculated with the help of a linear interpolation between $D/L = 1{,}0$ and $D/L = 2{,}0$ to $C_{D,P} = 1{,}73$. The ratio R/D is set to zero.

The drag coefficient for the columns is $C_{D,C} = 1{,}0$ with $D/L = 1{,}0$.

M. Modal analysis

The table below shows the determined eigenfrequencies of the platform and the tower.

Parameter	BEM	BEM+Morison	Morison
Surge	0,007	0,007	0,007
Sway	0,006	0,006	0,006
Heave	0,07	0,07	0,07
Roll	0,039	0,039	0,039
Pitch	0,039	0,039	0,039
Yaw	0,010	0,010	0,010
First fore-aft acceleration	0,43	0,43	0,40
First ide-side acceleration	0,45	0,45	0,41

Hochschule für Angewandte Wissenschaften Hamburg
Hamburg University of Applied Sciences

Erklärung zur selbstständigen Bearbeitung einer Abschlussarbeit

Gemäß der Allgemeinen Prüfungs- und Studienordnung ist zusammen mit der Abschlussarbeit eine schriftliche Erklärung abzugeben, in der der Studierende bestätigt, dass die Abschlussarbeit „– bei einer Gruppenarbeit die entsprechend gekennzeichneten Teile der Arbeit [(§ 18 Abs. 1 APSO-TI-BM bzw. § 21 Abs. 1 APSO-INGI)] – ohne fremde Hilfe selbständig verfasst und nur die angegebenen Quellen und Hilfsmittel benutzt wurden. Wörtlich oder dem Sinn nach aus anderen Werken entnommene Stellen sind unter Angabe der Quellen kenntlich zu machen."

Quelle: § 16 Abs. 5 APSO-TI-BM bzw. § 15 Abs. 6 APSO-INGI

Dieses Blatt, mit der folgenden Erklärung, ist nach Fertigstellung der Abschlussarbeit durch den Studierenden auszufüllen und jeweils mit Originalunterschrift als letztes Blatt in das Prüfungsexemplar der Abschlussarbeit einzubinden.
Eine unrichtig abgegebene Erklärung kann -auch nachträglich- zur Ungültigkeit des Studienabschlusses führen.

Erklärung zur selbstständigen Bearbeitung der Arbeit

Hiermit versichere ich,

Name: [redacted]

Vorname: [redacted]

dass ich die vorliegende Masterarbeit bzw. bei einer Gruppenarbeit die entsprechend gekennzeichneten Teile der Arbeit – mit dem Thema:

Two-bladed floating offshore wind turbines - Comparison of existing floating support structure concepts and aero-hydro-servo-elastic simulation

ohne fremde Hilfe selbständig verfasst und nur die angegebenen Quellen und Hilfsmittel benutzt habe. Wörtlich oder dem Sinn nach aus anderen Werken entnommene Stellen sind unter Angabe der Quellen kenntlich gemacht.

- die folgende Aussage ist bei Gruppenarbeiten auszufüllen und entfällt bei Einzelarbeiten -

Die Kennzeichnung der von mir erstellten und verantworteten Teile der -bitte auswählen- ist erfolgt durch:

[redacted] Ort   [redacted] Datum   Unterschrift im Original